UNIVERSITY OF CALIFORNIA, SAN DIEGO
SAN DIEGO STATE UNIVERSITY

# Biophysical and Biochemical Effects of Mono-Ubiquitination on Engineered Proteins

A dissertation submitted in partial satisfaction of the requirements for the degree

Doctor of Philosophy

in

Chemistry

by

Mario Fco. Navarro

Committee in charge:

University of California, San Diego

Professor Russell Doolittle
Professor Patricia Jennings
Professor Elizabeth Komives

San Diego State University

Professor John J. Love, Chair
Professor Greg Harris
Professor Tom Huxford

2013

The dissertation of Mario Fco. Navarro is approved, and it is acceptable in quality and form for publication on microfilm and electronically:

_____

_____

_____

_____

_____

_____
Chair

University of California, San Diego

San Diego State University

2013

# DEDICATION

I dedicate this dissertation to the following people:

My wife, Glenda Castro, who supported me before, during and after my graduate studies and beyond (in time and space)….  XOXO….

My daughter, Noemi who is the greatest motivation… and a Big, Big Friend!!!

My parents, Alfredo and Guadalupe for their love and support.

TABLE OF CONTENTS

LIST OF ABBREVIATIONS

| | |
|---|---|
| CP | core particle |
| °C | degrees Celsius |
| 1D | one dimensional |
| 2D | two-dimensional |
| 3D | three-dimensional |
| CD | circular dichroism |
| DTT | Dithiothreitol |
| DUBs | DeUbiquitinating enzymes |
| HSQC | Heteronuclear Single Quantum Coherence |
| IPT | Isopropyl β-D-1-thiogalactopyranoside |
| kD | kilo Dalton |
| L | liter |
| Lys | Lysine |
| MHC I | Major Histocompatibility One |
| MDa | Megadalton |
| NED8 | Neural-precursor-cell-expressed developmentally downregulated protein-8 |
| MHz | megahertz |
| Hz | hertz |
| ml | mililiter |
| msec | milisecond |
| nm | nanometer |

| | |
|---|---|
| NMR | nuclear magnatic resonance |
| ns | nanosecond ` |
| OD | optical density |
| $OD_{600}$ | optical density at 600 nanometers |
| ODC | Ornithine Decarboxylase |
| PAGE | polyacrylamide gel electrophoresis |
| PCR | polymerase chain reaction |
| PDB | protein databank |
| polyUb | poly ubiquitination |
| ppm | parts per million |
| RP | regulatory particle |
| SDS | sodium dodecyl sulfate |
| $T_m$ | melting temperature |
| Tris | tris(Hydroxymethyl) aminomethane |
| Ub | ubiquitin |
| Ub-MonA | ubiquitin monomer A |
| UbA-Mon(Y45A) | ubiquitin monomer A (tyrosine 45 to alanine) |
| Ub-MonB | ubiquiin monomer B |
| Ub-MonB(A45F) | ubiquitin monomer B (alanine 45 to phenylalanine F) |
| Ub-G | ubiquitin protein G |
| Ub-Ub | ubiquitin ubiquitin |
| UbUb-22 | ubiquitin ubiquitin 22-mer |
| UCH-L3 | ubiquitin carboxy hydrolase-L3 |

| | |
|---|---|
| UCHL3-TKT | ubiquitin carboxy hydrolase-L3 insertion mutant (threonine, lysine and threonine) |
| UPS | Ubiquitin Proteasome System |
| UV | ultraviolet spectroscopy |
| μl | microliter |
| μM | micromolar |

LIST OF FIGURES

LIST OF TABLES

ACKNOWLEDGEMENTS

Chapter III and Chapter IV, in part are reprints of the material as appear in Navarro M., Carmody L., Romo O., and Love J. (2013) “Biochemical and biophysical effects of N-terminal monoubiquitination of small proteins”. Manuscript in final stages of preparation.

I thank Dr. Love for his support, his mentoring, scientific input and also for giving me the guided-freedom necessary to pursue my own scientific ideas. I am very grateful for the support of faculty from the Chemistry Department at San Diego State University, especially to Dr. Aileen Knowles, Dr. William Stumph and to Dr. Tom Huxford as well as to Dr. Greg Harris from the Biology Department for their scientific and professional advice and for sharing their own resources. I thank my second family, all the past and current students from the Love’s lab with whom I laughed and learned. Especially I thank Lisa Carmody and Octavio Romo. I would like to thank to my loving, caring and supporting wife Glenda Castro for being supportive during my graduate studies and to our daughter Noemi who makes it all funnier and more meaningful. Also I need to acknowledge my in-laws, Ana and Fred Castro for their great help and for babysitting, educating and entertaining Noemi. I need to express my gratitude to my parents, Alfredo and Guadalupe for bringing me to this planet and of course to my siblings Ernesto, Karina and Alfredo. I need to acknowledge Hélène Citeau, Sharon Ferguson, and Danny Rillera at the University of San Diego for their extensive and always friendly assistance in the use of the CD spectrometer. Finally I thank my sources of funding: Consejo Nacional de Ciencia y Tecnologia (Mexico) and the California Metabolic Research Foundation.

VITA

**Education**

2001 B.S. Clinical Biochemistry
Universidad Autonoma de Baja California. Tijuana BC, Mexico

2004 Ms. Sc. Marine Biotechnology
Centro de Educacion Cientifica y Educacion Superior de Ensenada. Ensenada BC, Mexico

2013 Ph. D., Chemistry,
San Diego State University and University of California, San Diego (Joint Doctoral Program)

**Publication**

Navarro M., Carmody L., Romo O., and Love J. "Biochemical and biophysical effects of N-terminal monoubiquitination of small protein". Manuscript in final stages of preparation.

**Honors and Awards**

2007 Recipient of the Scholarship for Doctoral Students Overseas, National Center for Science and Technology, Mexico.

2009 FASEB MARC Minority Student Travel Award to attend the 23rd Symposium of the Protein Society. Boston, Massachusetts.

2009 Peer Mentor at the Annual Biomedical Research Conference for Minority Students (ABRCMS). FASEB-MARC.

2010 Peer Mentor at the Annual Biomedical Research Conference for Minority Students (ABRCMS). FASEB-MARC.

2010 Recipient of an Arne N. Wick Pre-doctoral Research Fellowship form the California Metabolic Research Foundation.

2011Peer Mentor at the Annual Biomedical Research Conference for Minority Students (ABRCMS). FASEB-MARC.

ABSTRACT OF THE DISSERTATION

Biophysical and Biochemical Effects of Mono-Ubiquitination on Engineered Proteins

by

Mario Fco. Navarro

Doctor of Philosophy in Chemistry

University of California, San Diego, 2013

San Diego State University, 2013

Professor John J. Love, Chair

The integrated efforts of biologists and chemists have resulted in a greater understanding of the function, structure, regulation and biomedical relevance of the ubiquitin-proteasome system (UPS). Ubiquitin, a key and central component of the UPS, is normally described primarily as a molecular tag that directs proteins to the proteasome for the purpose of degradation. Over the past 20 years several authors have speculated on the role ubiquitin possibly plays in triggering substrate unfolding to facilitate target degradation by the proteasome. The overall goal of my thesis project was to provide insights into the potential influence ubiquitin on the biophysical and biochemical properties of proteins to which it is covalently attached.

To achieve this goal we study the more straightforward means by which ubiquitin is attached to target proteins, *i.e.,* N-terminal mono-ubiquitination. By means of rational design we engineered a panel of small test proteins that exhibited variable thermal stabilities. These 'test' proteins were biophysically characterized as stand-alone, 'free' proteins in addition to being characterized as genetic fusions to the C-terminus of ubiquitin. Our results show that the thermal stabilities of the designed variants, both before and after monoubiquitination, are very similar and, more importantly, the addition of ubiquitin at the N-terminus of the test variants did not grossly alter the thermal stabilities of the test proteins.

To investigate the biochemical relevance of mono-ubiquitinated proteins that exhibit variable thermal stabilities we characterized the engineered mono-ubiquitinated substrates in the context of the deubiquitinase Human Carboxy Hydrolase-L3 (UCH-L3). UCH-L3 removes small and unfolded peptide extensions from the C-terminus of ubiquitin. However no systematic analysis has been performed to evaluate the effect of the thermal stability of these extensions beyond their amino acid sequence and size. The hydrolysis assays performed on the engineered ubiquitin fusions demonstrate that differences in thermal stabilities of the proteins attached to ubiquitin greatly affect the capacity of UCH-L3 to process the substrates. Generally, unstable fusions are hydrolyzed at a significantly faster rate relative to stable fusions. Finally, we speculate on how these findings might provide additional insights into the roles that ubiquitin and the enzyme UCH-L3 play in natural systems.

# CHAPTER I
# Introduction

## 1.1 Protein Degradation: A Historical Perspective

Intracellular protein degradation is not a random process but instead an exquisitely controlled cellular event that enables cells to respond to different metabolic needs and to adapt to their ever changing environment [1]. Important examples that exemplify the necessity for regulated protein degradation include the removal of misfolded proteins to avoid toxicity, the termination of signaling cascades for cell communication, and antigen processing during the adaptive immune response [2, 3]. Although the significance of these processes was recognized early on, the molecular details remained obscure for a long time. The molecular mechanisms that provide some proteins with a half-life of minutes and others with that of days were not well appreciated at the time and studies of how proteins are produced rather than how these are destroyed were favored [4]. This changed with the serendipitous discovery of the lysosome in 1956 by de Duve and his findings twelve years later that this cell structure played a role in protein degradation [4] . It was not until 1977, however, when Poole established the lysosome as the primary cell component for degradation of proteins of extracellular origin [5, 6]. Moreover, by utilizing lysosome specific drugs (lysosomotropics), Poole concluded that these drugs inhibited only degradation of extracellular but not intracellular proteins, speculating on the existence of a non-lysosomal system for the degradation of intracellular proteins [6]. This hypothesis was supported by the observation that reticulocytes, cells that lack lysosomes, still performed protein degradation. Notably, in 1977 Goldberg used rabbit reticulocytes to establish the occurrence of a soluble, ATP

dependent, non-lysosomal proteolytic system capable of degrading polypeptides in a cell-free extract with rates that paralleled those obtained in whole cells [7]. Concomitantly, in 1978 Ciechanover described a polypeptide component of this system with remarkable heat-stability named ATP-dependent proteolysis factor 1 (APF-1) [8]. Two years later Wilkinson positively identified that APF-1 as a small protein named ubiquitin [9].

### 1.2 The Ubiquitin-Proteasome System: The Canonical View

The elucidation of the non-lysosomal system required for degradation of intracellular proteins was initiated in the late 1970's [10]. This intricate system, termed the ubiquitin-proteasome (UPS) is composed of several structural proteins plus other functional elements (Figure 1-1). The functional involvements of the UPS extend beyond protein degradation to maintain the amino acid pool as initially thought since is also relevant in regulation of signaling pathways, cell cycle progression, DNA repair and apoptosis [11, 12, 13]. The importance of the proteasome is perhaps better illustrated in diseases in which some of its components malfunction leading to several forms of cancer, aging, obesity and degenerative diseases such as Parkinson's disease [14, 15, 16,17].

*Ubiquitin.* One of the first elements of the UPS to be described was ubiquitin, a highly conserved, ubiquitous small protein of 76 amino acids with a molecular weight of 8.5 kDa and encoded by a multigene family [19, 20]. Initial studies regarded ubiquitin to be just a "tag" to signal protein degradation when was covalently attached to lysine residues in target proteins, earning the ignominious label of "The kiss of death" [21, 22]. However, this small molecule is now known to be engaged in multiple biological roles that should not be considered as secondary to protein degradation (see below).

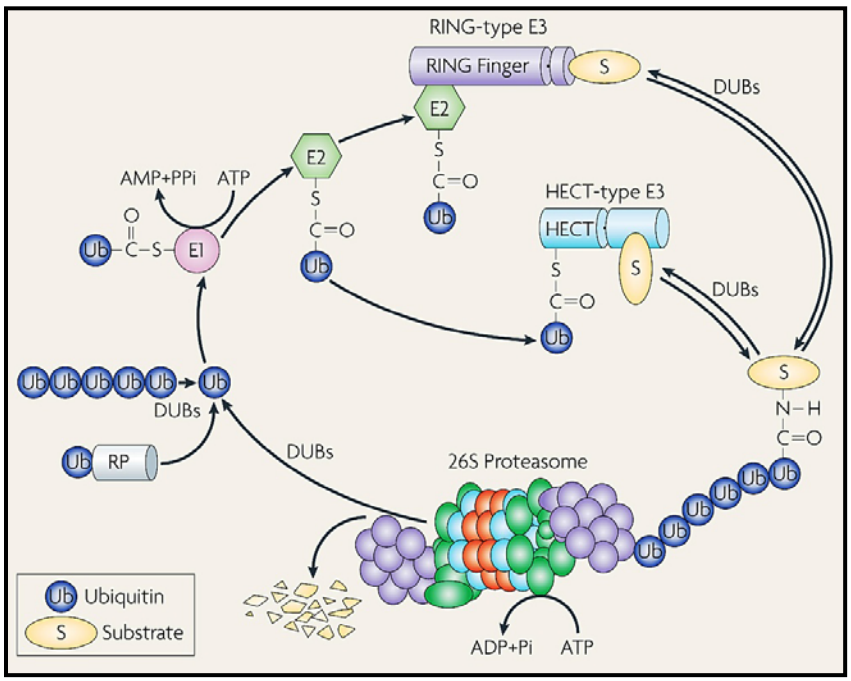


**Figure 1.1.** The ubiquitin-proteasome system (UPS). Multiple structural and functional elements coordinate to degrade intracellular proteins in a timely, specific and rapid fashion. First, activated ubiquitin is transferred to the target substrate (substrate tagging), then polyubiquination occurs and finally the substrate is degraded in a sequential manner. DUBs deubiquitinases, RP regulatory particle. Further details provided in the text [modified from 18].

*The Proteasome.* This protein complex, located in the cytosol and the nucleus, constitutes up to 2% of cell mass and is better defined as a large multicatalytic, 26S protease that degrades polyubiquitylated proteins to produce small peptides. The 26S proteasome is composed of one 20S core particle (CP) plus one or two 19S regulatory particles (RP) for a total molecular mass of approximately 2.5 MDa. The 20S CP is shaped like a barrel assembled by a stack of two inner rings (β-rings) and two outer rings (α-rings), each one composed of seven subunits that form a central channel (Figure 1-2). Catalysis within the proteasome is provided by three subunits in each β-ring, for a total of six proteolytic active sites per proteasome while the α-rings regulate the entry of substrates prior to catalysis [3, 23]. The 19S RP, on the other hand, can be dissected into

two stable subcomplexes; a lid composed of eight subunits and a base formed by nine subunits. The RP is a multifunctional element composed of six subunits with ATPase activity (Rpt1-6) that gate the entrance to the degradation channel and participate in substrate recognition, unfolding and translocation into the 20S core particle [3, 23, 24, 25].

*Proteasomal Degradation.* Degradation of proteins through the UPS requires energy in the form of ATP and involves two phases: 1) covalent attachment of multiple ubiquitin units to the target protein (tagging) and 2) degradation of the tagged protein through the 26S proteasome to generate free ubiquitin and small peptides, both of which can be recycled afterwards (Figure 1-1) [4, 11].

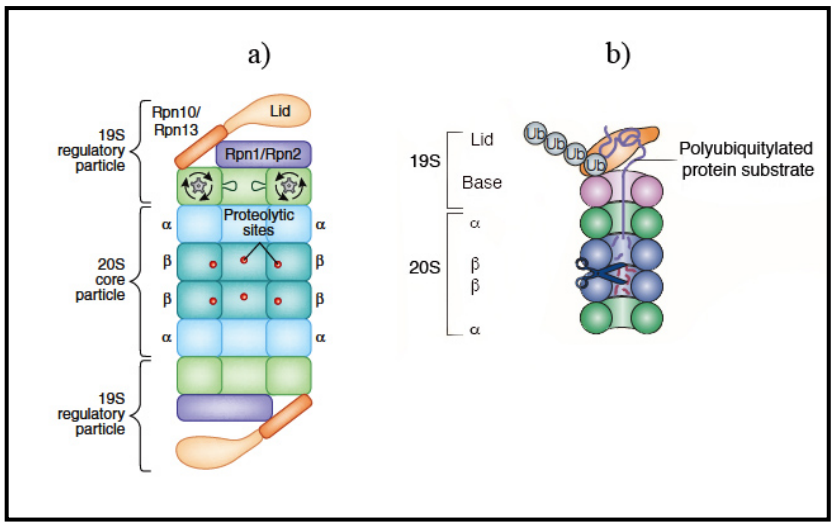


**Figure 1.2.** Structural and functional components of the eukaryotic 26S proteasome. a) The 26S proteasome with its multiple structural elements, the regulatory particle and the core particle. Rpn 10/13 are regarded as ubiquitin receptors and Rpn1/2 function as scaffold proteins. b) Depiction of unfolded polyubiquitylated substrate as it travels through the proteasome where proteolysis occurs as indicated by scissors [3, 23].

In the first phase, tagging of target proteins by ubiquitin is accomplished in three consecutive steps catalyzed by enzymes E1 (activator), E2 (carrier) and E3 (ligase).

During the ligation step, one of three types of E3 ligases may come into play; RING-type (most of the cases), U-box-type and HECT-type. RING-type and U-box-type ligases serve as scaffolds that bring E2 and the target protein in close proximity, enabling the direct transfer of ubiquitin, while HECT-type ligases transfer ubiquitin from E2 to itself prior to its conjugation to the target (Fig. 1.1) [4, 6, 18, 26, 27]. Whether conjugation of the first ubiquitin molecule to the target occurs via a RING, U-box-type or HECT-type ligases the vast majority of examples described report that an isopeptide bond is formed between the carboxy-terminal of Gly76 in ubiquitin and the ε-amino group of an internal lysine in the target protein [28]. Once the first ubiquitin moiety is added to the target, ubiquitin polymerization with the assistance of the elongation factor E4 is necessary. Specifically, the C terminus of the incoming molecule is attached to the ε-amino group of an internal lysine (*e.g.* Lys48) in the previously attached ubiquitin moiety [29]. The second phase of the proteasomal degradation takes place in a series of successive events defined as follows: 1) ubiquitin recognition 2) substrate binding 3) deubiquitination 4) unfolding and translocation of the substrate and ultimately 5) proteolysis.

### 1.3 Ubiquitination

*Ubiquitin, One Molecule Several Possibilities.* While protein degradation through the UPS is the best characterized and perhaps the most dominating role of ubiquitin, this post-translational modification is also involved in other molecular and cellular events such as enzyme regulation, endocytosis, transcriptional regulation, nuclear transport and DNA repair [30, 31, 32]. A logical question at this point is as follows: how can a single molecule be involved in such diverse functions? The complex diversity of the

ubiquitination reactions may bring reasonable insights. Three elements contributing to such diversity are: the number of ubiquitin molecules polymerized, the lysine residue in ubiquitin used for addition of extra moieties, and the type of amino acid in the target protein where direct attachment of ubiquitin occurs.

*Number of Ubiquitin Molecules Polymerized.* The extent of ubiquitin polymerization has decidedly profound effects on the destiny of a protein. Two broad categories can be considered: monoubiquitination and polyubiquitination. Monoubiquitination, which is the addition of a single ubiquitin moiety to a protein, may result in endocytosis, transcriptional regulation and budding of retroviruses [30, 33, 34]. Regulation of gene transcription can be achieved by monoubiquitination of histones, providing both positive and negative effects depending on particular examples, although other mechanisms are possible [34]. An interesting case is that of p53, a tumor suppressor which on one hand, undergoes monoubiquitination when levels of Mdm2 (an E3 ligase) are low, resulting in its nuclear export, but on the other hand, if levels of Mdm2 are high, p53 is polyubiquitinated and undergoes nuclear degradation. The physiological significance of these two types of modifications are possibly complementary; monoubiquitination provides a fast, transient and energy efficient mechanism for down regulation, while polyubiquitination represents a higher energy-cost alternative but also a more definitive mechanism to down regulate the activity of p53 [34, 35]. Interestingly enough, multiple-monoubiquitination in which single ubiquitin units are attached to proteins on multiple sites has also been shown to occur. Two examples of this type of modification are provided by receptor tyrosine kinases (RTKs) such as the epidermal growth factor receptor (EGFR) and the platelet-derived growth factor receptor

(PDGFR) that are degraded upon multiple-monoubiquitination [36]. On the other hand, polyubiquitination has been introduced earlier and, as described, this type of ubiquitination is frequently associated with proteasomal degradation.

*Lysine Residue in Ubiquitin Used for Polymerization*. There are seven lysine residues in ubiquitin: Lys6, Lys11, Lys27, Lys29, Lys33, Lys48 and Lys63. Out of these seven, Lys48 is the most common residue associated with protein degradation by the UPS [1, 37], yet ubiquitin polymerization occurs not only through Lys48. Several reports provide evidence that the other Lys residues are also positions for ubiquitin condensation [38, 39]. Figure 1-3 illustrates the positions of all seven Lys residues in ubiquitin together with their putative biological roles. Most notably, polyubiquitination, where the initial point of attachment is Lys29, results in degradation mediated through the lysosome and not through the proteasome [40, 41].

*Type of Amino Acid in the Target Protein where Attachment of Ubiquitin Occurs.* Several laboratories have confirmed that, in addition to the side chain of lysine, other points of covalent attachment provide the necessary chemistry to react with the C-terminus of ubiquitin. For example, its C-terminus can also react with the sulfhydryl group (–SH) of cysteine (Cys) and the hydroxyl group (–OH) of serine (Ser) and threonine (Thr) side chains. The most studied example of this type of ubiquitination is in fact a particular viral strategy aimed to block the detection of virally-infected cells by the immune system. Key players here are the E3 ligases kK3 and kK5 from the Kaposi's sarcoma-associated herpesvirus and the ligase mK3 from the murine γ-herpes virus 68 (HV68) [38, 39]. kK3 and kK5 promote ubiquitination of the major histocompatibility complex class I heavy chain (MHC I) on Cys or Lys while mK3 ubiquitinates Ser, Thr or

Lys. In both cases degradation of ubiquitinated MHC I is the end result. However, kK3 and kK5 induce rapid endocytosis and degradation in the lysosome whereas mK3 promotes endoplasmic reticulum associated protein degradation (ERAD) [42, 43, 44].

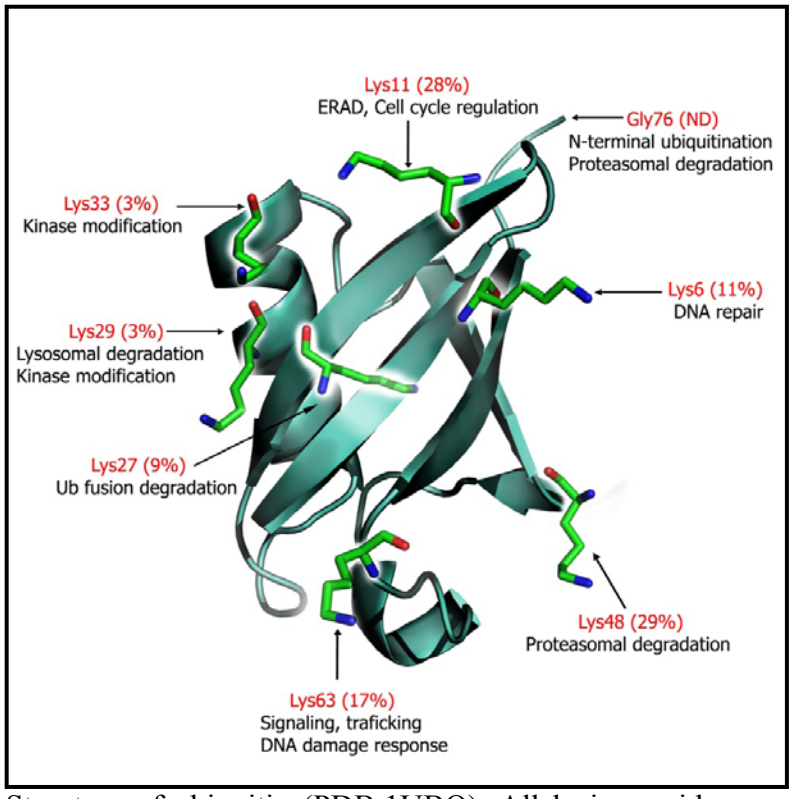


**Figure 1.3.** Structure of ubiquitin (PDB:1UBQ). All lysine residues used in ubiquitin polymerization are indicated in red and known biological relevance in black. Percentage indicates relative abundance of the particular linkage in *S. cerevisiae* [modified from 38].

Of special interest for the work presented in this thesis is N-terminal ubiquitination (N-tUb), which is the covalent addition of a polyubiquitin chain to the α-NH2 group in the N-terminal residue of certain proteins. N-tUb, is a post-translational modification that should be differentiated from a form of ubiquitination in which certain proteins are translated as in-frame fusions to the C-terminus of ubiquitin [45, 46]. Two examples that fall in this distinction are ribosomal proteins in yeast and rat [45, 46]. The

production of these fusion proteins seems to assist in ribosome biogenesis, attributing a role to ubiquitin in which it possibly functions as a “chaperone”.

N-tUb was first described during studies of the rapid turnover of MyoD; a transcriptional activator engaged in muscle development [47]. Degradation of MyoD was established to require ubiquitin and the proteasome however, when all nine lysine residues were mutated to arginine (thus preventing standard ubiquitination) MyoD was still degraded efficiently in a ubiquitin and proteasome dependent manner [47]. Accordingly, blocking of the N-terminus by carbamylation in wt MyoD and in the lysine-less mutant resulted in stabilization of these constructs. Following this report, other proteins were also proposed to be naturally ubiquitinated at the N-terminus and thereafter degraded by the UPS. Among these were the Latent Membrane Protein 1 (LMP1) from the Epstein-Barr virus, the Early 7 protein (E7) from the human papilomavirus and the cyclin kinase Inhibitor p21 [48, 49, 50]. However, the evidence provided to support the existence of N-tUb, was indirect. The data demonstrated 1) stabilization of constructs upon N-terminal blockage, 2) *in vitro* proteasome-mediated degradation of N-terminally ubiquitinated substrates that were generated synthetically and 3) absence of degradation of these synthetic substrates when the proteasome was inhibited.

Direct evidence for the occurrence of N-terminal ubiquitination was provided independently by two groups when peptides formed between C-terminal residues of ubiquitin and N-terminal residues of the extracellular signal-regulated kinase 3 (ERK3), p21 and E7 were detected by mass spectrometry [51, 52]. The identification of these ubiquitin conjugates offered unequivocal verification on the natural occurrence N-tUb.

Our understanding of N-tUb is far from complete, however some of the key features are now beginning to be elucidated. One of these elements is a large 600 kDa system responsible for the assembly of a linear head to tail polyubiquitin chain, the Linear Ubiquitin Chain Assembly Complex (LUBAC). The most prominent attribute of this complex is that upon recognition of ubiquitin moieties conjugated to proteins (either N-terminally or to internal Lys residues), LUBAC adds additional ubiquitin molecules in a linear fashion (C- to N- terminal) which may function as a degradation signal or as a docking signal for the recruitment and binding of different components of signaling pathways [53, 54]. Moreover, proteasomal degradation of N-terminally ubiquitinated substrates has been shown to also be stimulated through the Ubiquitin Fusion Degradation pathway (UFD), in which the N-terminal ubiquitin moiety of a substrate is ubiquitinated at Lys29 and Lys48 by a specific enzymatic system of ubiquitin ligases (UFD4 and UFD2) [53, 55]. The biological significance of N-tUb is now beginning to be uncovered as proteins undergoing this form of ubiquitination, and subsequent proteasomal degradation, have been found to participate directly in processes such as viral infection, oncogenisis, cell cycle regulation, tumor suppression, apoptosis and cell differentiation [48, 49, 50, 51, 56, 57].

*Does Ubiquitin Function Solely as a Molecular Tag?* Based on the application of various biochemical tools and structural biology methods, the fundamentals of the UPS, in the context of biology and disease, have begun to be better understood. Consequently, defined functions are now attributed to precise players (*e.g.* ubiquitination by ligases or protein degradation by the proteasome) and events have been explicitly defined in time and space (*e.g.* ubiquitination of RTKs in cytosolic domains, internalization, fusion to

lysosomes and degradation) [4, 58]. In addition, some authors suggest that ubiquitin not only acts as a molecular tag, but it also may modify the biophysical properties of certain proteins. The attached ubiquitin moiety may, in part, function to decrease the structural stability of the target protein by partially unfolding it, and thus further preparing it for subsequent degradation via the proteasome [59]. Modulation of the biophysical properties of proteins by covalent modifications has been studied most widely with respect to phosphorylation and glycosylation. Phosphorylation introduces two negative charges in any of five amino acids: Ser, Thr, Tyr, His and Asp. In the particular case of protein kinases, phosphorylation induces a conformational change that allows the formation of the substrate-binding site, and the alignment of catalytic residues or those involved in metal coordination [60, 61, 62]. Molecular dynamic (MD) simulations of peptide fragments indicate that phosphorylation may increase local structural ordering. Two examples are the cAMP response element-binding domain (CREB) and the smooth muscle myosin regulatory light chain (RLC), the phosphorylation of which results in increased helical content [61]. Glycosylation is a more diverse protein modification in which several of thirteen carbohydrates may be attached to any of eight amino acids: Asn, Arg, Ser, Trp, Thr, Tyr, Hyl (hydroxylysine) and Hyp (hydroxyproline) [63]. Some forms of glycosylation occur during protein synthesis as the unfolded protein is being translocated into the endoplasmic reticulum while other forms occur after protein synthesis is complete and the protein is fully folded. The complexity of the sugar moieties (glycans) varies in both monosaccharide composition as well as size [64]. In some cases, this form of post-translation modification has been shown to enhance protein thermal stability and assist in the kinetics of folding [64].

Whereas the concept that ubiquitin may facilitate protein unfolding to aid protein degradation is intuitively attractive, evidence supporting this notion is currently somewhat scarce [59]. In an attempt to gain insight into this phenomenon *in silico* techniques have been applied to assess the effect of ubiquitination on protein stability and folding [65]. This study was performed on proteins modified by one of several forms of ubiquitination (monoubiquitination, at Lys48 as well as Lys63-linked tetraubiquitination). Although these computer simulations indicate a complex scenario, the results show that 1) monoubiquitination had the least effect on the target protein's stability, 2) Lys63-mediated tetraubiquitination had an increased effect and 3) tetraubiquitination at position Lys48 resulted in considerable thermal destabilization and strong local unwinding [65]. From a functional perspective, the lower stability and increased protein unfolding induced by Lys48-linked polyubiquitination are consistent with the outcome most commonly attributed to this form of ubiquitination: protein degradation through the UPS [65]. The minimal effect induced by monoubiquitination revealed by this *in silico* approach has been expanded recently in the study of the mono-ubiquitinated proliferating cell nuclear antigen (PCNA), a sliding-clamp processivity factor involved in DNA replication [66]. It has been demonstrated that, *in vivo*, PCNA is ubiquitinated at position Lys164, however obtaining appreciable amounts of ubiquitinated PCNA ($^{Ubi}$PCNA) hampered further characterization. A strategy to overcome this limitation was to split PCNA into two polypeptides: an N-terminal portion ($PCN_{1-163}$) and an N-terminally ubiquitinated C-terminal portion (Ub-$PCN_{165-258}$). Functional assays demonstrated that these two polypeptides self-assembled into a functional $^{Ubi}$PCNA trimer, capable of stimulating DNA polymerazation. More importantly, an overlay between the structures of

the intact non-ubiquitinated PCNA and that of the split $^{Ubi}$PCNA showed that ubiquitin produced minimal structural effects (r.m.s. 0.6 Å) [66].

Beyond the direct effect that ubiquitin may exert on proteins, an indirect role in protein degradation is plausible; proteins targeted for proteasomal degradation may be retained at the proteasome where ubiquitin acts as a tether, positioning substrates to be unfolded at the RP in an ATP-dependent mechanism [67].

### 1.4 Deubiquitination and Deubiquitinases

Details concerning ubiquitination by ligases, such as the sequential reactions, biochemical mechanisms, targeted molecules, and types of linkages formed are now fairly well characterized. On the other hand, deubiquitination is less well understood. Ubiquitination and deubiquitination are dynamic and reversible processes that involve multiple enzymes such as the ligases discussed above and a class of enzymes termed deUbiquitinases (DUBs). These enzymes function to remove ubiquitin from proteins that have been post-translationally modified by ligases as well as from proteins that are produced as N-terminal genetic fusions to ubiquitin (Fig. 1.4). Some of the reactions in which DUBs participate are: 1) release of monomeric ubiquitin from a polyubiquitin precursor or from premature ubiquitinated ribosomal proteins, 2) release of ubiquitin from small cellular nucleophiles that it may react with (*e.g.*, glutathione), 3) removal of regulatory ubiquitin, 4) removal of polyubiquitin chains from substrates of the 26S proteasome and 5) amendment of inappropriately ubiquitinated proteins [68, 69]. Biologically, deubiquitination is not just the counterbalance of ubiquitination but is also

known to be important for cell cycle regulation, proteasome and lysosome dependent protein degradation, gene expression, kinase activation, and DNA repair [70].

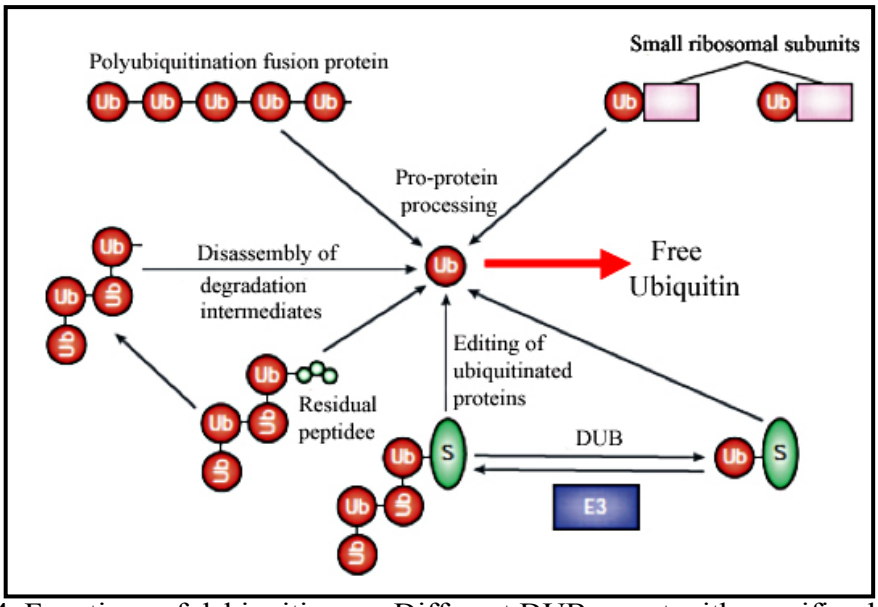


**Figure 1.4.** Functions of debiquitinases. Different DUBs react with specific ubiquitinated proteins in several biological contexts, generating free ubiquitin molecules that can be used in subsequent ubiquitination reactions [modified from 69].

*The Ubiquitin Carboxy Terminal Hydrolase Family*. The human genome encodes ~100 DUBs that remove not only ubiquitin but also ubiquitin-like proteins and are classified into five families: 1) ubiquitin C-terminal hydrolases (UCH) 2) the ubiquitin specific protease (USP/UBP) 3) the ovarian tumor domain (OUT) 4) the Josephin domain, and 5) the JAB1/MPN/Moc34 metalloenzyme (JAMM) [70, 71].

The first four families are cysteine proteases while the last is a zinc-dependent metalloprotease. Of particular interest for our work is the human UCH family composed of four isozymes: UCH-L1, UCH-L3, BP1 and UCH37 (formerly known as UCH-L5). In turn, the UCH family is grouped in two subsets; enzymes that contain just the globular

UCH fold like UCH-L1 and UCH-L3 and the group in which enzymes have an additional C-terminal extension, exemplified by BAP1 and UCH37 [70, 72]. The catalytic core of the members of the UCH family is formed by ~230 amino acids with a fold, a catalytic triad geometry, as well as an oxyanion hole similar to that of papain [70].

The catalytic triad consists of three amino acids: Cys, His and Asp that react with the substrate using a catalytic mechanism comparable to that described for papain [28]. One of the primary features of the mechanism of cysteine proteases is the formation of a covalent intermediate, the acyl-enzyme complex that results from the nucleophilic attack of the active site thiol group on the carbonyl carbon of the scissile peptide bond on the substrate (Figure 1.5). In the subsequent step, a first product, the C-terminal portion of the peptide substrate is released to generate a second acyl-enzyme species that reacts with a water molecule to form the second product, ubiquitin. Upon releasing of this second product, the free enzyme is also generated [73].

Although UCHs are clearly identified as enzymes that remove ubiquitin, their specific functions *in vivo* still remain poorly defined. Some of the possible activities assigned to UCHs are recycling of ubiquitin conjugated inappropriately to small molecule (*e.g.* glutathione or polyamines) and processing of newly synthesized ubiquitin translated as polyubiquitin [71].

In addition, results from *in vitro* experiments imply other potential activities for UCHs: removal of ubiquitin from N-terminal linear fusions and removal of ubiquitin conjugated to small peptides through isopeptide bonds formed with lysine [28].

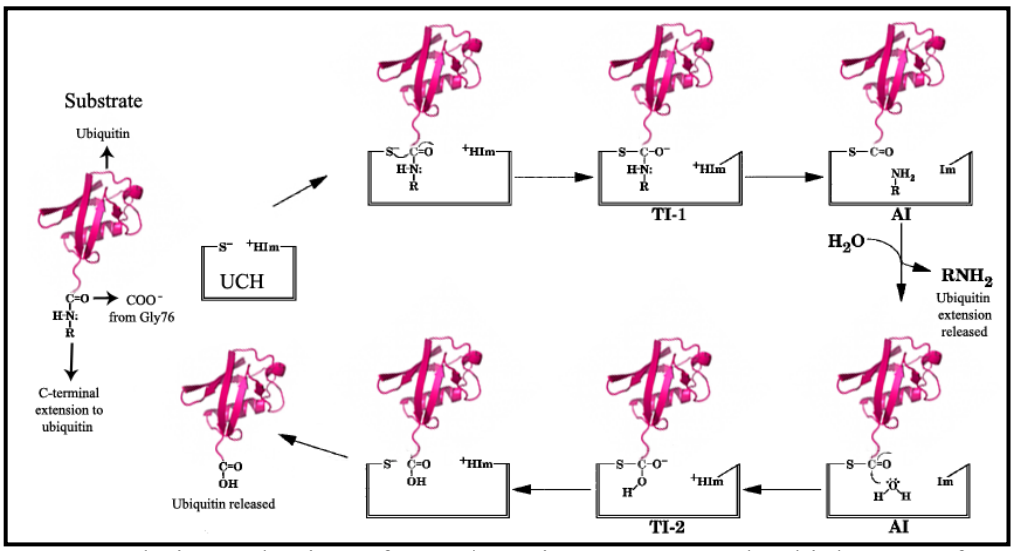


**Figure 1.5.** Catalytic mechanism of UCH/cysteine proteases. The thiol group of cysteine first attacks the carbonyl group of Gly76 in ubiquitin to form a tetrahedral intermediate. Next, an acyl-enzyme complex is generated and the first product, the molecule fused C-terminally to ubiquitin, is released. Finally, the acyl-enzyme complex reacts with a water molecule to release the second product, free ubiquitin. Substrate: Ubiquitin N-terminal fusion; $S^-$, from cysteine thiol; $^+$Him, imidazole from histidine; AI, Acyl intermediate; TI-1 and TI-2, high energy tetrahedral intermediates [modified from 74].

An exception to the UCH enzymes with poorly defined *in vivo* substrates is UCH37, the only member found in complex with the proteasome. This complex occurs through the interaction of the C-terminal domain of UCH37 and the C-terminal domain of the Adrm1 lid subunit localized in the 19S RP [70]. Deubiquitination by UCH37 occurs at the distal end of the polyubiquitin chains to disassemble ubiquitin chains polymerized through Lys6, Lys11 and Lys48. However, UCH37 can only process α-linked diUbiquitin when in complex with the whole 19S RP [75]. The isopeptidase activity of full-length UCH37 is rather low, yet an increment of one to two orders of magnitude is experienced by this hydrolase upon interacting with Adrm, a ubiquitin receptor located on the proteasome [72, 75]. This is explained by virtue of the interaction between the C-terminal extension of UCH37 and the C-terminal portion of Adrm1,

resulting in relief of the autoinhibition of UCH37 as demonstrated by the catalysis of ubiquitin-7-amido-4-methylcoumarin (Ub-AMC) a model fluorescent substrate in DUBs research [76].

The biochemical properties of UCH37 are hypothesized to result in different, yet antagonizing biological outcomes. First, it has been suggested that UCH37 has a negative effect in protein degradation, thus functioning as a down regulator. Studies show that UCH37 inhibits degradation of ubiquitinated proteins; presumably, removal of ubiquitin rescues proteins from being channeled into the proteasome. As a consequence, depletion of UCH37 leads to a decrease in the levels of cellular polyubiquitinated substrates. Second, UCH37 seems to specifically facilitate the destruction of some proteins at the proteasome such as the inducible nitric oxide synthase and IκB-α [72].

*Ubiquitin Carboxy Terminal L3*. The most studied members of the UCH family are the isozymes 1 and 3 that exhibit specific tissue distribution. Expression of UCH-L1 is confined to neurons, testis and ovaries while expression of UCH-L3 is more ubiquitous and is found in hematopoietic cells, testis, heart kidney, liver and muscle [28, 77, 78]. Concomitant with the different expression patterns, these two enzymes are observed to be involved in different pathologies. UCH-L1 is a highly abundant protein in the brain (1-2%) hence its involvement on a neurological disorder is not surprising. A point mutation in UCH-L1 (I93M) is linked to Parkinson's disease (PD) and results in partial loss of its hydrolytic activity [79]. In addition to this, a loss in the activity of UCH-L1 was also observed under a different circumstance, from which lessons in molecular biology and biochemistry were learned. *In vitro* experiments demonstrated that, as a function of concentration, UCH-L1 displays two different enzymatic activities. At low

concentrations UCH-L1 is a monomer that acts as a ubiquitin hydrolase. On the other hand, when its concentration is increased, UCH-L1 dimerizes and functions as a ubiquitin ligase [79, 80]. These findings challenge the paradigm of one gene, one protein since the same gene gives rise to two proteins with two opposing catalytic activities: a deubiquitinase and a ubiquitin ligase. An interesting biological effect under investigation is the apparent correlation between the decrease or loss of activity of UCH-L1 and the accumulation of the protein α-synuclein (that above a threshold concentration forms pathogenic aggregates known as protofibrils) [79].

In addition to the role UCH-L1 may play in neurodegenerative diseases both UCH-L1 and UCH-L3 have been evaluated for possible links to cancer and for their potential as biological markers for diagnosis and prognosis. High expression levels of UCH-L1 and UCH-L3 have been detected in several forms of cancer that affect various organs and tissues such as the esophagus, thyroid, colon, breast, leukemia and pancreas among others [78, 81]. A relevant finding is the presence of autoantibodies against UCH-L3 in patients suffering from colon cancer [81]. This is a particularly intriguing discovery because it is the wild type form of the enzyme and not the product of a mutated gene that the antibodies recognize. This observation indicated that detection of autoantibodies against UCH-L3 may be useful in early cancer detection [81].

The biochemical characterization of UCH-L1 and UCH-L3 developed in parallel and, in general, these two enzymes process ε-linked amide bonds at the C-terminus of ubiquitin, peptides α-linked to the C-terminus of ubiquitin, in addition to thioesters and amide-linked adducts [68]. The sequence identity between UCH-L1 and UCH-L3 is 52%, yet the enzymatic activities of these enzymes, as determined *in vitro*, are considerably

different. UCH-L3 is 200-fold more active when its hydrolytic activities are characterized using the non-native substrate ubiquitin-AMC [79]. In addition to this difference, UCH-L3 is more amenable to experimental settings given its higher solubility, enabling a more extensive analysis [28]. The structure of UCH-L3 resembles that of members of the papain-like family of cysteine proteases, specifically in regards to the catalytic triad in the active site (formed by Cys95, His169 and Asp184) and the oxyanion hole residue Gln89 [68]. Conversely, the most prominent differences are strand and helix connectivity as well as a 20 amino acid loop (residues 147 to166) that lacked defined electron density in the crystal structure due to its flexibility and disordered character [68]. At the moment, the significance of this loop could only be speculated. The Initial argument proposed that the loop was positioned over the active site to define substrate specificity by blocking access to large substrates. Evidence to support this argument was obtained latter when the structure of the only UCH from yeast, ubiquitin hydrolase 1 (YUH) was solved in complex with a ubiquitin-aldehyde inhibitor. YUH posses a low 33% identity with UCH-L3, yet, YUH1 also contains a 21 amino acid disordered loop (residues 144-164) [74]. The loops from these enzymes share 28% identity and are referred to as the 'active-site-crossover loop' that undergoes a dramatic conformational change, transitioning from a disordered structure to pass directly on top of the active site when YUH1 is bound to the inhibitor [74].

In order to examine the crossover loop in greater detail, a structural comparison of the free enzyme and the enzyme in complex with a substrate was sought. This comparison was enabled when the structure of UCH-L3 was solved in complex with a suicide substrate, ubiquitin vinylmethylester (Ub-VME), which irreversibly blocks

further cycles of catalysis by UCH-L3 [82]. The structure of this complex revealed the occurrence of a large structural rearrangement of the crossover loop into a helix (residues 142-154) followed by an S-shaped loop (residues 155-167) that crosses over the active site of the enzyme (Fig. 1.6). Even though the structure of the crossover loop was solved in the catalytically competent form of the enzyme, its function to restrict the size of the substrate or to assist its proper positioning for catalysis was not verified experimentally and was only a matter of speculation.

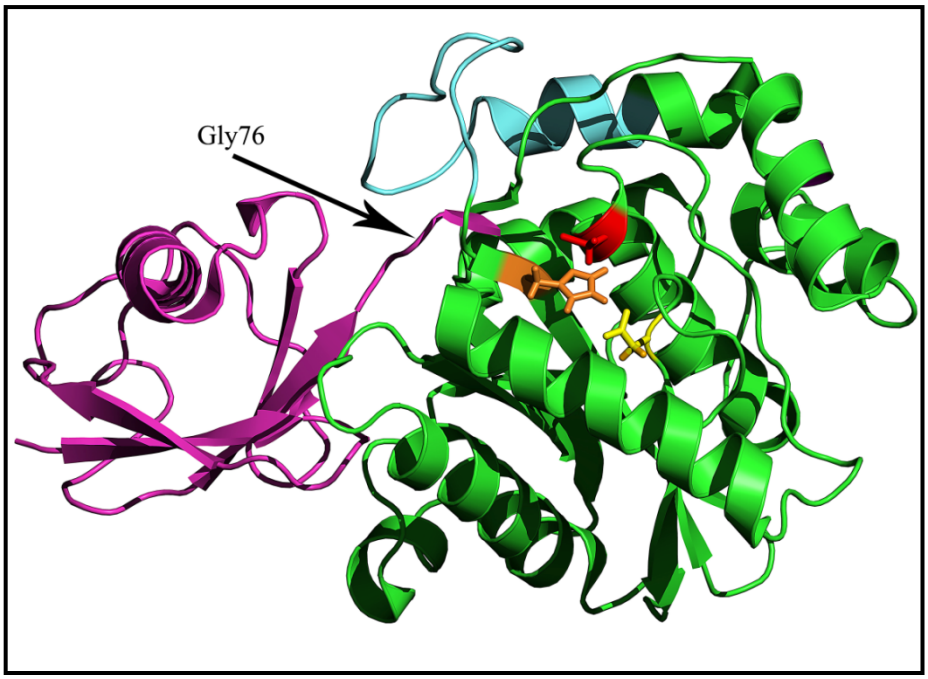


**Figure 1.6.** Structure of UCH-L3 in complex with suicide substrate, Ub-VME. Ubiquitin (dark pink) interacts with UCH-L3 (green) to bring the C-terminal extensions directly attached to Gly76 in proximity to the residues that form the active site: Cys95 (red), His169 (orange) and Asp 184 (yellow). A disordered crossover loop (teal) rearranges partially into a helix when UCH-L3 is bound to the substrate (PDB: 1XD3 ).

Recently Popp *et al.* used "sortagging," a chemical biology technique, to provide further understanding of the biophysical properties of the crossover loop [83]. By using

this approach the backbone connectivity of the crossover loop to the C-terminal half of the enzyme was interrupted upon cleavage with a site-specific sortase enzyme. The authors reasoned that the speculated substrate size limitation conferred by the loop could be relieved upon cleavage, and this would allow larger substrates to be hydrolyzed. Certainly, Lys63-linked diUbiquitin is not a substrate for wild type UCH-L3, however it was processed by the sortase-cleaved UCH-L3, rendering monomeric ubiquitin [83]. To further explore the concept that the crossover loop restricts the size of the leaving group that can be processed by UCH-L3, a series of consecutive glycine residues were added C-terminally to the loop. In doing so, the authors found that extension of the loop with 5 glycine residues enabled hydrolysis of both Lys63 and Lys48-linked diUbiquitin, but required prior sortase cleavage first. Processing of these same substrates improved when the loop contained a longer, 10 glycine residue extension while no hydrolysis was detected with wild type UCH-L3 [83].

In spite of the research on human UCH-L3, a conclusive *in vivo* substrate remains to be identified. *In vitro* experiments have established a preference of this enzyme for cleaving small and unfolded amino acid extensions off the C-terminal of ubiquitin. Surprisingly, the mouse orthologue of UCH-L3 has been strongly implicated in deubiquitination of the membrane bound epithelial sodium channel (ENaC). ENaC participates in regulation of salt and fluid homeostasis, and its concentration in the cell membrane is regulated by endocytosis, mediated in turn by ubiquitination [84]. When cultured kidney cells isolated from mice were treated with a small molecule inhibitor of UCH-L3, increased accumulation of ubiquitinated ENaC was observed, leading to its removal from the membranes by endocytosis [85]. This same effect was observed when

expression of UCH-L3 was reduced by means of siRNA knockdown. Whether the activity of UCH-L3 was reduced by the use of an inhibitor or by siRNA knockdown, increased ubiquitination of ENaC was not followed by its degradation but instead, endocytosis and later recycling back to the membrane of apical cells was detected [85].

From this study, UCH-L3 is attributed a role that has not been described before, participating as a key regulator in the dynamics of ion channel population in cell membranes [85]. An important consideration emerging from this study is the possibility of identifying a physiological involvement for UCH-L3 given the high amino acid identity of 96% between the mouse and human UCH-L3. Engagement of mouse UCH-L3 in processing a large, folded protein such as an ion channel represents a contradiction to the general understanding that UCH-L3 preferentially processes small molecules attached to ubiquitin. This development would also question the idea of the crossover loop serves as a filter for the size of the substrate to be processed. Expectedly, from the biophysical and biochemical body of knowledge generated thus far no viable explanation can still be formulated.

*Bispecific Properties of UCH-L3*. The compact fold of ubiquitin consists of two α-helices and five β-strands arranged in a ββαββαβ orientation that forms a structural motif termed the β-grasp. This fold is also present in a number of molecules that constitute the ubiquitin-like (Ubl) family of proteins [86]. The common traits of Ubl-proteins or ubiquitons, are their relative low molecular weight, low or absent sequence identity with ubiquitin (10-58%) and the most prominent feature, the ubiquitin fold (Fig. 1-7) [87].

In humans, at least 12 ubiquitons have been described to date. Examples of these include a protein named SUMO (Small Ubiquitin-like Modifier), associated with transcriptional repression; FAT10 implicated in cell cycle regulation and the neuronal-precursor-cell-expressed developmentally downregulated protein-8 (NEDD8) [87, 88, 89].

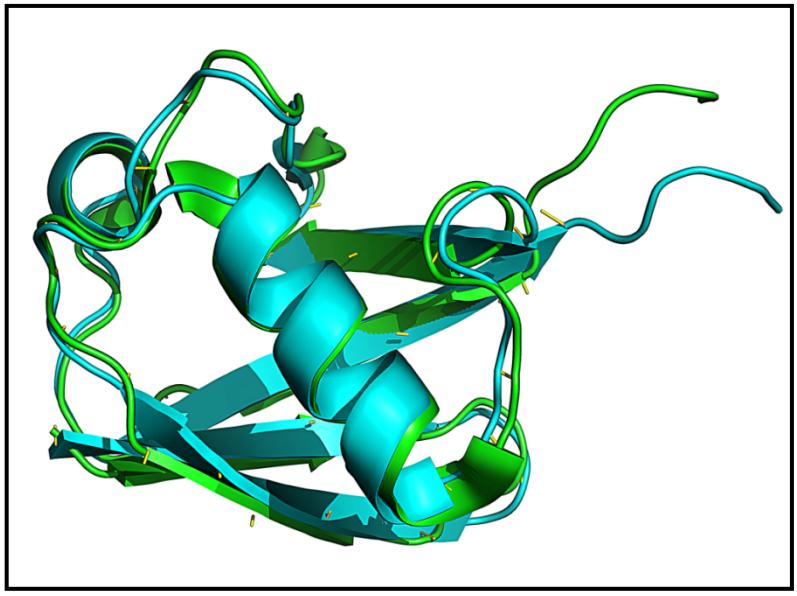

**Figure 1.7**. Members of the Ubl-family of proteins contain the ubiquitin fold. The structural features of NEDD8 (teal, PDB: 2KO3) and ubiquitin (green, PDB: 1UBQ) are shown, revealing their highly similar secondary structure (RMSD value of 0.7 Å).

NEDD8 is synthesized as an 81 amino acid pro-peptide that is processed by UCH-L3 to generate a mature 76 amino acid protein with 68% identity to ubiquitin [87, 90]. Since the last four residues of ubiquitin and NEDD8 are identical (Leu-Arg-Gly-Gly) and the global fold between these two proteins is similar (Fig 1.7), is not surprising that UCH-L3 displays dual specificity since this enzyme hydrolyzes peptides C-terminally fused to NEDD8 as demonstrated by *in vitro* assays [91, 92]. Once in its mature form,

NEDD8 can be used to covalently modify proteins such as p53, MDM2 and members of the human cullin family [87, 89, 93, 94]. However, UCH-L3 does not remove NEDD8 from proteins modified with this ubiquiton, instead proteases like USP21, DEN/NEDP1 and the COP9 complex are responsible for NEDD8 removal [93]. Although the dual specificity of UCH-L3 is now clearly established, its involvement in the context of NEDD8 has been demonstrated to be restricted to pro-peptide maturation. Accordingly, steady-state kinetic studies determined that the binding affinity of UCH-L3 for ubiquitin is higher than for NEDD8 and this enzyme preferentially catalyzes Ub-AMC over NEDD8-AMC [95].

*The Use of UCH-L3 as a Tool in Biotechnology.* The application of recombinant technology has enabled the introduction of a number of recombinant proteins to the market, with insulin being one of the earliest and most successful examples to date [96]. Unfortunately, a large number of recombinant proteins and peptides are poorly expressed, are not biologically active due to missfolding or are unstable [97]. Nevertheless a technology that has provided some solutions for the expression of very small proteins and peptides, production of difficult-to-express proteins, or proteins that are unstable is based on genetic fusions of the problem protein to a stably expressed protein. An example of one of these technologies is the fusion of the highly expressed λ cII gene from *E. Coli,* followed by the cleavage site of the coagulation factor $X_a$ and finally the protein of interest [97]. One downside of this system is that non-natural (scar) amino acids associated with the factor $X_a$ cleavage site may remain on the N-terminus of the target protein after hydrolysis [97]. Another system based on genetic fusions involves the cloning of ubiquitin to the N-terminus of a protein of interest and hydrolysis with UCH-

L3 to release the desired product [98]. This system results in proteins with the intended N-terminal sequence and since only one single cleavage site exists at the C-terminus of ubiquitin the target proteins are not cleaved internally. The optimization of this expression system, downstream purification and processing of the ubiquitin fusions with UCH-L3 has resulted in yields as high as 330 mg/L of pure peptides, representing a cost-effective and scaleable bioprocessing system [98, 99]. In a different scheme, a tripartite fusion system has been implemented to make possible the secretion of peptides to the periplasmic space of *E. coli* since this may result in improved folding, simplified downstream processing and higher stability [100]. This tripartite system consists of: 1) ecotin, a protease inhibitor 2) ubiquitin b from mouse and 3) the target peptide. After purification of the tripartite fusion from the periplasm, and its processing by the rabbit homolog of UCH-L3, yields of a peptide have reached 1.78 mg per gram of dry cell pellet [100].

### 1.5 Protein Stability

Studies that explore and/or are designed to increase protein stability have been catalyzed not only by scientific curiosity but also by commercial interest. Sales of industrial enzymes are expected to reach $2.7 billion in 2012 while the global market for therapeutic proteins reached over $100 billion in 2010 [101, 102]. The success of these protein-based products is in part dependent on their structural and functional integrity. In turn there is an intimate relationship between the structure/function of proteins and their stability, hence the interest in understanding and manipulating this biophysical property.

At the molecular level protein stability emerges as a consequence of multiple effects such as disulfide bonds, aromatic interactions, hydrogen bonds, ion pairs, metal binding and the hydrophobic effect as a main driving force [103]. A useful approach to advance the understanding of protein stability is the comparison of proteins from hyperthermophiles such as *Thermotoga maritima* with those from the mesophiles counterparts. Available data indicate that the high stability of hyperthermophiles cannot be explained by one mechanism alone; instead minor structural changes underlie their enhanced stability. Overall, the higher thermal stability is the result of increased number of atomic contacts within the protein (contact order), which leads to increased protein compactness [104]. Likewise, protein compactness rather than the increased content of secondary structure (*e.g.* decreased loop content) helps to explain the differences between mesophiles and hyperthermophiles. Application of the knowledge gained through these comparisons and the understanding of properties from specific families of proteins has lead to chemical and thermal stabilization of enzymes such as subtilisin used in detergents, lipases used in baking and ∝-amylases used for glucose production [105, 106].

*Stability Vs. Function and Flexibility.* Is there a correlation between protein stability and function? Several lines of evidence strongly suggest that an inverse correlation between these two properties exists. This correlation implies an evolutionary pressure to optimize function over stability, emerging from this the generally accepted principle of "stability-function tradeoff" [107]. This tradeoff was observed upon the analysis of the catalytic residues that, in part, form the active sites of enzymes. From the perspective of protein stability, the organization of active sites is unfavorable since

functional residues that are generally charged or polar, are embedded in hydrophobic clefts and often, are proximal to residues with like charges [107]. In addition, key catalytic residues possess unfavorable backbone angles [107]. As a result, mutations in positions relevant to the function of proteins may increase the stability at the expense of activity and vice versa [107]. Early work that illustrates this trade off involves the bacterial RNAse from *Bacillus amyloliquefaciens* (barnase) and its inhibitor, barstar. The interaction between this enzyme and the inhibitor is driven by acidic amino acids Asp35, Asp39, Glu76 and Glu80 in barstar. If any of these amino acids are mutated to Ala, the binding affinity of these two proteins decreases from two to five orders of magnitude, while stability increases by 0.3 to 2.1 kcal $mol^{-1}$ [108]. Conversely when basic amino acids Lys27, Arg59 and His102 in barnase are mutated to Ala, a large decrease in the enzymatic activity occurs, accompanied by increased stability [109]. Still, enzyme thermostabilization without significant loss of catalytic efficiency has been possible. Using RossettaDesign, a sophisticated suite of protein design algorithms, and cytosine deamidase as a model, Korkegian *et al.* obtained a variant with an increased thermal stability of 10 °C [110]. To design this variant, the authors focused in positions 4 Å away from the active, isolating a triple mutant that suffered a slight reduction on the *Vmax* and *Km*, although the catalytic efficiency (*kcat/Km*) remained unchanged [110]. Furthermore, the increased stability on the triple variant extended the half-life activity of the enzyme at 50 °C, from ~4 hours to ~117 hours (30-fold increase) [110].

What accounts for increased stability and reduced protein function? A well established biochemical principle, indicates that the function of a protein is intimately related to its three-dimensional structure, nevertheless the dynamics and flexibility of the

polypeptide chain are also crucial properties [111]. Proteins do not exist in a static state, rather multiple structural fluctuations occur within “fast” and “slow” time scales, from femtoseconds to milliseconds [112, 113]. These structural fluctuations are central to protein function since a wide range of molecular and biological events such as enzyme catalysis, ligand-receptor interactions, protein-protein interactions and signal transduction occur in these times scales [112, 113]. Therefore the function of a protein is also impacted by factors that modify its dynamic character and its flexibility [112, 113]. Accordingly, several studies have shown that hyperthermophiles tend to be less flexible than their mesophilic homologs, suggesting an inverse relationship between stability and dynamics/flexibility [114]. Furthermore, Tehei *et al.* proposed that enzymes have evolved conformational flexibility according to their optimum working temperature [115]. Tehi *et al.* analyzed the flexibility and stability of Malate Dehydrogenase (MalDH) from the hyperthermophile *Methanococcus jannaschii (*Mj) and Lactate Dehydrogenase (LDH) from the mesophile *Oryctolagus cunniculus* (Oc). This analysis found that the flexibility values observed for LDH *Oc* and MalDH *Mj* at the temperatures of optimal activity (37 °C and 90 °C) are basically identical [115]. In a different approach Tsai *et al.* studied lysozyme and Ribonuclease A under dehydrated (*e.g.* powder form that favors thermal stability) and in hydrated forms. Under stable conditions the results imply that proteins are prevented from significant conformational sampling however, when these are hydrated the solvent facilitates conformational sampling when sufficient thermal energy is available [114]. In other words, higher stability restricts structural dynamics (conformational fluctuations) and these may be essential for events associated with protein functions such as substrate binding and catalysis.

**1.6 N-terminal Monoubiquitination and Ubiquitin Carboxy Hydrolase-L3.**

The extensive studies on the UPS have increased our knowledge on key aspects of the biology and chemistry of this system. The combined efforts of biologists, biochemists and structural biologists have dissected the function, the structure and regulation of the multiple components of the UPS. In addition, the use of modern tools like proteomics and bioinformatics produce a wealth of data that make possible the simultaneous identification of numerous proteins modified by ubiquitin. The application of this type of systematic assessment has been performed in human cell lines, enabling the identification of up to 5,000 ubiquitinated proteins in a single study [116]. Likewise one study was sufficient to establish that besides the canonical Lys48-linked polyubiquitin chains, non-conventional chains (*i.e.,* those linked through Lys6, Lys11, Lys27, and Lys33) also mediate protein degradation. Surprisingly, it was shown that these forms of polyubiquitination occur in levels higher than those anticipated originally [39].

The improved understanding of the components and regulation of the UPS has transcended the boundaries of basic science to impact the field of biomedical and clinical research. Low levels of ubiquitin in plasma are correlated with obesity, the loss of activity of Parkin, an E2 ligase, is associated with Parkinson's disease and unregulated levels of several DUBs are found in various types of malignancies such as acute lymphoblastic leukemia, non-small cell lung cancer and colorectal cancer among others [14, 16, 17]. As far as therapy, the Food and Drug Administration has approved bortezomib an inhibitor of the proteasome for the treatment of multiple myeloma. At the same time studies continue to evaluate the therapeutic effect of bortezomib to treat non-Hodgkin's lymphoma, prostate, breast and non-small-cell lung cancer [117].

Although accomplishments of this nature represent considerable advances in the overall characterization of the ubiquitinome, other fundamental questions remain to be answered. Specifically, the direct biophysical effects of protein ubiquitination have been minimally explored [66, 65]. In part, this is due to the fact that protein ubiquitination may generate a complex multitude of modified proteins as in multimono-ubiquitination, polyubiquitination, or ubiquitin chains polymerized through Lys6, Lys11, Lys27, Lys29 or Lys33 [38, 39, 28]. From this picture it is clear that establishing a system to produce more homogenous and less convoluted ubiquitinated proteins would be advantageous for biophysical studies. In this thesis we are interested in exploring what is the significance of N-terminal mono-ubiquitination (N-tmUb) as a model to garner important data that may provide insights into more complicated forms of ubiquitination. Specifically, we wish to determine what is the effect of attaching a single ubiquitin moiety to the N-terminus of small proteins in the context of the protein's thermal stability. Such studies can be extended to naturally occurring N-terminally ubiquitinated proteins in the future.

For these studies we have rationally designed a panel of proteins derived from the β1 domain of streptococcal protein G (Gβ1) and their thermal stability determined. To critically assess the effect of ubiquitination we added a single ubiquitin moiety to the N-terminus of all the variants derived from Gβ1 and the impact of this modification on the thermal stability of the variants was analyzed. Furthermore we investigate if the catalytic properties of UCH-L3, a deubiquitinase known to remove ubiquitin from small and unfolded C-terminal extensions, are affected by the thermal stability of the protein fused to ubiquitin. In doing so, we provide simplified experimental means to study naturally occurring N-terminally ubiquitination. Thus, we intend to bridge the biophysical

properties of ubiquitinated substrates with the catalysis by UCH-L3 and determine if any possible correlation occurs.

The design implemented confirms the relevance of single point mutations in the thermal stability of Gβ1 variants. The characterization of the variants shows that these proteins span a range of thermal stability from 38 °C to >100 °C. The studies on the ubiquitinated versions of the Gβ1 variants indicate that N-terminal monoUbiquitination results for the most part in slight thermal destabilization. Finally, we demonstrate that the differences in thermal stabilities of the extensions attached to the C-terminus of ubiquitin directly affect the catalytic rate of hydrolysis by UCH-L3. We found a direct correlation between the thermal stability of the fusion and the hydrolysis rate by UCH-L3. Generally, unstable ubiquitin fusions are hydrolyzed at a faster rate than stable fusions. Surprisingly, single point mutations that affect the thermal stability of the Gβ1 variants and that of the ubiquitin fusion also impact the rate of hydrolysis by UCH-L3.

**References**

1. Hochstrasser, M. (1992). Ubiquitin and intracellular protein degradation. *Curr Opin Cell biol* **4**, 1024-1031.

2. Wolfe, M. S. (2009). Intramembrane proteolysis. *Chem Rev* **109**, 1599-612.

3. Schrader, E. K., Harstad, K. G. & Matouschek, A. (2009). Targeting proteins for degradation. *Nat Chem Biol* **5**, 815-822.

4. Glickman, M. H. & Ciechanover, A. (2001). The Ubiquitin-Proteasome Proteolytic Pathway: Destruction for the Sake of Construction. *Physiol Rev* **82**, 373-428.

5. Coffey, J. W. & De Duve, C. (1968). Digestive activity of lysosomes. I. The digestion of proteins by extracts of rat liver lysosomes. *J Biol Chem* **243**, 3255-63.

6. Ciechanover, A. (2005). Intracellular protein degradation: from a vague idea thru the lysosome and the ubiquitin–proteasome system and onto human diseases and drug targeting. *Cell Death Differ* **12**, 1178-1190.

7. Etlinger, J. D. & Goldberg, A. L. (1977). A soluble ATP-dependent proteolytic system responsible for the degradation of abnormal proteins in reticulocytes. *Proc Natl Acad Sci U S A* **74**, 54-8.

8. Ciehanover, A., Hod, Y. & Hershko, A. (1978). A heat-stable polypeptide component of an ATP-dependent proteolytic system from reticulocytes. *Biochem Biophys Res Commun* **81**, 1100-5.

9. Wilkinson, K. D., Urban, M. K. & Haas, A. L. (1980). Ubiquitin is the ATP-dependent proteolysis factor I of rabbit reticulocytes. *J Biol Chem* **255**, 7529-32.

10. Kresge, N., Simoni, R. & Hill, R. (2006). The Discovery of Ubiquitin-mediated Proteolysis by Aaron Ciechanover, Avram Hershko, and Irwin Rose. *J Biol Chem* **255**, 7525-75258.

11. Prakash, S., Tian, L., Ratliff, K. S., Lehotzky, R. E. & Matouschek, A. (2004). An unstructured initiation site is required for efficient proteasome-mediated degradation. *Nat Struct Mol Biol* **11**, 830-7.

12. Rahighi, S., Ikeda, F., Kawasaki, M., Akutsu, M., Suzuki, N., Kato, R., Kensche, T., Uejima, T., Bloor, S., Komander, D., Randow, F., Wakatsuki, S. & Dikic, I. (2009). Specific Recognition of Linear Ubiquitin Chains by NEMO Is Important for NF-kB Activation. *Cell* **136**, 1098-1109.

13. Kimura, Y., Yashiroda, H., Kudo, T., Koitabashi, S., Murata, S., Kakizuka, A. & Tanaka, K. (2009). An inhibitor of a deubiquitinating enzyme regulates ubiquitin homeostasis. *Cell* **137**, 549-59.

14. Chang, T. L., Chang, C. J., Lee, W. Y., Lin, M. N., Huang, Y. W. & Fan, K. (2009). The roles of ubiquitin and 26S proteasome in human obesity. *Metabolism Clinical and Experimental* **58**, 1643-8.

15. Dahlmann, B. (2007). Role of proteasomes in disease. *BMC Biochem* **8 Suppl 1**, S3.

16. Fang, Y., Fu, D. & Shen, X. Z. (2010). The potential role of ubiquitin c-terminal hydrolases in oncogenesis. *Biochim Biophys Acta* **1806**, 1-6.

17. Olanow, C. W. & McNaught, K. S. (2006). Ubiquitin-proteasome system and Parkinson's disease. *Mov Disord* **21**, 1806-23.

18. Murata, S., Yashiroda, H. & Tanaka, K. (2009). Molecular mechanisms of proteasome assembly. *Nat Rev Mol Cell Biol* **10**, 104-15.

19. Ciechanover, A., Elias, S., Heller, H., Ferber, S. & Hershko, A. (1980). Characterization of the heat-stable polypeptide of the ATP-dependent proteolytic system from reticulocytes. *J Biol Chem* **255**, 7525-8.

20. Nei, M., Rogozin, I. B. & Piontkivska, H. (2000). Purifying selection and birth-and-death evolution in the ubiquitin gene family. *Proc Natl Acad Sci U S A* **97**, 10866-71.

21. Drahl, C. (2009). Prelude To A Kiss Of Death. *Chemical & Engineering News* **87**, 41-43.

22. Behuliak, M., Celec, P., Gardlik, R. & Palffy, R. (2005). Ubiquitin--the kiss of death goes Nobel. Will you be quitting? *Bratisl Lek Listy* **106**, 93-100.

23. Ciechanover, A. (2005). Proteolysis: from the lysosome to ubiquitin and the proteasome. *Nat Rev Mol Cell Biol* **6**, 79-87.

24. Lecker, S. H., Goldberg, A. L. & Mitch, W. E. (2006). Protein degradation by the ubiquitin-proteasome pathway in normal and disease states. *J Am Soc Nephrol* **17**, 1807-19.

25. Rosenzweig, R., Osmulski, P. A., Gaczynska, M. & Glickman, M. H. (2008). The central unit within the 19S regulatory particle of the proteasome. *Nat Struct Mol Biol* **15**, 573-80.

26. Ye, Y. & Rape, M. (2009). Building ubiquitin chains: E2 enzymes at work. *Nat Rev Mol Cell Biol* **10**, 755-64.

27. Ardley, H. & Robinson, P. (2005). E3 ubiquitin ligases. *Essays in Biochemistry* **041**, 15-30.

28. Larsen, C. N., Krantz, B. A. & Wilkinson, K. D. (1998). Substrate specificity of deubiquitinating enzymes: ubiquitin C-terminal hydrolases. *Biochemistry* **37**, 3358-68.

29. Koegl, M., Hoppe, T., Schlenker, S., Ulrich, H. D., Mayer, T. U. & Jentsch, S. (1999). A novel ubiquitination factor, E4, is involved in multiubiquitin chain assembly. *Cell* **96**, 635-44.

30. Ciechanover, A., Orian, A. & Schwartz, A. L. (2000). The ubiquitin-mediated proteolytic pathway: mode of action and clinical implications. *J Cell Biochem Suppl* **34**, 40-51.

31. Maccario, H., Perera, N. M., Gray, A., Downes, C. P. & Leslie, N. R. (2010). Ubiquitination of PTEN (phosphatase and tensin homolog) inhibits phosphatase activity and is enhanced by membrane targeting and hyperosmotic stress. *J Biol Chem* **285**, 12620-8.

32. Muyang Li, C. L. B., Foon Wu-Baer, Delin Chen, Richard Baer, Wei Gu. (2003). Mono- Versus Polyubiquitination: Differential Control of p53 Fate by Mdm2. *Science* **302**.

33. Zhou, W., Zhu, P., Wang, J., Pascual, G., Ohgi, K. A., Lozach, J., Glass, C. K. & Rosenfeld, M. G. (2008). Histone H2A monoubiquitination represses transcription by inhibiting RNA polymerase II transcriptional elongation. *Mol Cell* **29**, 69-80.

34. Hicke, L. (2001). Protein regulation by monoubiquitin. *Nat Rev Mol Cell Biol* **2**, 195-201.

35. Li, M., Brooks, C. L., Wu-Baer, F., Chen, D., Baer, R. & Gu, W. (2003). Mono- versus polyubiquitination: differential control of p53 fate by Mdm2. *Science* **302**, 1972-5.

36. Haglund, K., Sigismund, S., Polo, S., Szymkiewicz, I., Di Fiore, P. P. & Dikic, I. (2003). Multiple monoubiquitination of RTKs is sufficient for their endocytosis and degradation. *Nat Cell Biol* **5**, 461-6.

37. Hershko, A. & Ciechanover, A. (1998). The ubiquitin system. *Annu Rev Biochem* **67**, 425-79.

38. Komander, D. (2009). The emerging complexity of protein ubiquitination. *Biochem Soc Trans* **37**, 937-53.

39. Xu, P., Duong, D. M., Seyfried, N. T., Cheng, D., Xie, Y., Robert, J., Rush, J., Hochstrasser, M., Finley, D. & Peng, J. (2009). Quantitative proteomics reveals the function of unconventional ubiquitin chains in proteasomal degradation. *Cell* **137**, 133-45.

40. Haglund, K., Sigismund, S., Polo, S., Szymkiewicz, I., Di Fiore, P. & Dikic, I. (2003). Multiple monoubiquitination of RTKs is sufficient for their endocytosis and degradation. *Nat Cell Biol* **5**, 461-466.

41. Chastagner, P., Israel, A. & Brou, C. (2008). AIP4/Itch regulates Notch receptor degradation in the absence of ligand. *PLoS One* **3**, e2735.

42. Cadwell, K. & Coscoy, L. (2005). Ubiquitination on nonlysine residues by a viral E3 ubiquitin ligase. *Science* **309**, 127-30.

43. Wang, X., Herr, R. A., Chua, W. J., Lybarger, L., Wiertz, E. J. & Hansen, T. H. (2007). Ubiquitination of serine, threonine, or lysine residues on the cytoplasmic tail can induce ERAD of MHC-I by viral E3 ligase mK3. *J Cell Biol* **177**, 613-24.

44. Wang, X., Herr, R. A., Rabelink, M., Hoeben, R. C., Wiertz, E. J. & Hansen, T. H. (2009). Ube2j2 ubiquitinates hydroxylated amino acids on ER-associated degradation substrates. *J Cell Biol* **187**, 655-68.

45. Finley, D., Bartel, B. & Varshavsky, A. (1989). The tails of ubiquitin precursors are ribosomal proteins whose fusion to ubiquitin facilitates ribosome biogenesis. *Nature* **338**, 394-401.

46. Olvera, J. & Wool, I. G. (1993). The carboxyl extension of a ubiquitin-like protein is rat ribosomal protein S30. *J Biol Chem* **268**, 17967-74.

47. Breitschopf, K., Bengal, E., Ziv, T., Admon, A. & Ciechanover, A. (1998). A novel site for ubiquitination: the N-terminal residue, and not internal lysines of MyoD, is essential for conjugation and degradation of the protein. *EMBO J* **17**, 5964-73.

48. Aviel, S., Winberg, G., Massucci, M. & Ciechanover, A. (2000). Degradation of the Epstein-Barr Virus Latent Membrane Protein 1 (LMP1) by the Ubiquitin-Proteasome Pathway. *J Biol Chem* **275**, 23491-23499.

49. Reinstein, E., Scheffner, M., Oren, M., Ciechanover, A. & Schwartz, A. (2000). Degradation of the E7 human papillomavirus oncoprotein by the ubiquitin-proteasome system: targeting via ubiquitination of the N-terminal residue. *Oncogene* **19**, 5944-5950.

50. Bloom, J., Amador, V., Bartolini, F., DeMartino, G. & Pagano, M. (2003). Proteasome-Mediated Degradation of p21 via N-Terminal Ubiquitinylation. *Cell* **115**, 71-87.

51. Ben-Saadon, R., Fajerman, I., Ziv, T., Hellman, U., Schwartz, A. L. & Ciechanover, A. (2004). The tumor suppressor protein p16(INK4a) and the human papillomavirus oncoprotein-58 E7 are naturally occurring lysine-less proteins that are degraded by the ubiquitin system. Direct evidence for ubiquitination at the N-terminal residue. *J Biol Chem* **279**, 41414-21.

52. Coulombe, P., Rodier, G., Bonneil, E., Thibault, P. & Meloche, S. (2004). N-Terminal ubiquitination of extracellular signal-regulated kinase 3 and p21 directs their degradation by the proteasome. *Mol Cell Biol* **24**, 6140-50.

53. Kirisako, T., Kamei, K., Murata, S., Kato, M., Fukumoto, H., Kanie, M., Sano, S., Tokunaga, F., Tanaka, K. & Iwai, K. (2006). A ubiquitin ligase complex assembles linear polyubiquitin chains. *EMBO J* **25**, 4877-87.

54. Tokunaga, F., Sakata, S., Saeki, Y., Satomi, Y., Kirisako, T., Kamei, K., Nakagawa, T., Kato, M., Murata, S., Yamaoka, S., Yamamoto, M., Akira, S., Takao, T., Tanaka, K. & Iwai, K. (2009). Involvement of linear polyubiquitylation of NEMO in NF-kappaB activation. *Nat Cell Biol* **11**, 123-32.

55. Johnson, E. S., Ma, P. C., Ota, I. M. & Varshavsky, A. (1995). A proteolytic pathway that recognizes ubiquitin as a degradation signal. *J Biol Chem* **270**, 17442-56.

56. Fajerman, I., Schwartz, A. L. & Ciechanover, A. (2004). Degradation of the Id2 developmental regulator: targeting via N-terminal ubiquitination. *Biochem Biophys Res Commun* **314**, 505-12.

57. Tait, S. W., de Vries, E., Maas, C., Keller, A. M., D'Santos, C. S. & Borst, J. (2007). Apoptosis induction by Bid requires unconventional ubiquitination and degradation of its N-terminal fragment. *J Cell Biol* **179**, 1453-66.

58. Marmor, M. D. & Yarden, Y. (2004). Role of protein ubiquitylation in regulating endocytosis of receptor tyrosine kinases. *Oncogene* **23**, 2057-70.

59. Hochstrasser, M. (1996). Ubiquitin-dependent protein degradation. *Annu Rev Genet* **30**, 405-39.

60. Thomason, P. & Kay, R. (2000). Eukaryotic signal transduction via histidine-aspartate phosphorelay. *J Cell Sci* **113 ( Pt 18)**, 3141-50.

61. Narayanan, A. & Jacobson, M. P. (2009). Computational studies of protein regulation by post-translational phosphorylation. *Curr Opin Struct Biol* **19**, 156-63.

62. Lehninger, A. L., Nelson, D. L. & Cox, M. M. (2008). *Lehninger principles of biochemistry*. 5th edit, W.H. Freeman, New York.

63. Spiro, R. G. (2002). Protein glycosylation: nature, distribution, enzymatic formation, and disease implications of glycopeptide bonds. *Glycobiology* **12**, 43R-56R.

64. Shental-Bechor, D. & Levy, Y. (2009). Folding of glycoproteins: toward understanding the biophysics of the glycosylation code. *Curr Opin Struct Biol* **19**, 524-33.

65. Hagai, T. & Levy, Y. (2010). Ubiquitin not only serves as a tag but also assists degradation by inducing protein unfolding. *Proc Natl Acad Sci U S A* **107**, 2001-6.

66. Freudenthal, B. D., Gakhar, L., Ramaswamy, S. & Washington, M. T. (2010). Structure of monoubiquitinated PCNA and implications for translesion synthesis and DNA polymerase exchange. *Nat Struct Mol Biol* **17**, 479-84.

67. Henderson, A., Erales, J., Hoyt, M. A. & Coffino, P. (2011). Dependence of proteasome processing rate on substrate unfolding. *J Biol Chem* **286**, 17495-502.

68. Johnston, S. C., Larsen, C. N., Cook, W. J., Wilkinson, K. D. & Hill, C. P. (1997). Crystal structure of a deubiquitinating enzyme (human UCH-L3) at 1.8 A resolution. *EMBO J* **16**, 3787-96.

69. Weissman, A. M. (2001). Themes and variations on ubiquitylation. *Nat Rev Mol Cell Biol* **2**, 169-78.

70. Reyes-Turcu, F. E., Ventii, K. H. & Wilkinson, K. D. (2009). Regulation and cellular roles of ubiquitin-specific deubiquitinating enzymes. *Annu Rev Biochem* **78**, 363-97.

71. Nijman, S. M., Luna-Vargas, M. P., Velds, A., Brummelkamp, T. R., Dirac, A. M., Sixma, T. K. & Bernards, R. (2005). A genomic and functional inventory of deubiquitinating enzymes. *Cell* **123**, 773-86.

72. Sethe Burgie, E., Bingman, C. A., Soni, A. B. & Phillips, G. N. (2011). Structural characterization of human Uch37. *Proteins: Structure, Function, and Bioinformatics*, n/a-n/a.

73. Cstorer, A. & Ménard, R. (1994). [33] Catalytic mechanism in papain family of cysteine peptidases. In *Methods in Enzymology* (Alan, J. B., ed.), Vol. Volume 244, pp. 486-500. Academic Press.

74. Johnston, S. C., Riddle, S. M., Cohen, R. E. & Hill, C. P. (1999). Structural basis for the specificity of ubiquitin C-terminal hydrolases. *EMBO J* **18**, 3877-87.

75. Nishio, K., Kim, S. W., Kawai, K., Mizushima, T., Yamane, T., Hamazaki, J., Murata, S., Tanaka, K. & Morimoto, Y. (2009). Crystal structure of the de-ubiquitinating enzyme UCH37 (human UCH-L5) catalytic domain. *Biochem Biophys Res Commun* **390**, 855-60.

76. Yao, T., Song, L., Xu, W., DeMartino, G. N., Florens, L., Swanson, S. K., Washburn, M. P., Conaway, R. C., Conaway, J. W. & Cohen, R. E. (2006).

Proteasome recruitment and activation of the Uch37 deubiquitinating enzyme by Adrm1. *Nat Cell Biol* **8**, 994-1002.

77. Wilkinson, K. D., Deshpande, S. & Larsen, C. N. (1992). Comparisons of neuronal (PGP 9.5) and non-neuronal ubiquitin C-terminal hydrolases. *Biochem Soc Trans* **20**, 631-7.

78. Miyoshi, Y., Nakayama, S., Torikoshi, Y., Tanaka, S., Ishihara, H., Taguchi, T., Tamaki, Y. & Noguchi, S. (2006). High expression of ubiquitin carboxy-terminal hydrolase-L1 and -L3 mRNA predicts early recurrence in patients with invasive breast cancer. *Cancer Sci* **97**, 523-9.

79. Liu, Y., Fallon, L., Lashuel, H. A., Liu, Z. & Lansbury, P. T., Jr. (2002). The UCH-L1 gene encodes two opposing enzymatic activities that affect alpha-synuclein degradation and Parkinson's disease susceptibility. *Cell* **111**, 209-18.

80. Carmine Belin, A., Westerlund, M., Bergman, O., Nissbrandt, H., Lind, C., Sydow, O. & Galter, D. (2007). S18Y in ubiquitin carboxy-terminal hydrolase L1 (UCH-L1) associated with decreased risk of Parkinson's disease in Sweden. *Parkinsonism Relat Disord* **13**, 295-8.

81. Nam, M. J., Madoz-Gurpide, J., Wang, H., Lescure, P., Schmalbach, C. E., Zhao, R., Misek, D. E., Kuick, R., Brenner, D. E. & Hanash, S. M. (2003). Molecular profiling of the immune response in colon cancer using protein microarrays: occurrence of autoantibodies to ubiquitin C-terminal hydrolase L3. *Proteomics* **3**, 2108-15.

82. Misaghi, S., Galardy, P. J., Meester, W. J., Ovaa, H., Ploegh, H. L. & Gaudet, R. (2005). Structure of the ubiquitin hydrolase UCH-L3 complexed with a suicide substrate. *J Biol Chem* **280**, 1512-20.

83. Popp, M. W., Artavanis-Tsakonas, K. & Ploegh, H. L. (2009). Substrate filtering by the active site crossover loop in UCHL3 revealed by sortagging and gain-of-function mutations. *J Biol Chem* **284**, 3593-602.

84. Miranda, M. & Sorkin, A. (2007). Regulation of receptors and transporters by ubiquitination: new insights into surprisingly similar mechanisms. *Mol Interv* **7**, 157-67.

85. Butterworth, M. B., Edinger, R. S., Frizzell, R. A. & Johnson, J. P. (2009). Regulation of the epithelial sodium channel by membrane trafficking. *Am J Physiol Renal Physiol* **296**, F10-24.

86. Madsen, L., Schulze, A., Seeger, M. & Hartmann-Petersen, R. (2007). Ubiquitin domain proteins in disease. *BMC Biochem* **8 Suppl 1**, S1.

87. Welchman, R. L., Gordon, C. & Mayer, R. J. (2005). Ubiquitin and ubiquitin-like proteins as multifunctional signals. *Nat Rev Mol Cell Biol* **6**, 599-609.

88. Liu, Y. C., Pan, J., Zhang, C., Fan, W., Collinge, M., Bender, J. R. & Weissman, S. M. (1999). A MHC-encoded ubiquitin-like protein (FAT10) binds noncovalently to the spindle assembly checkpoint protein MAD2. *Proc Natl Acad Sci U S A* **96**, 4313-8.

89. Kirkin, V. & Dikic, I. (2007). Role of ubiquitin- and Ubl-binding proteins in cell signaling. *Curr Opin Cell Biol* **19**, 199-205.

90. Setsuie, R., Sakurai, M., Sakaguchi, Y. & Wada, K. (2009). Ubiquitin dimers control the hydrolase activity of UCH-L3. *Neurochem Int* **54**, 314-21.

91. Hemelaar, J., Borodovsky, A., Kessler, B. M., Reverter, D., Cook, J., Kolli, N., Gan-Erdene, T., Wilkinson, K. D., Gill, G., Lima, C. D., Ploegh, H. L. & Ovaa, H. (2004). Specific and covalent targeting of conjugating and deconjugating enzymes of ubiquitin-like proteins. *Mol Cell Biol* **24**, 84-95.

92. Wada, H., Kito, K., Caskey, L. S., Yeh, E. T. & Kamitani, T. (1998). Cleavage of the C-terminus of NEDD8 by UCH-L3. *Biochem Biophys Res Commun* **251**, 688-92.

93. Soucy, T. A., Dick, L. R., Smith, P. G., Milhollen, M. A. & Brownell, J. E. (2010). The NEDD8 Conjugation Pathway and Its Relevance in Cancer Biology and Therapy. *Genes Cancer* **1**, 708-16.

94. Whitby, F. G., Xia, G., Pickart, C. M. & Hill, C. P. (1998). Crystal structure of the human ubiquitin-like protein NEDD8 and interactions with ubiquitin pathway enzymes. *J Biol Chem* **273**, 34983-91.

95. Gan-Erdene, T., Nagamalleswari, K., Yin, L., Wu, K., Pan, Z. Q. & Wilkinson, K. D. (2003). Identification and characterization of DEN1, a deneddylase of the ULP family. *J Biol Chem* **278**, 28892-900.

96. Keen, H., Glynne, A., Pickup, J. C., Viberti, G. C., Bilous, R. W., Jarrett, R. J. & Marsden, R. (1980). Human insulin produced by recombinant DNA technology: safety and hypoglycaemic potency in healthy men. *Lancet* **2**, 398-401.

97. Butt, T. R., Jonnalagadda, S., Monia, B. P., Sternberg, E. J., Marsh, J. A., Stadel, J. M., Ecker, D. J. & Crooke, S. T. (1989). Ubiquitin fusion augments the yield of cloned gene products in Escherichia coli. *Proc Natl Acad Sci U S A* **86**, 2540-4.

98. Pilon, A., Yost, P., Chase, T. E., Lohnas, G., Burkett, T., Roberts, S. & Bentley, W. E. (1997). Ubiquitin fusion technology: bioprocessing of peptides. *Biotechnol Prog* **13**, 374-9.

99. Pilon, A. L., Yost, P., Chase, T. E., Lohnas, G. L. & Bentley, W. E. (1996). High-level expression and efficient recovery of ubiquitin fusion proteins from Escherichia coli. *Biotechnol Prog* **12**, 331-7.

100. Paal, M., Heel, T., Schneider, R. & Auer, B. (2009). A novel Ecotin-Ubiquitin-Tag (ECUT) for efficient, soluble peptide production in the periplasm of Escherichia coli. *Microb Cell Fact* **8**, 7.

101. Elvin, J., Couston, R. & van der Wallace, C. (2011). Therapeutic antibodies: Market Considerations, Disease Targets and Bioprocessing. *International Journal of Pharmaceutics*.

102. Iyer, P. V. & Ananthanarayan, L. (2008). Enzyme Stability and Stabilization-Aqueous and Non-Aqueous Environment. *Process Biochemistry* **43**, 1019-1032.

103. Vieille, C. & Zeikus, G. J. (2001). Hyperthermophilic enzymes: sources, uses, and molecular mechanisms for thermostability. *Microbiol Mol Biol Rev* **65**, 1-43.

104. Pechkova, E., Sivozhelezov, V. & Nicolini, C. (2007). Protein thermal stability: the role of protein structure and aqueous environment. *Arch Biochem Biophys* **466**, 40-8.

105. Shaw, A., Bott, R. & Day, A. G. (1999). Protein engineering of alpha-amylase for low pH performance. *Curr Opin Biotechnol* **10**, 349-52.

106. Fágáin, C. Ó. (2003). Enzyme stabilization,Äîrecent experimental progress. *Enzyme and Microbial Technology* **33**, 137-149.

107. Tokuriki, N., Stricher, F., Serrano, L. & Tawfik, D. S. (2008). How protein stability and new functions trade off. *PLoS Comput Biol* **4**, e1000002.

108. Schreiber, G., Buckle, A. M. & Fersht, A. R. (1994). Stability and function: two constraints in the evolution of barstar and other proteins. *Structure* **2**, 945-51.

109. Meiering, E. M., Serrano, L. & Fersht, A. R. (1992). Effect of active site residues in barnase on activity and stability. *J Mol Biol* **225**, 585-9.

110. Korkegian, A., Black, M. E., Baker, D. & Stoddard, B. L. (2005). Computational thermostabilization of an enzyme. *Science* **308**, 857-60.

111. Meinhold, L., Clement, D., Tehei, M., Daniel, R., Finney, J. L. & Smith, J. C. (2008). Protein dynamics and stability: the distribution of atomic fluctuations in thermophilic and mesophilic dihydrofolate reductase derived using elastic incoherent neutron scattering. *Biophys J* **94**, 4812-8.

112. Henzler-Wildman, K. & Kern, D. (2007). Dynamic personalities of proteins. *Nature* **450**, 964-72.

113. Lill, M. A. (2011). Efficient incorporation of protein flexibility and dynamics into molecular docking simulations. *Biochemistry* **50**, 6157-69.

114. Tsai, A. M., Udovic, T. J. & Neumann, D. A. (2001). The inverse relationship between protein dynamics and thermal stability. *Biophys J* **81**, 2339-43.

115. Tehei, M. & Zaccai, G. (2007). Adaptation to high temperatures through macromolecular dynamics by neutron scattering. *FEBS J* **274**, 4034-43.

116. Kim, W., Bennett, E. J., Huttlin, E. L., Guo, A., Li, J., Possemato, A., Sowa, M. E., Rad, R., Rush, J., Comb, M. J., Harper, J. W. & Gygi, S. P. (2011). Systematic and quantitative assessment of the ubiquitin-modified proteome. *Mol Cell* **44**, 325-40.

117. Nalepa, G., Rolfe, M. & Harper, J. W. (2006). Drug discovery in the ubiquitin-proteasome system. *Nat Rev Drug Discov* **5**, 596-613.

# CHAPTER II
# Materials and Methods

## 2.1 Introduction

Deciphering the multiple patterns of ubiquitination and their functional diversity has called for considerable efforts, yet the biophysical analysis of ubiquitinated proteins has received limited attention. Factors such as the number of ubiquitin molecules polymerized and the specific lysine residue within ubiquitin used for the addition of extra moieties contribute to the significant complexity in the patterns of ubiquitination [1]. To expand our understanding of the biophysical and biochemical consequences of protein ubiquitination we have studied the effect of N-terminal monoUbiquitination in the context of protein thermal stability. To accomplish this goal we have designed mutants derived from the β1-domain of streptococcal protein G (Gβ1) and their thermal stability characterized by spectroscopical techniques. In addition we investigate if the catalytic properties of a deubiquitinase, Ubiquitin Carboxy Hidrolase-L3 (UCH-L3) are affected by the thermal stability of the test proteins attached to the C-terminus of ubiquitin. In the present chapter we provide a description of the materials and the methods used throughout this thesis.

## 2.2 Materials

All chemicals used for HPLC purification were HPLC grade, obtained from primarily from Fisher Scientific. The C8 Dynamax column for HPLC purifications was purchased from Varian Inc. All oligonucleotides were purchased from IDT Technologies and their sequences are listed in the Appendix I. QuickChange® kit, *Pfu* DNA

polymerase and the plasmid pBT were purchased from Stratagene. High fidelity DNA poymerase Phusion and the PageRuler$^{TM}$ prestained protein ladder were purchased from Thermo Scientific. Enzymes DpnI, BamHI and EcoRI were purchased from New England Biolabs. KspI was purchased from Roche. NucleoSpin Plasmid kit, Ni-TED columns and NucleoSpin Extrac II kit were purchased from E&K Scientific. T4 ligase and IAEDANS were purchased from Invitrogen. IPTG was purchased from Genesee Scientific. Amicon Centricons were purchased from Milipore. BSA was purchased from Fisher Scientific. The Superdex$^{TM}$ 75 analytical column and the low molecular weight gel filtration calibration kit were purchased from GE Healthcare.

## 2.3 Methods

Molecular Biology

2.2.1 Gβ1 and Variants

In a previous study Gβ1 was redesigned to generate two variants: Monomer A (MonA) and Monomer B (MonB) [2]. For the project described herein one point mutation for each one of these parent molecules were created using the commercially available technique QuickChange®. The plasmid coding for MonB was used as template and the oligonucleotides OCN58 monB (A45F), OCN59 monB (A45F) Rev were utilized to introduce the desired mutation (PCR conditions Table 2.1). The typical reaction mixture used in all PCR amplifications is shown in Table 2.2. Upon amplification the reaction was digested with DpnI, incubated for 6 hrs at 37 °C and 10 μL transformed in chemically competent *E. coli* (Top10 cells). Transformed cells were plated on LB agar plates that contained ampicillin (60 μg/mL) and incubated for 12 hrs at 37 °C. Plasmids

from individual colonies were isolated using the NucleoSpin plasmid kit and the correct DNA composition was verified via DNA standard sequencing. The amino acid sequence of all five variants studied is shown in Fig. 2.1. The designed mutants MonA(Y45A) and MonB(A45F) were implemented on the rationale that position 45 plays a key role in the thermal stability of the parent molecule [3, 4].

**Table 2.1.** PCR parameters used to produce mutant MonB(A45F).

| ***Step*** | ***Temperature*** | ***Time*** | ***Cycles*** |
|---|---|---|---|
| 1. | 95 °C | 30” | 1 |
| 2. | 95 °C | 30” | 16 |
| 3. | 55 °C | 1’ | 16 |
| 4. | 68 °C | 5’ | 16 |
| Store at 4 °C | | | |

**Table 2.2.** Typical reaction mix used for all PCR experiments. Total volume: 50 μL.

| ***Component*** | ***Amount*** |
|---|---|
| DNA Template | 100 ng |
| Oligonucleotide Forward | 125 ng |
| Oligonucleotide Reverse | 125 ng |
| *dNTP mix | 1 μL |
| 10X Reaction Buffer | 5 μL |
| **DNA Polymerase (*Pfu*) | 0.5 μL |

* 10 mM Stock (Fermentas)
**2.5 U/μL (Stratagene)

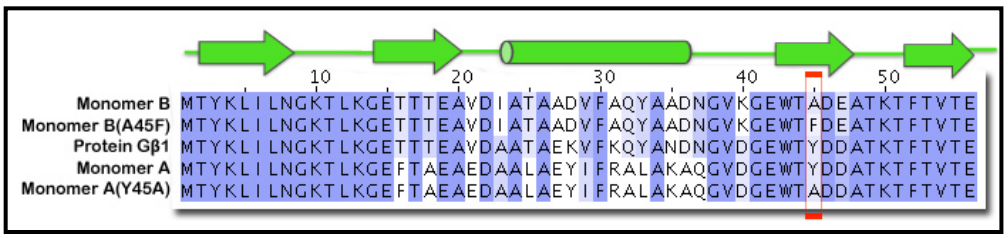


**Figure 2.1.** Sequence alignment of Gβ1 and variants studied in this thesis. Sequences are matched to elements of secondary structure in Gβ1. Position 45 is boxed in red. Arrows indicate β-sheets and the cylinder an α-helix.

2.2.2 N-terminal Ubiquitin Fusions

In order to generate ubiquitinated proteins the genes coding for wild-type Gβ1, MonA, MonA(Y45A), MonB, and MonB(A45F) were amplified by PCR using oligonucleotides OCN25 Ubi:ProG For and OCN26 Ubi:ProG Rev for Gβ1 and OCN28 Ubi:MonAB Rev and OCN27 Ubi:MonAB for the rest of the proteins (PCR conditions Table 2.3). The two forward oligonucleotides contain a KspI site and the reverse oligonucleotides contain a site for BamHI. Addition of these two restriction sites enabled ligation of the amplified genes at the 3' end of ubiquitin in plasmid pUBQ. This cloning scheme was followed to generate all the N-terminally monoUbiquitinated variants and functions as a cassette system (Fig. 2.2).

**Table 2.3** PCR conditions to amplify Gβ1, MonA, MonA(Y45A), MonB and MonB(A45F).

| ***Step*** | ***Temperature*** | ***Time*** | ***Cycles*** |
|---|---|---|---|
| 1. | 94 °C | 10' | 1 |
| 2. | 94 °C | 15'' | 30 |
| 3. | 55 °C | 30'' | 30 |
| 4. | 72 °C | 1' | 30 |
| 5. | 72 °C | 10' | 1 |
| Store at 4 °C | | | |

After purification using a NucleoSpin Extract II kit the PCR products as well as pUBQ were digested with KspI for 3 hrs at 37 °C, purified with Nucleospin extract II, digested with BamHI for 3 hrs at 37 °C and finally purified with Nucleospin extract II. A total of 50 ng of doubly digested PCR products were mixed with doubly digested pUBQ in different ratios (1:3, 1:9 and 1:12) and ligated in 20 μL reactions with T4 ligase for 90 minutes at room temperature.

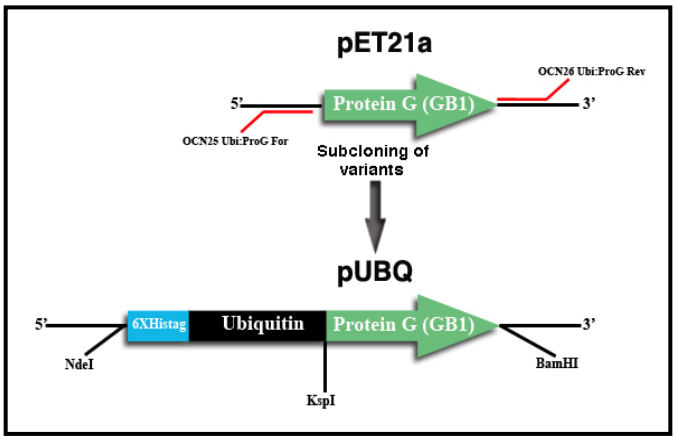


**Figure 2.2.** Cloning in position 3' to the end of ubiquitin in plasmid pUBQ generates N-terminally monoUbiquitinated proteins. This plasmid functions as a cassette system making possible to clone protein G and all the variants designed. An N-terminal 6XHisTag is included to aid in the protein purification of fusions.

Next, chemically competent *E. coli* cells (strain Top10) were transformed with 10 μL of the ligation reactions, plated on LB agar plates that contained ampicillin (60 μg/mL) and incubated for 12 hrs at 37 °C. Plasmids from individual colonies were isolated using the NucleoSpin plasmid kit and the correct DNA composition was verified via DNA standard sequencing. The prefix "Ub" was added to the name of each variant to indicate an N-terminal monoUbiquitinated protein, *i.e.,* Ub-G, Ub-MonA, Ub-MonA(Y45A), Ub-MonB and Ub-MonB(A45F).

In addition to the above described variants, we also created two more fusions: a di-ubiquitin fusion (Ub-Ub) and a di-ubiquitin fusion with an extended 22 amino acids scrambled peptide at the C-terminus of the distal ubiquitin (UbUb-22) (see Fig. 2.3). To generate the Ub-Ub fusion, oligonucleotides OCN67Ubi:Ubi For, OCN69Ubi:Ubi Rev and template pUBQ were used (PCR conditions table 2.4). UbUb-22 was generated by introducing an additional distal ubiquitin and by substituting the stop codon with that of Met, extending the open reading frame for additional 22 amino acids downstream of the distal ubiquitin (Fig 2.3). To produce this fusion oligonucleotides OCN67 Ubi:Ubi For and OCN68 Ubi:Ubi Rev and template pUBQ were utilized (PCR conditions table 2.4). Cloning of these two ubiquitin fusions required digestion of the genes with KspI and BamHI and ligation into pUBQ using the same cloning scheme described above for the other ubiquitin fusions (Fig. 2.2).

**Table 2.4.** PCR conditions to amplify ubiquitin and ubiquitin with a C-terminal extension of 22 amino acids.

| ***Step*** | ***Temperature*** | ***Time*** | ***Cycles*** |
|---|---|---|---|
| 1. | 94 °C | 10’ | 1 |
| 2. | 94 °C | 30’’ | 30 |
| 3. | 55 °C | 30’’ | 30 |
| 4. | 72 °C | 1’ | 30 |
| 5. | 72 °C | 10’ | 1 |
| Store at 4 °C | | | |

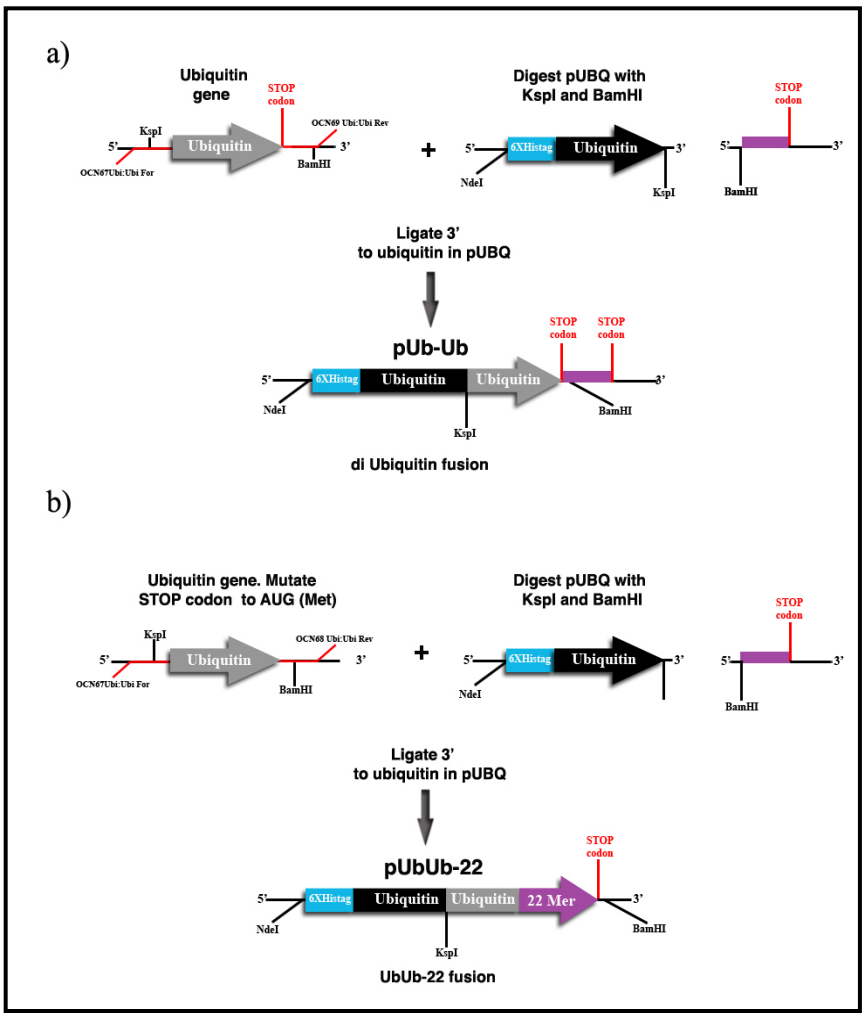


**Figure 2.3.** Cloning strategy used to generate a) Ub-Ub, the di-ubiquitin fusion and b) UbUb-22, the di-ubiquitin fusion with a scrambled peptide at the C-terminus of the distal ubiquitin. Generation of these two fusions required the same DNA template (pUBQ) and the same forward oligonucleotide. a) The ubiquitin gene is amplified and ligated into pUBQ. b) The reverse oligonucleotide OCN68 Ubi:Ubi Rev substitutes the STOP codon for a Met codon at the end of the distal ubiquitin, extending the open reading frame to generate a 22-mer in the C terminus of the distal ubiquitin. The actual codon to stop translation is already contained in the plasmid backbone.

### 2.2.3 Subcloning of UCH-L3 in pBT-λCI

To perform co-translational studies the genes of the hydrolase and the ubiquitin fusion substrates were cloned into two different plasmids with compatible origins of replication (Fig. 2.4). The gene coding for Ubiquitin Carboxy Hydrolase–L3 (UCH-L3)

was amplified using the template plasmid pET19b/UCH-L3 and oligonucleotides OCN6 UCH-Nde I-For and OCN7 UCH-EcoR I-Rev (PCR conditions Table 2.5). The PCR product obtained was purified and digested with EcoRI and NdeI simultaneously for 12 hours at 37 °C. UCH-L3 DNA was subcloned in plasmid pBT (a component of the BacterioMatch® Two-Hybrid System) under the control of the lac-UV5 promoter in a region outside of the multiple cloning site (MCS). Prior to this subcloning step pBT had to be modified to delete the lambda cI (λcI) repressor gene, which was substituted with the gene for UCH-L3. To achieve this pBT was amplified with the oligonucleotides OCN 4pBT--LcI–For and OCN5 pBT--LcI-Rev (PCR conditions Table 2.6). The forward primer contains a site for the enzyme EcoRI and the reverse contains a site for NdeI. Upon completion of the PCR reaction this was incubated with DpnI to digest the methylated parent plasmid. With this strategy we amplified the entire plasmid, excluding the λcI gene (Fig. 2.3).

**Table 2.5.** PCR Conditions to amplify the gene for UCH-L3

| ***Step*** | ***Temperature*** | ***Time*** | ***Cycles*** |
|---|---|---|---|
| 1. | 94 °C | 10’ | 1 |
| 2. | 94 °C | 15” | 30 |
| 3. | 55 °C | 30’’ | 30 |
| 4. | 72 °C | 1’ | 30 |
| 5. | 72 °C | 10’ | 1 |
| Store at 4 °C | | | |

Once purified and doubly digested the UCH-L3 gene and the amplified plasmid pBT-λcI (minus the λcI gene) were mixed at different ratios (1:3 and 1:9) and ligated with T4 ligase. *E. coli* cells (strain JM109) were transformed with 10 μL of ligation

reaction. Since pBT is a low copy plasmid individual colonies were grown in 25 mL of LB plus chloramphenicol (45 μg/mL) to obtain enough amounts of DNA for sequencing and further experimentation. Sequencing of genes cloned outside of the MCS in pBT required the design of two oligonucleotides: OCN18 Seq pBT LcI-For and PC19 seq pBT LcI-Rev.

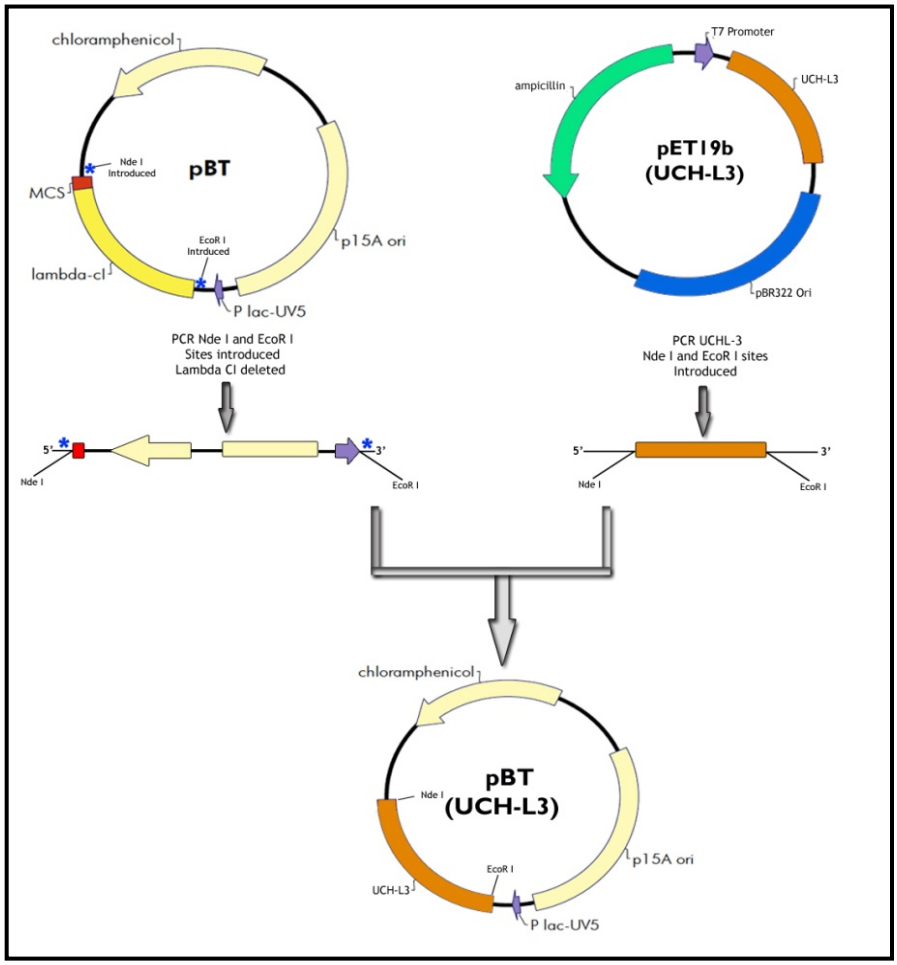


**Figure 2.4.** Generation of plasmid pBT/UCH-L3 for co-translational studies entailed the deletion of the λcI repressor gene from pBT and its substitution by the gene of UCH-L3. Specific antibiotic resistance is indicated for each plasmid. The origin of replication in pBT/UCH-L3 (p15 Ori) allows compatibility with the origin of replication found in plasmids from the pET system (pBR322 Ori) in which the fusions are cloned. Plasmid compatibility is necessary for co-transformation of *E. coli* cells with plasmids that bear UCH-L3 and the substrates (see section 2.5.1).

**Table 2.6.** PCR Conditions to amplify pBT and delete the λCI gene

| ***Step*** | ***Temperature*** | ***Time*** | ***Cycles*** |
|---|---|---|---|
| 1. | 95 °C | 30’ | 1 |
| 2. | 95 °C | 30’’ | 16 |
| 3. | 55 °C | 1’ | 16 |
| 4. | 68 °C | 4’ | 16 |
| 5. | 72 °C | 10’ | 1 |
| Store at 4 °C | | | |

2.2.4 Generation of Insertion Mutant of UCH-L3

Recent publications have established that the crossover loop positioned on top of the active site of UCH-L3 during catalysis functions to regulate the size of the substrate that this enzyme can process [5, 6]. To test the potential role of this loop in the hydrolysis of the substrates introduced here we generated a mutant previously described by Zhou *et al*. [6]. Since UCH-L5 is known to hydrolyze a Lys-48 linked diubiquitin substrate Zhou *et al.* reasoned that the extra residues found in the loop of UCH-L5 could enable other deubiquitinases to accommodate and hydrolyze larger ubiquitin substrates as well. This approach resulted in the design of two insertion variants derived from UCH-L1 and UCH-L3. These insertions mutants were capable of hydrolyzing the Lys-48 linked diubiquitin substrate that the wild type enzymes did not process [6]. The position and the amino acids inserted were selected as a result of an alignment of UCH-L5 against UCH-L1 and UCH-L3 (Fig. 2.5). In the UCH-L3 mutant designed three consecutive amino acids (Thr, Lys and Thr) were inserted to extend the loop.


**Figure. 2.5.** Alignment of crossover loops from UCH-L1, UCH-L3 and UCH-L5. The alignment of these isoenzymes shows that the crossover loop in the hydrolase domain of UCH-L5 is larger than that of UCH-L1 and UCH-L3 by six and three amino acids, respectively. In bold are the three amino acids in UCH-L5 that were introduced in UCH-L3 [Modified from 6].

Generation of the UCH-L3 insertion mutant (UCHL3-TKT) was performed through site directed mutagenesis. For this reaction we used the high fidelity DNA poymerase Phusion, the plasmid containing the wild type gene of UCH-L3 as template and oligonucleotides OCN71 UCHL3TKT(SDM)-For and OCN72 UCHL3TKT(SDM)-Rev (conditions of reaction in Table 2.7). The amplified PCR product was digested with DpnI and incubated for 2 hrs at 37 °C. Plasmids generated in this reaction were transformed in chemically competent *E. coli* (Top10 cells). Plasmids from individual colonies were isolated and the correct incorporation of the three consecutive codons for Thre, Lys and Thre was confirmed via DNA standard sequencing.

**Table 2.7.** PCR Conditions to introduce the sequence of amino acids TKT in the crossover loop of UCH-L3

| ***Step*** | ***Temperature*** | ***Time*** | ***Cycles*** |
|---|---|---|---|
| 1. | 98 °C | 10’ | 1 |
| 2. | 98 °C | 30’’ | 18 |
| 3. | 55 °C | 40’’ | 18 |
| 4. | 72 °C | 5’ | 18 |
| 5. | 72 °C | 10’ | 1 |
| Store at 4 °C | | | |

2.2.5 Generation of Variants for FRET Studies

As a means to characterize the catalytic properties of UCH-L3 in the context of the ubiquitin fusions, we devised a system based on the Fluorescence Resonance Energy Transfer (FRET) phenomena. FRET systems require the establishment of a donor/acceptor pair. To fulfill this requirement we took advantage of a naturally occurring tryptophan in position 43 present in Gβ1 and the other protein-G variants and used it as a donor. As an acceptor we used IAEDANS, a commercially available fluorophore. This fluorophore is a thiol-reactive probe that covalently binds to the sufhydrl group in cysteine residues (Fig. 2.6) [7].

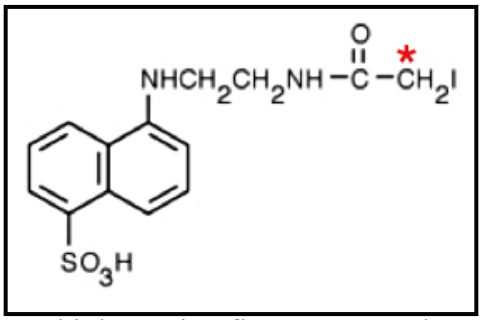


**Figure 2.6.** IAEDANS is a thiol-reactive fluorescent probe. The reaction between the α-carbon (*) in the iodoacetyl group and the sulfhydryl group from cysteine residues generates a stable thioether linkage (Modified from http://www. invitrogen.com).

Since cysteine is not present in ubiquitin this had to be introduced by site directed mutagenesis. With the goal of locating a surface residue with potential to be mutated to cysteine we analyzed the crystal structure of ubiquitin (PDB: 1UBQ). Our analysis indicated that threonine in position 14 was a reasonable candidate. Therefore, mutants Ub(T14C)-G, Ub(T14C)-MonA, Ub(T14C)-MonA(Y45A) and Ub(14C)-MonB were created using oligonucleotides OCN39 Ubi:GAB TtoC For and OCN40 Ubi:GAB TtoC

Rev as well as the specific templates from the corresponding ubiquitin fusion (PCR conditions Table 2.8). The amplified PCR products were digested with DpnI and incubated for 2 hours at 37 °C. Plasmids generated in this reaction were transformed in chemically competent *E. coli* (Top10) cells and plasmid from individual colonies isolated. The correct change T14 to C14 in ubiquitin was confirmed via DNA standard sequencing.

**Table 2.8.** PCR Conditions to generate ubiquitin (T14C) in ubiquitin fusions.

| ***Step*** | ***Temperature*** | ***Time*** | ***Cycles*** |
|---|---|---|---|
| 1. | 95 °C | 30’ | 1 |
| 2. | 95 °C | 30’’ | 16 |
| 3. | 55 °C | 1’ | 16 |
| 4. | 68 °C | 4’ | 16 |
| 5. | 72 °C | 10’ | 1 |
| Store at 4 °C | | | |

2.2.6 DNA and Protein Sequences

Sequencing of all the genes associated with this project was performed in the MicroChemical Core Facility at San Diego State University and by Retrogen Inc. Analysis of DNA and protein sequences was performed with Enzyme X and 4 Peaks software (http://www.mekentosj.com).

## 2.4 Protein Production and Purification

2.3.1 Gβ1 and Variants

The plasmids containing the genes coding for Gβ1 and variants were transformed into chemically competent *E. coli* (BL21 strain). A single colony from a plate was

inoculated 100 mL of LB media that contained ampicillin (45 μg/mL). The flask was rotated in an incubator at 275 rpm at 37 °C. After ~4 hours of growth the culture was transferred into 900 mL of fresh LB media. To monitor cell growth, absorbance (optical density) of the liquid culture was read every ~1 hour. When the culture reached an $OD_{600}$ of 0.6, protein production was induced by adding IPTG to a final concentration of 1 mM, followed by incubation for additional 3 hours. Upon completion of protein induction, the entire culture was centrifuged and the cell pellet subjected to three rounds of freeze/thaw (ethanol/dry ice bath for 10 minutes, water/ice bath for 30 minutes and room temperature for 15 minutes). The pellet from this step was resuspended in 20 mL of PBS buffer per liter of growth which resulted in a crude extract rich in proteins of interest [8]. The suspension was centrifuged for 35 min at 10,000 RPM and the supernatant collected. As a pre-purification step, some native proteins from *E. coli* were precipitated and removed by an acetonitrile cut. For this purpose, the supernatant from the previous step was diluted using 100% acetonitrile to a final concentration of 50% for the wild-type Gβ1 preparation and the MonA preparation and 30% for all other variants. This solution was incubated at room temperature for 30 minutes and centrifuged for 30 minutes at 10,000 RPM at 4 °C to remove insoluble material. The supernatant from this step was lyophilized for 24 hrs. Lyophilized material was resuspended in water, passed through a 0.45 μm filter and subjected to reverse phase HPLC using a C8 Dynamax column, applying a linear gradient of 1% $min^{-1}$ acetonitrile/water. Purified protein fractions from the HPLC were pooled, lyophilized, dissolved in 50 mM sodium phosphate at pH 6.5 and concentrated with centricons with a cut-off of 3 kDa. Protein purity was assessed by SDS-PAGE and

concentrations determined using the molar extension coefficients for tryptophan (5,500) and tyrosine (1,490) residues (Table 2.9).

**Table 2.9.** Spectral and physical properties of all proteins used in this thesis

| Protein | Number of amino acids | Molecular Weight (kDa) | Extinction Coeficcient ($M^{-1}$ $cm^{-1}$) |
|---|---|---|---|
| Protein G | 56 | 6.29 | 9970 |
| MonA | 56 | 6.20 | 9970 |
| MonB | 56 | 6.00 | 8480 |
| MonA(Y45A) | 56 | 6.15 | 8480 |
| MonB(A45F) | 56 | 6.07 | 8480 |
| Ubiquitin | 86 | 9.72 | 1490 |
| Ub-Ub | 162 | 18.26 | 2980 |
| UbUb-22 | 184 | 20.89 | 8480 |
| UCH-L3 | 252 | 28.7 | 20065 |
| Ub-G | 143 | 15.99 | 11460 |
| Ub-MonA | 142 | 15.90 | 11460 |
| Ub-MonB | 142 | 15.70 | 9970 |
| Ub-MonA(Y45A) | 142 | 15.81 | 9970 |
| Ub-MonB(A45F) | 142 | 15.77 | 9970 |

*Properties were computed using the amino acid sequences for each protein, including the HisTag. These calculations were performed in the website: http://web.expasy.org/protparam/

2.3.2 Ubiquitin and Ubiquitin Fusions

To achieve expression of ubiquitin and all the fusions we used the same protocol as that described in section 2.3.1. To extract the proteins of interest after induction, the cell pellet from 1 L of bacterial culture was resuspended in 40 mL of LEW buffer (Lysis-Equilibration-Wash: 50mM $NaH_2PO_4$, 300 mM NaCl, pH 8.0), pre-incubated on ice for 15 minutes and sonicated at room temperature 5X for 30 seconds with 1 minute of incubation on ice in between sonication cycles. The sonicated extract was cleared by centrifugation and taking advantage of the stability of ubiquitin at high temperatures the

supernatant was heated from 3-10 minutes at ~85 °C which resulted in substantial precipitation of native *E. coli's* proteins [9]. Next the supernatant was incubated on ice for 7 minutes and the insoluble material was removed by centrifugation for 10 minutes at 10,000 RPM. The clear supernatant was processed further; since ubiquitin and all fusions contain an N-terminal 6xHistag we used Ni-TED columns to perform immobilized metal affinity chromatography (IMAC). Cleared supernatants were loaded into a Ni-TED column, rinsed with LEW buffer and proteins bound specifically to the column were eluted with LEW buffer containing 250 mM imidazole. The eluted fractions from the column were concentrated with 6 kDa cut-off centricons for ubiquitin and 10 kDa cut-off centricons for fusions. Proteins were stored in 25 mM sodium phosphate buffer and 10 mM DTT at pH 6.8 at -20 ° C. Concentration of proteins was determined using standard UV-vis spectroscopy and extinction coefficients for each fusion (Table 2.7).

### 2.3.3 Ubiquitin Carboxy Hydrolase–L3 and UCHL3-TKT Insertion Variant

To achieve expression of UCH-L3 and the insertion variant (UCHL3-TKT) we used the protocol described in section 2.3.1. Since the gene for both forms of the enzyme contains an N-terminal 6xHistag we followed the same procedure to purify these enzymes as with the his-tagged ubiquitin and the fusions, except that the heat shock step that was omitted. Buffer composition for IMAC purification was also different. The equilibration buffer consists of: 20 mM sodium phosphate, 0.5 M sodium chloride and 20 mM imidazole at pH 7.4. The elution buffer consists of: 20 mM sodium phosphate, 0.5 M sodium chloride and 0.5 mM imidazole at pH 7.4. The eluted fractions were concentrated with centricons that had a molecular weight cut-off of 30 kDa. Enzyme was immediately

frozen in liquid nitrogen and stored at -80 °C in 20 mM sodium phosphate, 0.5 M sodium chloride and 10 mM DTT at pH 7.4. Enzyme concentration was determined as described in section 2.3.1.

**2.5 Circular dichroism.**

Circular dichroism data were collected for ubiquitin, MonA(Y45A), MonB(A45F), as well as fusions Ub-Ub, Ub-G, Ub-MonA, Ub-Mon(Y45A), Ub-MonB and Ub-Mon(BA45F) at protein concentrations of 50 μM in 50 mM sodium phosphate at pH 6.5. Collection of data was performed on a Jasco-810 spectrometer equipped with a thermoelectric unit and using a 0.1 mm path length cell. Initially, far UV continuous scanning from 260 to 195 nm was collected to assess secondary structure content at 25 °C. Thermal denaturation curves were monitored every 1 °C from 5 to 95 °C at 218 nm for Mon-A(Y45A), Mon-B(A45F) and fusions Ub-G, Ub-MonA, Ub-MonA(Y45A), Ub-MonB and Ub-MonB(A45F) and at 208 nm for ubiquitin and Ub-Ub. To determine the thermal denaturation point ($T_m$) the inflection in the melting curve was calculated by performing nonlinear regression analysis using the Boltzman equation [10, 11] for a sigmoidal curve:

$$OD = \frac{(A_1 - A_2)}{1+\exp\,(T-Tm)/dx} + A_2$$

Where $A_1$ is the low limit in the Y axis, $A_2$ is the high limit in the Y axis, $T$ is temperature in °C, $T_m$ is the inflection point in the fitted curve and $dx$ is the rate. This equation was solved using the IGOR PRO software package (version 6.11). In order to calculate of the $T_m$ of the fusion Ub-Ub the Boltzman equation was modified to include

the terms that fit the linear segment in the denaturation curve observed from 5 °C to 80°C:

$$OD = \frac{a+b*T(A_1 - A_2)}{1+\exp(T-Tm)/dx} + A_2$$

Where *a*= 0 (intercept in Y axis), *b*= 0.11816 (slope), *dc*=1 (rate), and $T_m$ = 85 °C. Similarly, to calculate the $T_m$ of the fusion Ub-G the Boltzman equation was modified to include the term that fits the polynomial segment in the denaturation curve, observed from 45 °C to 75°C.

$$OD = \frac{a+b*T^2(A_1 - A_2)}{1+\exp(T-Tm)/dx} + A_2$$

Where *a*= -3.04, *b*= 0.144, *dc*= 3.9, and $T_m$ = 78.7 °C. Normalization of thermal denaturation curves was performed by linearly shifting all points such that $[\theta]_{208}$ or $[\theta]_{218}$ value at 5 °C equaled zero. Next, a scaling factor was obtained for each set by dividing the maximum $[\theta]_{208}$ or $[\theta]_{218}$ value for all sets at 95 °C by the $[\theta]_{208}$ or $[\theta]_{218}$ value at 95 °C for each set. All data points for each set were then scaled by the unique scaling factor calculated separately for the set of Gβ1 and variants and one more for the set of ubiquitin fusions.

**2.6 Hydrolysis of Ubiquitin Fusions by UCH-L3.**

2.5.1 Co-translational Studies.

As a first approximation to estimate the extent of hydrolysis of ubiquitin fusions by UCH-L3 we performed co-translational studies. Under this format BL21 cells are

transformed with the plasmid coding for UCH-L3 and then individually with those of the ubiquitin fusions. By following this protocol the concomitant expression of both the substrate and the enzyme are possible, enabling the hydrolysis reaction to take place *in vivo* inside of the cell [12]. The advantages of this method are that small volumes of cultures can be used for analysis, no purification of the substrate or the enzyme are required and samples can be analyzed on SDS-PAGE without further processing. First, the preparation of chemically competent BL21 cells previously transformed with pBT/UCH-L3 was necessary. Then, competent BL21 (pBT/UCH-L3) cells were transformed with the individual plasmids containing the genes for the ubiquitin fusions. A single colony for each fusion was grown in 10 mL of LB media plus ampicillin (45 μg/mL) and chloramphenicol (45 μg/mL). The culture was rotated at 275 rpm and incubated at 37 °C until the $OD_{600}$ reached ~0.6. Induction of both the substrate and the enzyme was achieved simultaneously by the addition of 1 mM IPTG. Thereafter 0.5 mL aliquots of cultures were taken at 30, 60, 90, 120, 180 and 360 minutes, spun down for 3 minutes at 10,000 rpm on a bench top centrifuge and the supernatant discarded. For normalization of the cell pellets 2X loading dye was added in a proportion of 40 μL per $OD_{600}$ of 1. Normalized cell lysates were boiled for 3 min at 94 °C and centrifuged 1 minute at 13,000 rpm. Aliquots of the supernatants from the different time points were run on 15% SDS-PAGE, stained with Coomassie brilliant blue and inspected visually to assess substrate hydrolysis.

2.5.2 FRET Assay

For FRET studies we used Ub(T14C)-MonB as a model substrate. This ubiquitin fusion was produced and extracted with three cycles of freeze/thaw and the pellet resuspended in 20 mL of PBS pH 7.4 (see protocol 2.3.1, acetonitrile cut omitted). Assuming a protein yield of 4 mg/L of fusion [2] a 20 molar excess of the probe, IAEDANS, in solid form was added to the extract and incubated in the dark for 12 hours at 4 °C. Although this fusion can be purified by IMAC, separation of labeled from unlabeled substrate is not possible with this form of chromatography. Therefore separation of these two species was performed by HPLC as described in section 2.3.1. As a control unlabeled Ub(T14C)-MonB was purified under the same conditions in order to determine if the retention time had changed in the IAEDANS-labeled sample. For hydrolysis experiments reactions of 50 μM of substrate with 1.5 μM of enzyme were incubated in 250 μL at 37 °C. Data were collected at different times on a Fluoromax 3 fluorimeter (Horiba Corporation) with an excitation wavelength of 295 nm and a scanning range of 600 to 310 nm for acquisition.

2.5.3 *in vitro* Hydrolysis, SDS-PAGE

As an alternative to analyze the hydrolytic activity of UCH-L3 we implemented two different assays that require densitometric measurements of the hydrolyzed fusions run on SDS-PAGE gels. First, a time course-type of assay was run. Here for every time point analyzed a fixed amount of enzyme (10 pmole) was mixed with a fixed amount of substrate (70 pmole) and 0.5 μg of BSA as loading control. The reaction mixture was brought up to a final volume of 8 μL per time point with reaction buffer (25mM sodium

phosphate buffer and 10 mM DTT at pH 6.8) and incubated at 37 °C. To assess the progress of the reaction 8 μL aliquots were drawn at different time points, 2 μL of 4X loading dye added and rapidly heated for 3 minutes at 96 °C to stop the reaction. The protein components of the reactions were separated on 15% SDS-PAGE and gels were stained with Coomassie brilliant blue. The intensity of the band (in pixels) corresponding to the substrate was quantified with ImageJ software (v.1.43) [13]. The log of the band intensity corresponding to unreacted substrate was plotted against time to obtain a linear curve. From this curve the time point at which 50% of the substrate is hydrolyzed ($H_{50\%}$) was derived solving the equation for the linear curve in the form $y=mx+b$. In the second type of hydrolysis assay individual reactions with increasing amounts of enzyme (3.5, 7.0, 70.0, 140 and 278 pmole) were incubated with a fixed amount of the substrates (70 pmole) and 0.5 μg of BSA as loading control. The reactions wwere brought up to a final volume of 8 μL with reaction buffer and the mixtures incubated for 30 minutes at 37 °C. To stop the reactions 2 μL of 4X loading dye were added and rapidly heated for 3 minutes at 96 °C. The processed samples were run in SDS-PAGE gels and analyzed by densitometry with ImageJ. The percent of remaining substrate was obtained by dividing the intensity of the substrate's band by the intensity of the band from a control in which no enzyme was added (considered as 100%).

**2.7 Size Exclusion Chromatography of Ubiquitin Fusions**

The state of oligomerization of the ubiquitin fusions was assessed by means of size exclusion chromatography (SEC) in which a Superdex$^{TM}$ 75 analytical column was used in conjunction with an AKTA system. Buffer and flow rates used for all

experiments were 50 mM Tris, 100 mM NaCl at pH 8.0 at 0.8 mL/min. A total of ~5.5 μg of fusion protein in 100 to 150 μL of buffer were injected into the column. A calibration curve was prepared using a commercial low molecular weight gel filtration calibration kit. The three proteins used from the kit were chosen on the basis of the expected average molar mass of the fusions. To calculate the molar mass of each fusion the elution volumes were obtained from each individual chromatogram, the gel phase distribution coefficient ($K_{av}$) estimated and the molar mass derived by solving the equation for the standard curve generated. The $K_{av}$ were obtaine obtained as follows:

$$K_{av} = \frac{Ve-Vo}{Vc-Vo}$$

Ve= Elution volume of sample
*Vo=Void volume
*Vc=Column volume
*To obtain Vo and Vc blue dextran and ATP were run on the column

**2.7 Multidimensional NMR**

The overall fold of fusions Ub-G, Ub-MonA and Ub-MonB was investigated by means of multidimensional [$^{1}H$, $^{15}N$] heteronuclear single quantum coherence (HSQC) NMR. For this purpose proteins were produced and purified as described in section 2.1.2 with the exception that LB media was substituted with M9 minimal media containing $^{15}N$-ammonium sulfate (2 g/L). After purification proteins were diluted to ~650 μM in 50 mM sodium phosphate buffer at pH 6.5 prepared in a mixture containing 90% $H_2O$/ 10% $^{2}H_2O$. NMR spectra were collected at 20 °C on a Varian 600 MHz spectrometer using a pre-saturation sequence for solvent suppression. Data were processed with NMRPipe

(Varian) while NMR View (One Moon Scientific, Inc.) was used to generate and analyze spectra.

### 2.8 Molecular Visualization

All molecular representations were generated with MacPymol (DeLano Scientific LLC) [14].

## References


1. Komander, D. (2009). The emerging complexity of protein ubiquitination. *Biochem Soc Trans* **37**, 937-53.

2. Huang, P. S., Love, J. J. & Mayo, S. L. (2007). A de novo designed protein protein interface. *Protein Sci* **16**, 2770-4.

3. Patterson, M. (2008). Protein-Based Analysis of Amyloid Fibrilation and Inhibition Parameters. MSc Thesis. San Diego State University.

4. Barakat, N. H., Carmody, L. J. & Love, J. J. (2007). Exploiting elements of transcriptional machinery to enhance protein stability. *J Mol Biol* **366**, 103-16.

5. Popp, M. W., Artavanis-Tsakonas, K. & Ploegh, H. L. (2009). Substrate filtering by the active site crossover loop in UCHL3 revealed by sortagging and gain-of-function mutations. *J Biol Chem* **284**, 3593-602.

6. Zhou, Z. R., Zhang, Y. H., Liu, S., Song, A. X. & Hu, H. Y. (2012). Length of the active-site crossover loop defines the substrate specificity of ubiquitin C-terminal hydrolases for ubiquitin chains. *Biochem J* **441**, 143-9.

7. Jeganathan, S., von Bergen, M., Brutlach, H., Steinhoff, H. J. & Mandelkow, E. (2006). Global hairpin folding of tau in solution. *Biochemistry* **45**, 2283-93.

8. Johnson, B. H. & Hecht, M. H. (1994). Recombinant proteins can be isolated from E. coli cells by repeated cycles of freezing and thawing. *Biotechnology (N Y)* **12**, 1357-60.

9. Yost, P., Pilon, A. L., Lohnas, G. & Roberts, S. (1997). High-Level Expression and Efficient Recovery of Ubiquitin Fusion Proteins from Escherichia coli. *World Intellectual Property Organization.* **WO 97/001627**, 1-73

10. Christopoulos, M. H. a. *Fitting models to biological data using linear and nonlinear regression. A practical guide ti curve fitting.* , GraphPad Software Inc., San Diego., 2003.

11. Fiedler, J. D., Higginson, C., Hovlid, M. L., Kislukhin, A. A., Castillejos, A., Manzenrieder, F., Campbell, M. G., Voss, N. R., Potter, C. S., Carragher, B. & Finn, M. G. (2012). Engineered mutations change the structure and stability of a virus-like particle. *Biomacromolecules* **13**, 2339-48.

12. Larsen, C. N., Krantz, B. A. & Wilkinson, K. D. (1998). Substrate specificity of deubiquitinating enzymes: ubiquitin C-terminal hydrolases. *Biochemistry* **37**, 3358-68.

13. Abramoff, M. D., Magalhaes, P. J. & Ram, S. J. (2004). Image Processing with ImageJ. *Biophotonics International* **11**, 36-42.

14. Delano, W. L. & Lam, J. W. (2005). PyMOL: A communications tool for computational models. *Abstracts of Papers of the American Chemical Society,* **230**, U1371-U1372.

# CHAPTER III
# Biophysical Characterization of Free and N-Terminally Mono-ubiquitinated Variants of the Gβ1 Test Protein

## 3.1 Introduction

Ubiquitination of particular cellular protein results in the regulation of important processes such as gene transcription, nuclear export, vacuole localization and protein degradation [1, 2, 3, 4]. In addition, the integration of various "omics" tools has greatly expanded our view on alternative forms of protein ubiquitination and their functional significance [5]. Although the most highly utilized sites for ubiquitin attachment on target proteins are internal lysine residues, an alternative form of ubiquitination that occurs in the course of some viral infections, and the modification of tissues during oncogenesis, as well as cell cycle regulation, is N-terminal ubiquitination that also leads to protein degradation by the 26S proteasome [6, 7, 8, 9]. While ubiquitin has been the subject of extensive biophysical characterization, parallel studies on ubiquitinated proteins are only recently coming to light [10]. In the present chapter we explore the effects that N-terminal monoUbiquitination (N-tmUb) has on various biophysical properties of the resulting chimera (*i.e.,* ubiquitin and the C-terminally attached Gβ1 test variants). We describe first the rational design of small test proteins and the experimental assessment of their thermal stability. Furthermore, upon genetic fusion to ubiquitin the effect of N-tmUb on the thermal stability of these chimeric constructs is reported. The potential presence of oligomerization states of the ubiquitin fusions is also analyzed using size exclusion chromatography and finally, the extent of foldedness of some of the fusions is investigated by means of multidimensional NMR.

### 3.1.1 The β1 Domain of Streptococcal Protein G

Protein-G is a 65-kDa protein expressed in the cell surface of streptococcal bacteria from group G. It is believed that full-length protein-G functions to neutralize the mammalian immune response by binding to the Fc region of immunoglobulin G antibodies [11]. The Gβ1 domain from protein G has found widespread use in laboratories around the world for studies of protein folding and protein design from both theoretical and experimental perspectives [12]. Gβ1 is a small, independently folded, monomeric domain from protein-G that is composed of 56 amino acids. It is a thermophile ($T_m$ = 85 °C) that produces relatively high yields of protein when expressed in *E. coli* [13]. Structurally, Gβ1 consists of one α-helix and a four stranded β-sheet comprising two β hairpins (Fig. 3.1a).

Regions of the Gβ1 domain that are of physiological interest are the solvent-exposed residues located in the β strands (Fig. 3.1b). Variants of Gβ1 with mutations in these regions form fibril-like structures, thus serving as models for the *in vitro* study of amyloid fibrils, which are known to develop in pathologies such as familial amyloidosis and Alzheimer's disease [14, 15]. Similarly, different authors have explored the contribution of residues in the α-helix and the helix-sheet interface to the thermal stability of Gβ1 (Fig 3.1c) [16]. A five-fold variant with mutations in the α-helix produced a version of Gβ1 with a $T_m$ of 91 °C. At the same time, development of computational design methods in the field of protein design have been applied to reengineer the helix-sheet interface, producing hyperthermophiles with increased thermodynamic stability and melting temperatures that are greater than 100 °C [17, 18].

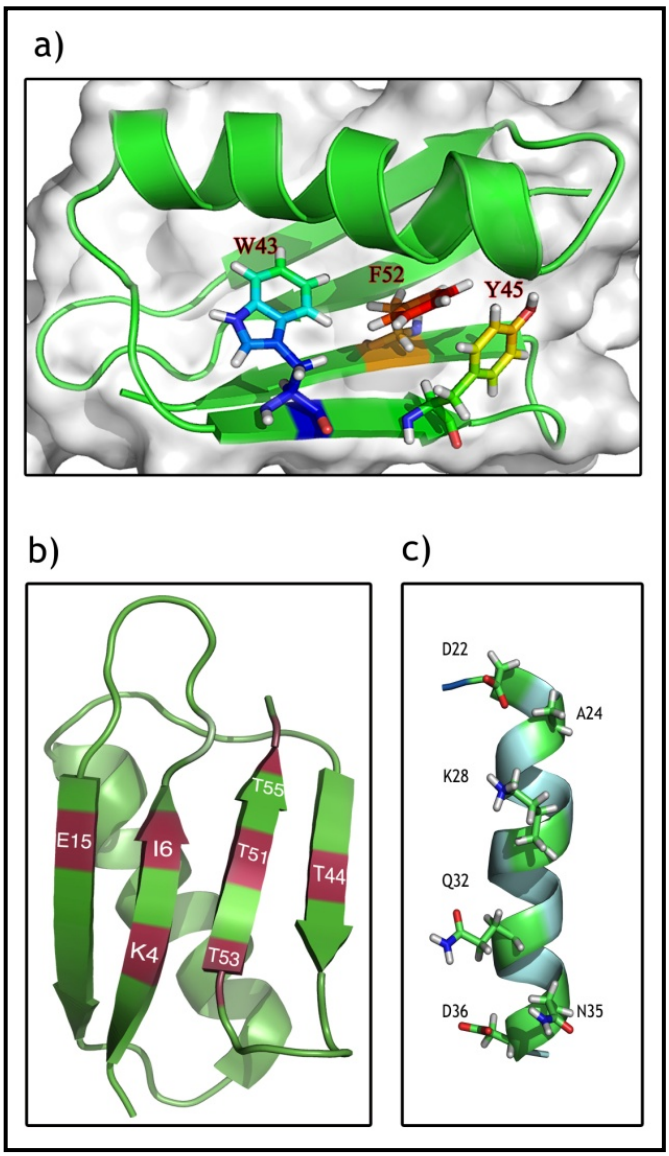


**Figure 3.1.** Structure of Gβ1 and positions explored in mutagenic studies. a) Tertiary structure of Gβ1 indicating the three amino acids that form an aromatic cluster: Trp43, Tyr45 and Phe52 [19]. b) Mutations in β-strands in positions indicated have generated variants that form fibril-like structures used to study the kinetics of fibril formation [14, 15]. c) Positions within the α-helix are relevant to the thermal stability of Gβ1 [16]. The introduction of residues with higher helical propensity results in increased stabilization due to favorable interactions with the helix dipole [16]. In addition, significant increased thermal stabilization has been achieved by introducing at α/β-interface residues that optimize its hydrophobic character and the geometry within the hydrophobic core [19] (PDB: 2GB1).

## 3.2 Results and Discussion

### 3.2.1. Protein Design

In a previous study, two variants of Gβ1 were engineered and are referred to as Monomer A (MonA) and Monomer B (MonB). MonA (a 12-fold mutant) is a hyperthermophile with a $T_m$ >100 °C and MonB (an 8-fold mutant) is a thermally destabilized variant with a modest $T_m$ of 38 °C [18]. Subsequent work performed in our laboratory showed that single point mutations at position 45 usually have a fairly significant effect on the structural stability of Gβ1. Mutation of alanine to tyrosine at position 45 in the context of the MonB sequence increased the stability of this variant from 38 °C to 72 °C and, conversely, mutation of tyrosine to alanine in the context of the Gβ1 wild-type sequence decreased the $T_m$ of this protein by 30 °C, from 85 °C to 55°C [19]. Based on these findings, we engineered two more mutants to alter the thermal stability of 'wild-type' MonA and 'wild-type' MonB, producing MonA(Y45A) and MonB(A45F) (amino acid sequences shown in Fig. 2.1).

### 3.2.2. Thermal Stability of G1β and Variants

The mutations introduced in MonA and MonB focused on position 45, which forms part of the aromatic cluster of the Gβ1 fold (Fig. 3.2). Our expectations were that MonB(A45F) would be more thermally stable than MonB and MonA(Y45A) would be less stable than MonA. The method used to measure the thermal stability and assess the secondary structure of these variants was circular dichroism spectroscopy (CD). Far ultraviolet (UV) CD spectra of MonA(Y45A) and Mono-B(A45F) are similar to that of

Gβ1 with a minima (where maximum negative signal intensity is observed) at ~218 nm (Fig. 3.3).

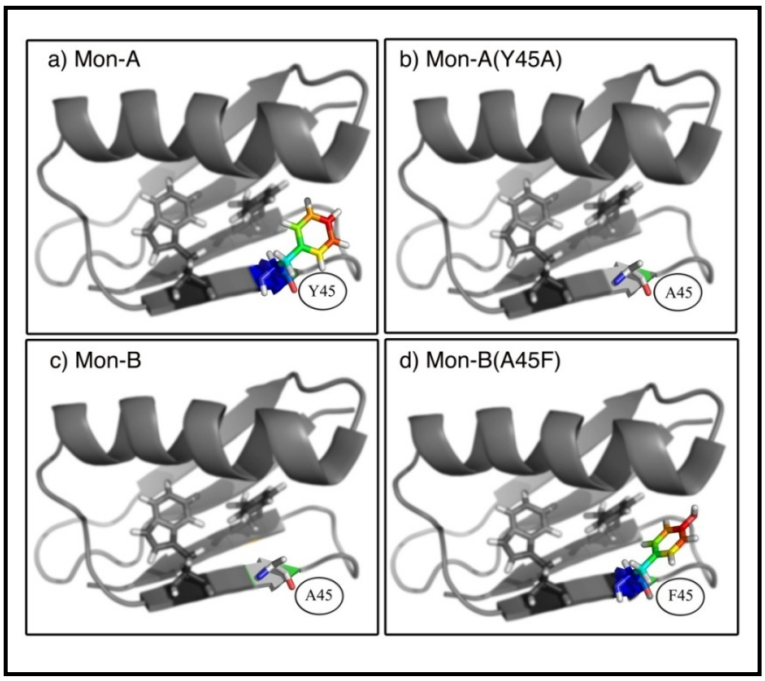


**Figure 3.2**. Positions of mutations for the engineered Gβ1 variants are shown in color. For MonA the tyrosine at position 45 was substituted by alanine to produce MonA(Y45A) (panels a and b). For MonB, the alanine at position 45 was substituted with a phenylalanine side-chain to produce MonB(A45F) (panels c and d). Stick projections in black and white indicate the other two amino acids that form the aromatic cluster, Trp43 and Phe52 (PDB: 2GB1).

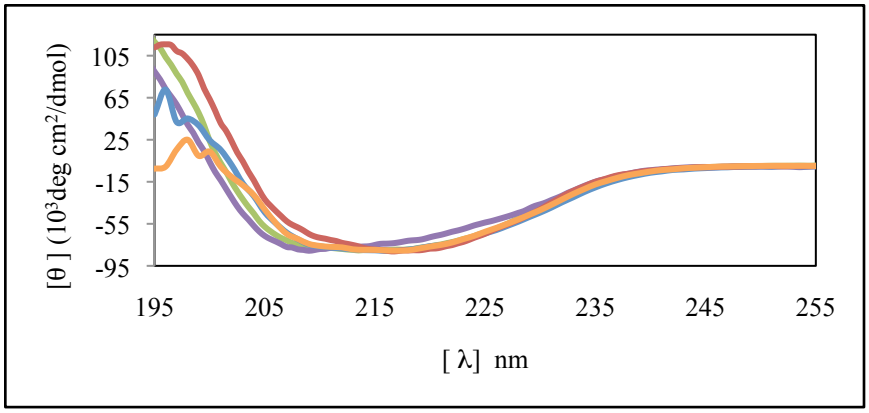


**Figure 3.3**. Normalized far UV CD scans at 25 °C from 195 to 260 nm. Gβ1, MonA, MonA(Y45A), MonB and MonB(A45F).The overall shape in the spectra for MonA(Y45A) and MonB(A45F) indicate an approximate and consistent α/β fold with respect to wild type Gβ1.

These similarities indicated that these variants most likely preserved the fold of the wild-type Gβ1 domain. To obtain thermal unfolding curves, protein unfolding was monitored at 218 nm and recorded every 1 °C from 5 °C to 95 °C (Fig 3.4). The slopes and the sigmoidal trajectory of the denaturation curves of MonA(Y45A) and MonB(A45F) are consistent with those of proteins that experience cooperative unfolding, a property also observed for Gβ1-WT [19]. This result provided additional evidence that MonA(Y45A) and MonB(A45F) most likely retained the native α/β fold of Gβ1.

The single amino acid changes made in MonA and MonB were introduced on the basis that the mutated residues may act independently to disrupt or complement the aromatic cluster formed by Trp43, Tyr45 and Phe52 (Fig 3.2). This design would potentially increase or decrease the thermal stability of the variants as observed elsewhere [19, 20].

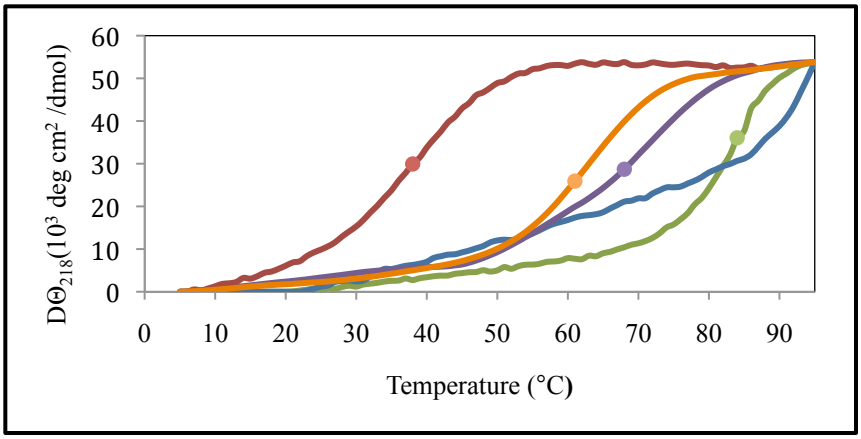


**Figure 3.4.** Normalized thermal unfolding curves for ■ Gβ1, ■ MonA, ■ MonA(Y45A), ■ MonB and ■ MonB(A45F). Signal was monitored at 218 nm. Except for MonA, the inflection point in each curve representing the $T_m$ is indicated by ( ● ).

The $T_m$*'s* derived from the unfolding curves (Fig. 3.4) confirm the expected effect of the mutations (Table 3.1). Substitution of a large aromatic residue Tyr by a small hydrophobic residue Ala, decreased the $T_m$ of MonA, from >100 °C to 68.7 °C. Likewise, the $T_m$ of MonB increased from 38 °C to 61.5 °C for the MonB(A45F) variant. In this case the substitution of Ala with Phe introduced a large aromatic residue that lead to stabilization, presumably by increasing the burial of hydrophobic surface area [17]. Upon collection of unfolding data, samples were cooled from 95 °C to 25 °C and scans from 195 nm to 260 nm were collected a second time to determine the reversibility of the unfolding process. A comparison of all the scans obtained pre and post thermal denaturation indicated that unfolding was likely reversible for all variants (data not shown).

**Table 3.1.** $T_m$ of Gβ1 and variants

| Protein Variant | $T_m$ (°C) |
|---|---|
| Protein Gβ1* | 85.0 |
| MonA* | >100 |
| MonA(Y45A) | 68.7 |
| MonB* | 38.0 |
| MonB(A45F) | 61.5 |

*Data from [18]

3.2.3 Thermal Stability of Ubiquitin

Ubiquitin is a key component of the ubiquitin proteasome system (UPS) and has been a model for biophysical studies on protein stability and folding [10, 21, 22]. This small protein composed of 76 amino acids (8.5 kDa) is chemically and thermally stable and has a compact fold that consists of two α-helices and a β-sheet made up of five β-strands (Fig. 3.5a) [10]. Of particular importance for the multiple biological roles ascribed to ubiquitin are the last four C-terminal amino acids Leu73, Arg74, Gly75 and Gly76; this sequence of amino acids form a stretch of unstructured residues (Fig. 3.5b) [23]. In most cases ubiquitination occurs when an isopeptide bond is formed between the carboxy-terminal Gly76 of ubiquitin and the ε-amino group of an internal lysine in the target protein. Subsequent ubiquitin polymerization by addition of distal ubiquitin moieties takes place in a similar fashion [24].

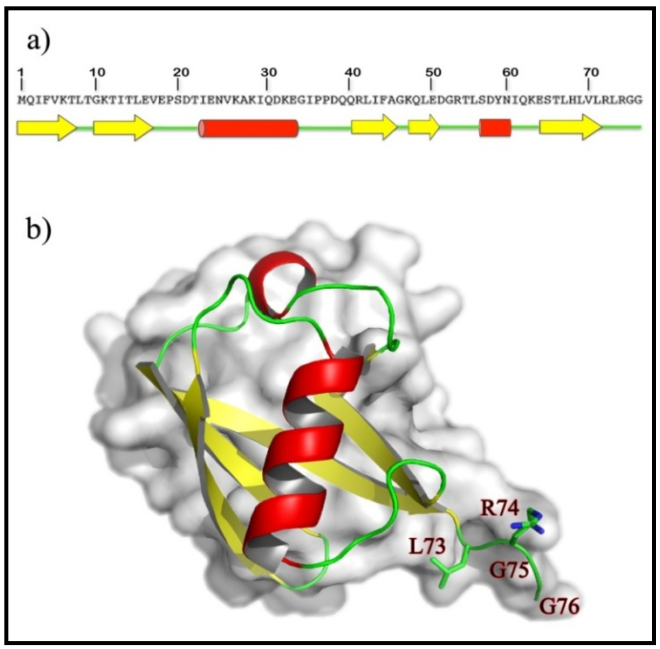


**Figure 3.5.** Structure of human ubiquitin. a) The amino acid sequence is matched to the elements of secondary structure. b) In the tertiary structure a stretch of unstructured amino acids at the C-terminus extends from the folded protein and is formed by Leu73, Arg74, Gly75, and Gly76 (PDB:1UBQ). The version of ubiquitin used in this thesis includes a six His-Tag at the N-terminus, which is also incorporated in all fusions.

One of the goals of our work was to investigate the thermal stability of N-terminally ubiquitinated proteins; therefore even though the thermal stability of ubiquitin is known we consider its characterization under our own experimental conditions to be essential [25]. To achieve this for ubiquitin we followed the same approach described above for the thermal characterization of variants derived from Gβ1. The far UV CD spectrum of ubiquitin collected at 25 °C is indicative of a well-structured protein with two minima at ~208 nm and ~228 nm (Fig. 3.6). Importantly, ubiquitin and Gβ1 were speculated to be evolutionary and structurally related, however the sequence identity between the two proteins is fairly low (*i.e.,* 12%), their functions are distant and their far UV spectra are also different (Fig. 3.2 and 3.6) [11, 26]. The differences in far UV

spectra of ubiquitin and Gβ1 will be relevant later when the spectral properties of the fusions between these two proteins are discussed.

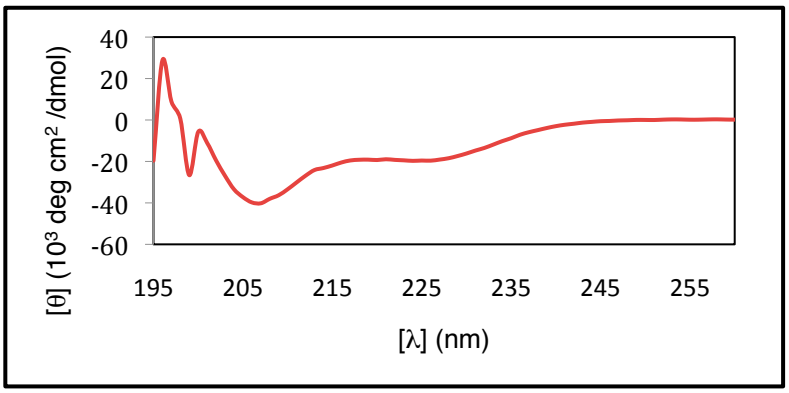


**Figure 3.6**. Far UV CD scan of ubiquitin at 25 °C from 195 nm to 260 nm. Two minima occur, one at ~208 nm and one more at ~228 nm.

The $T_m$ of ubiquitin was determined by monitoring the 208 nm signal intensity and was found to be 88 °C (Fig. 3.7). Thermal unfolding of ubiquitin takes place via a two-state mechanism (folded → unfolded) and the $T_m$ obtained here is comparable to other values previously reported under similar experimental conditions (*i.e.,* at pH 4, $T_m$ 91 °C) [25] corroborating that ubiquitin is a thermally stable protein.

These findings raise the question as to where does the stability of ubiquitin arise? The mechanisms of stabilization of this protein have been explored; ubiquitin does not contain disulphide bonds, it does not oligomerize, nor does it bind metal co-factors, which are all means by which stability is conferred in other proteins. Instead, van der Waals interactions and intramolecular hydrogen bonds appear to be the major contributors [25]. The structure of ubiquitin is tightly hydrogen-bonded with roughly 87% of the polypeptide chain involved in hydrogen-bonded secondary structure [23].

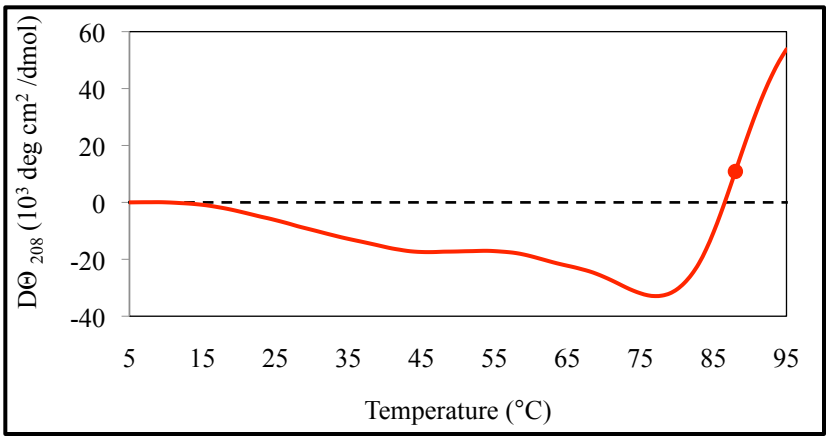


**Figure 3.7.** Thermal denaturation of ubiquitin monitored at 208 nm. Thermal denaturation occurs at 88 °C. The fact that ubiquitin exhibits cold denaturation is suggested by an increase in secondary structure content from ~20 °C to ~75 °C. Dashed line represents the 0 value of the Y-axis. The inflection point in the curve, representing the $T_m$ is indicated by ( ● ).

A comparison of the thermal denaturation curve of ubiquitin (Fig. 3.7) with those of Gβ1 and its variants (Fig. 3.3) reveal an interesting observation. While Gβ1 and its variants unfold as the temperature increases, the opposite is true for ubiquitin, to a point. At temperatures between ~20 °C and ~75 °C the signal falls below the baseline zero value mark in the $D\Theta_{208}$ axis and thus the secondary structure content of the protein appears to increase over this temperature span. This behavior, in which proteins gain secondary structure as a function of temperature, is indicative of cold denaturation and it was previously demonstrated to occur in ubiquitin [27, 28]. Cold denaturation derives from changes in the interaction between water molecules and non-polar side chains of amino acids. Mechanistically, cold denaturation initiates when the hydrophobic core of a protein is disrupted at low temperatures and the side chain of non-polar amino acids become hydrated due to increased exposure to the solvent [28, 29, 30]. In contrast to what one may expect, hydration of non-polar side chains is thermodynamically favorable (*i.e.,*

has a negative Gibbs energy of hydration) [28]. Following the thermal denaturation measurements of ubiquitin we observed a slight precipitation in the sample cells. This is consistent with a report that indicates that ubiquitin tends to aggregate after denaturation at pH >4.0 and our measurements were performed at pH 6.5 [25]. Still, a comparison of the scans from 195 nm to 260 nm pre- and post melting temperature measurement shows that remaining soluble ubiquitin experienced reversible unfolding.

### 3.2.4 Thermal Stability of N-terminally Mono-Ubiquitinated Variants

The two variants of MonA and MonB described above, in combination with Gβ1 make up a panel of five proteins with a range of thermal stabilities that run from 38°C to >100 °C (Table 3.1). We wished to evaluate the effect of N-terminal ubiquitination (N-tmUb) on the stability of Gβ1, MonA, MonA(Y45A), MonB and MonB(A45F). PCR was used to clone the genes for each variant behind the gene for ubiquitin and the resulting fused proteins are indicated with the prefix Ub: *i.e.,* Ub-G, Ub-MonA, Ub-MonA(Y45A), Ub-MonB and Ub-MonB(A45F). We also included in our studies a linear diUbiquitin fusion (Ub-Ub). The motivation to include this construct arose from reports demonstrating that this is a naturally occurring ubiquitin fusion that exists in the same format (*i.e.,* N- to C- terminal) implemented in the design of our ubiquitin-Gβ1 chimeras [31, 32]. Other examples of N- to C- ubiquitin fusions found *in vivo* are small ribosomal proteins discovered in several species including human, rat and yeast [33, 34]. The fact that N-terminal monoubiquitination is observed in nature increases the potential validity and biological relevance of our engineered chimeric substrates.

Since experimental data describing the biophysical effect of attaching ubiquitin to the N-terminus of a protein is not available we considered that three possible scenarios may occur regarding the thermal stability of the fused proteins: 1) the thermal stability of the fusions will be the average of the stability of ubiquitin and the attached test protein, or 2) the stability will match that of one of the two domains of the fusions, (either that of ubiquitin or that of the C-terminal test variant), or 3) the thermal melting curves would be complex and exhibit two or possibly multiple transitions. In an effort to address these questions we used CD spectroscopy to measure the melting temperatures of the fusions between ubiquitin and the Gβ1 test variants. Following the same experimental procedures described above, we assessed the content of secondary structure of the ubiquitin/Gβ1 chimeras and the linear Ub-Ub dimer. Fig. 3.8 shows the Far-UV scans of Gβ1 fusions indicating the presence of two minima ~208 nm and ~223 nm. This suggests that these proteins have spectral properties similar to those of ubiquitin (minima at ~208nm and ~228 nm) and Gβ1 (minima at ~218nm) (Figs. 3.3 and 3.6). The two minima in the traces of the fusions also indicate α-helical content [35], consistent with the fact that more residues in the fusions are involved in forming α-helices as opposed to the individual proteins on their own.

The spectrum of the Ub-Ub fusion nearly overlaps that of ubiquitin, implying that these two proteins are highly similar in their content of secondary structure. This conclusion is supported by a publication in which the two subunits in Ub-Ub were found to conserve the overall structural integrity of the monomer [36].

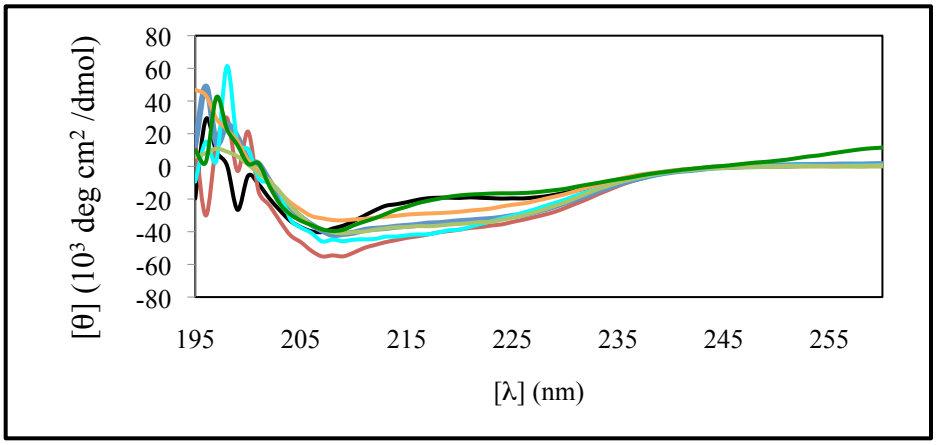


**Figure 3.8** Far UV CD scans at 25 °C from 195 nm to 260 nm. Ubiquitin, Ub-G, Ub-Ub, Ub-MonA, Ub-MonA(Y45A), Ub-MonB and Ub-MonB(A45F). The presence of two minima at ~208 and ~223 nm in the fusions indicate increased content of α-helical structure. The scan of ubiquitin is the same as that in Fig. 3.6 but is included here only as reference.

As suggested by the similarities in their far-UV spectra, we determined that the folding of the Gβ1 fusions was approximately conserved and proceeded to determine the thermal melts of all the fusions. Denaturation curves of all fusions reveal three notable findings (Fig. 3.9): 1) All curves show single mode transitions 2) the $T_m$'s of all the fusions are similar to that of the attached C-terminal test variant and 3) cold denaturation of ubiquitin in the fusions does not appear to occur in any of the denaturation curves obtained.

Considering that some of the Gβ1 variants have $T_m$'s markedly different from that of ubiquitin, we expected that the thermal denaturation curves of some of these fusions would possibly exhibit two transitions that potentially represent the individual and separate unfolding of each protein. A prime example of this assumption is represented by the fusion of ubiquitin with MonB; the difference in $T_m$ ($\Delta T_m$) between MonB and ubiquitin is 50 °C (38 °C and 88 °C respectively). Therefore we expected to possibly

observe two unfolding curves and two distinct transition points for the Ub-MonB fusion and that each would be close to the melting temperatures of each separate protein. In contrast, for the fusions of ubiquitin with more stable proteins such as Gβ1, which has a $\Delta T_m$ of 3 °C we anticipated a single transition point in the melting curve. Regardless of the substrate tested the thermal denaturation curves of all the ubiquitin fusions, including Ub-MonB exhibit only one transition (Fig. 3.9). A result similar to this was reported by Patel et al. Using linear fusions of ubiquitin and variants of a ubiquitin interacting motif (UIM1) it was found that all constructs analyzed displayed single sigmoidal transitions [37]. The analysis of the Ub-UIM1 variants by far- and near CD UV and differential scanning calorimetry revealed that these fusions could be fit to a two-state model of unfolding [37]. Likewise the two components of the fusions we have characterized (i.*e.,* ubiquitin and Gβ1) are known to undergo two-state unfolding transitions [25, 38]. Therefore, considering the cases of the Ub-UIM1, ubiquitin and Gβ1 we conclude that most likely Ub-G, Ub-MonA, Ub-MonA(Y45A), Ub-MonB, Ub-Mon(A45F) and Ub-Ub undergo two-state unfolding.

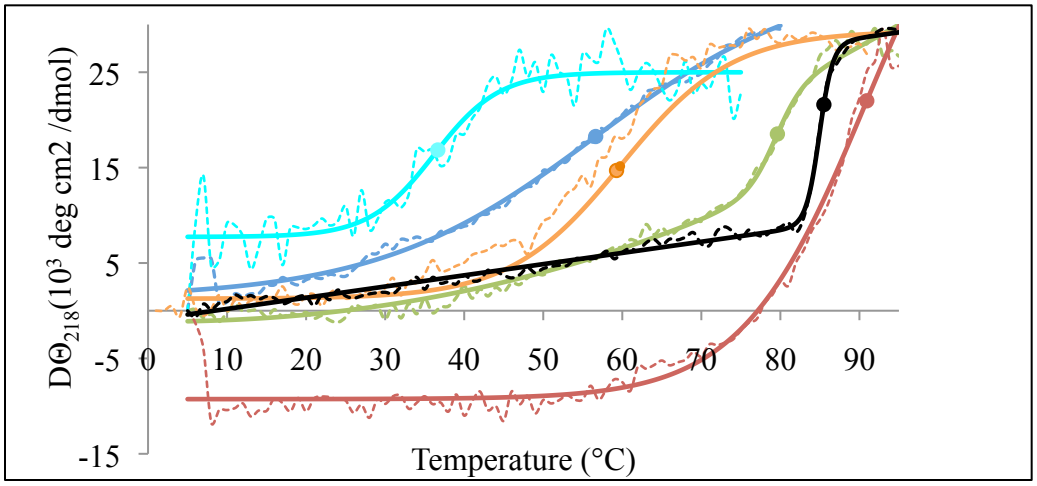


**Figure 3.9** Normalized thermal denaturation curves of ubiquitin fusions monitored at 218 nm for Gβ1 variants and at 208 nm for Ub-Ub. ■ Ub-G, ■ Ub-MonA, ■ Ub-MonA(Y45A), ■ Ub-MonB, and ■ Ub-MonB(A45F) and ■ Ub-Ub. The Inflection points in curves are indicated by (●). Solid lines show the results of the nonlinear regressions analysis according to the Boltzman equation. Signal for Ub-MonB and Ub-MonA(Y45A) was plotted to 70 °C and to 80 °C given a sudden drop of signal experienced at these temperatures. We attribute this to sample precipitation seen after the experiment was completed. Still, derivation of $T_m$s from these two curves was possible (see chapter II).

Regarding the second point raised above (*i.e.,* the $T_m$'s of all the fusions are similar to that of C-terminal test variant), a comparison of the stability of the ubiquitin fusions with the non-fused counterpart shows that the two versions of each protein (*i.e.,* unfused Gβ1 and the Ub-G fusion) have similar thermal stabilities (Table 3.2). Overall, the $T_m$'s of the fusions resemble the corresponding Gβ1variant rather than to that of ubiquitin. At the same time, when the stabilities of the free proteins are ranked in parallel with those of their ubiquitin-fused counterparts, a similar trend is observed (Fig. 3.10). Although a statistical analysis of significance of $T_m$'s (*i.e,* P value) is not possible since denaturation curves were collected only once, the high reproducibility of the values obtained by CD spectroscopy has been demonstrated [39]. Predki et al. used a series of 30 mutants of Rop, an all α-helix protein and showed that $T_m$'s of these variants were

reproducible in a range of ±0.5 °C [39]. Taken together, our data suggest that at least in the context of N-terminal mono-ubiquitination, ubiquitin does not increase the stability of the protein that is attached to, but instead has a slight destabilizing effect.

**Table 3.2.** $T_m$ of Gβ1, variants and ubiquitin fusions

| **Free Protein** | $T_m$ **(°C)** | **Ubiquitin Fusion** | $T_m$ **(°C)** |
|---|---|---|---|
| Ubiquitin | 88 | Ub-Ub | 85 |
| Protein-Gβ1* | 85 | Ub-G | 79.8 |
| MonA* | >100 | Ub-MonA | 90.7 |
| MonA(Y45A) | 68.7 | Ub-Mon(Y45A) | 56.6 |
| MonoB* | 38 | Ub-MonB | 36.2 |
| MonB(A45F) | 61.5 | Ub-MonB(A45F) | 59.8 |

*Data from [18]

Previous studies have successfully characterized the thermal and chemical stability of ubiquitin, however research aimed at exploring the influence of ubiquitination on the stability of targeted proteins has been limited [21, 27]. In one body of work Hagai et al. applied *in silico* techniques to modify Ubc7 (an E2 ubiquitin ligase) by mono-ubiquitination and tetra-ubiquitination on Lys18, Cys89 or Lys94 [40]. As we report here mono-ubiquitination resulted only in slight destabilization of the test proteins attached to ubiquitin. The *in silico* study demonstrated that lys63-linked tetraubiquitination on the same residues induced an increased destabilizing effect, while Lys48-linked tetraubiquitination induced the strongest thermal destabilization and local unwinding [40]. Our results are consistent with this publication, and support the concept that one ubiquitin moiety may not significantly alter the biophysical properties of proteins to which it is attached. Instead, the attachment of four or more moieties may be necessary for a pronounced effect to be observed.

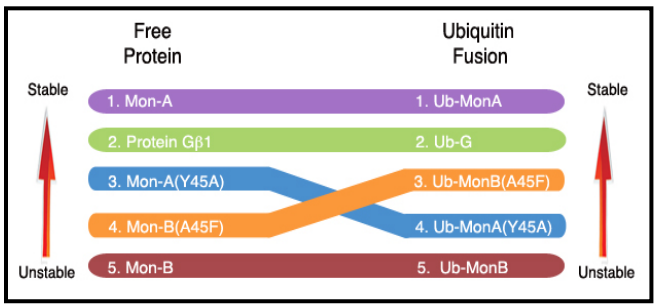


**Figure 3.10**. Ranking of thermal stability of proteins in free and fused forms. The stability rank in the free proteins is similar to that of the ubiquitinated forms. The exceptions to this observation are Ub-MonB(A45F) and Ub-MonA(Y45A). Still, the difference between these two fusions is only of 3.2 °C. The direction of the arrows indicates increasing thermal stability.

Furthermore, the slight destabilization observed in all of our fusions (Table 3.2) supports the findings of Hagai et al. that indicate that protein modification by ubiquitination may not only function as a tag for destruction, but it may also facilitate protein degradation through the UPS by inducing unfolding [40].

Finally, we return to the third notable finding described above (*i.e.,* cold denaturation of ubiquitin in the fusions does not seem to occur in any of the denaturation curves obtained). As measured by CD spectroscopy, one of the most unique properties of ubiquitin, cold denaturation, is not observed in any of the five fusions analyzed. Surprisingly this observation is also valid for the dimer of ubiquitin, Ub-Ub. Ubiquitin appears to gain secondary structure from ~20 °C to ~75 °C, which is explained as a tighter structural packing (Fig. 3.7). In contrast, in this range of temperatures only a constant unfolding and loss of $D\Theta_{208/218}$ signal is observed in all the fusions as well as in the non-fused variants. Similarly Patel et al. report near UV-CD melting profiles on five Ub-UIM1 variants that are consistent with our results [37]. All five curves presented in this publication are equivalent in terms of shape and trajectory to those of the Ub-Gβ1

chimeras and more interestingly, no evidence of cold denaturation of ubiquitin was observed.

Why is cold denaturation not observed when ubiquitin is N-terminally attached to other proteins? One obvious possibility is that this property is lost when ubiquitin is fused to other proteins. Another possible explanation is that the signal observed for the unfolding of the C-terminal test variant interferes with the detection of increasing secondary structure content for ubiquitin. Unfolding of the C-terminal test variant as the temperature increases and packing of ubiquitin are opposite phenomena. Possibly, the change in signal as unfolding of the C-terminal domain occurs is greater than the change in signal as packing of ubiquitin takes place, hence only the event with the largest change in $D\Theta_{218}$ is represented in the data. The analysis of cold denaturation imposes an evident limitation for its study by solution-based spectroscopic methods: buffers used to characterize proteins freeze at ~0°C. An experimental method that has overcome this limitation and may provide further insights on the structural features of ubiquitin fusions is based on NMR spectroscopy and protein encapsulation [41]. Multidimensional NMR and protein encapsulation on reverse micelles has been applied to study ubiquitin at negative temperatures [41]. When the spectra of ubiquitin were collected at +20 °C and -10 °C only subtle differences were seen. As the sample temperature was decreased, from -20 to -25 °C several $^{15}N$-$^{1}H$ crosspeaks were not detected and a transition took place that made only a few $^{15}N$-$^{1}H$ crosspeaks observable at -30 °C. All these effects were reversible until the sample was frozen at -35 °C [42]. Potentially, the direct observation of the fusions introduced here in a similar experimental setup would let us determine

more precisely if ubiquitin still undergoes cold denaturation when is attached to the N-terminus of other proteins.

### 3.2.5 Size Exclusion Chromatography

The oligomerization state of proteins has been investigated from the perspective of protein thermal stability. Several structural studies have shown a positive correlation between oligomerization and the stability of proteins that form homo-oligomeric structures [43, 44, 45]. Frequently, protein oligomerization involves the formation of interfacial interactions and a correlation has been show between oligomerization and the hyperthermostability of archeon proteins [45]. Within the context of our research, oligomerization may signify increased thermal stability in some of the fusions. In this analysis we did not include Ub-Ub since two groups have confirmed independently by X-Ray crystallography that this ubiquitin fusion is a monomer [36, 46].

In order to assess the potential presence of oligomers on the fusions we used size exclusions chromatography (SEC). SEC allows an approximation of the molecular mass of proteins and from this we can infer the possible occurrence of oligomers. A calibration curve was prepared using standard methods. The specific properties of aprotinin, ribonuclease A and carbonic anhydrase as well as the standards used to determine the column volume (Vc) and the void volume (Vo) are listed in table 3.3.

As shown in table 3.4 the molar masses of the fusions are generally larger than the expected values for monomers by an average of ~7.5 kDa (Table 3.4). A remote possibility for this discrepancy may be the result of post-translational modifications of the

fusions. *E. coli* is capable of producing post-translational modifications such as acetylation, methylation, phosphorylation and glycosylation [47, 48, 49, 50].

**Table 3.3.** Standards used to prepare the calibration curve and characterize the Superdex$^{TM}$ 75 SEC column

| ***Standard**** | ***Molar Mass Reported (Da)*** | ***Elution Volume Observed (mL)*** |
|---|---|---|
| Aprotinin | 6,500 | 15.76 |
| Ribonuclease A | 13,700 | 13.33 |
| Carbonic Anhydrase | 29,000 | 11.60 |
| ATP (Vc) | 507.18 | 18.0 |
| Blue dextran (Vo) | 2,000,000 | 7.63 |

*kit LMW (GE Healthcare). Vc: Column volume. Vo: Void volume

However, it is unlikely that any of these modifications (or combinations there of), would account for the increased molar masses observed, since neither human ubiquitin nor Gβ1 are known to be post-translationally modified when expressed in *E. coli* [13,51].

**Table 3.4.** Molar mass of ubiquitin fusions obtained experimentally

| ***Ubiquitin Fusion*** | ****Molar mass Expected (kDa)*** | ***Molar Mass Determined (kDa)*** |
|---|---|---|
| Ub-G | 15.99 | 23.44 |
| Ub-MonA | 15.90 | 25.18 |
| Ub-MonA(Y45A) | 15.81 | 22.38 |
| Ub-MonB | 15.70 | 23.33 |
| Ub-MonB(A45F) | 15.77 | 22.51 |

*Obtained by adding the individual molar mass of each amino acid in the peptide chain

Alternatively, separation of proteins and their distributions by SEC does not depend only on the molar mass but also on the hydrodynamic volume of the solutes (a function of size and shape of molecules) [52]. Consistently, the crystal structure of Ub-Ub shows that the region connecting both units is partially disordered, allowing this

dimer to adopt an “open” extended conformation that may increase its hydrodynamic volume and its apparent molar mass (Fig 3.11) [53]. The extended nature of this dimer is in agreement with the observation that the proximal and distal ubiquitin moieties do not interact with each other as it does happen in the Lys48-linked dimer [54]. The crystal structure of the Lys48-linked dimer shows that this protein exhibits a “closed,” compact conformation in which “Ile44 hydrophobic patch” in both units are packed against each other and shielded away from the solvent [54]. We consider these facts relevant because the Ub-Ub dimer is linked in the same format as the ubiquitin fusions studied here, from N- to C- terminal. Therefore is reasonable to consider that the ubiquitin-Gβ1 chimeras may exhibit an open conformation and consequently the molar masses observed by SEC may seem larger than expected.

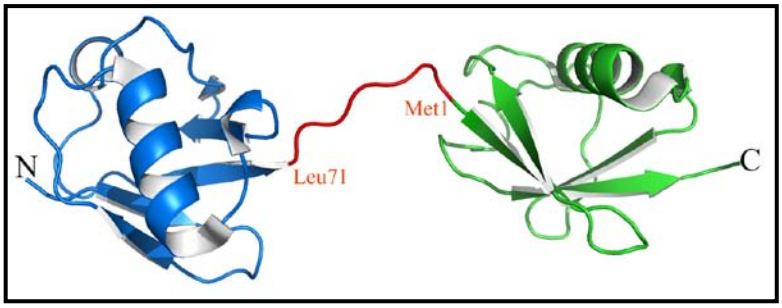


**Figure 3.11**. Structure of the linearly linked Ub-Ub dimer. The proximal ubiquitin is shown in blue and the distal ubiquitin in green. In red is the linkage that connects both ubiquitin units and extends for 7 amino acids, from Leu71 in the proximal moiety to Met1 in the distal one. The linkage is partly disordered with high temperature factors, consistent with intrinsic flexibility [46].

Furthermore, both ubiquitin and Gβ1 are determined to exist as monomers and it is unlikely that these two proteins will interact with each other to form oligomers when genetically fused [13, 51]. Finally, all the fusions eluted from the chromatographic

column at very similar volumes (from 11.84 to 12.15 mL) suggesting that these proteins occur in the same monomeric form, and therefore oligomerization does not account for the different thermal stabilities observed.

### 3.2.6 Structural Studies by Multi-Dimensional NMR

We have successfully demonstrated that the stability of N-terminal ubiquitin fusions parallels the stability of Gβ1 variants and established that all fusions exist in a monomeric state. Next we looked to correlate the thermal stability of some ubiquitin fusions with their conformational stability. In order to accomplish this goal, multidimensional NMR was employed. The Heteronuclear Single Quantum Coherence (HSQC) experiment is used to obtain a fingerprint of the folded state of a [$^{1}H^{15}N$]-labeled protein. The signal dispersion and high resolution in the spectra of Ub-G, Ub-MonA and Ub-MonB are properties consistent with those of well-folded proteins (Fig 3.11). This confirms the CD data (Fig. 3.8) and supports our observation that the Gβ1 topology is likely maintained in all five ubiquitin fusions.

Unexpectedly the spectrum of Ub-MonB, the least stable variant, indicates that this is a compact and significantly folded protein and no substantial differences are observed with the more stable variants, Ub-G and Ub-MonA. Still, some degree of conformational heterogeneity can be detected in Ub-MonB; multiple peaks are observed for the amide proton of Phe52 (*i.e.*, two peaks between ~10.05 and ~10.2 ppm in the proton scale in Fig. 3.11c). Multiple peaks arising from a single N-H bond are indicative of increased motion and dynamics. This is not observed in Ub-G and Ub-MonA that contain only one peak in this region of the spectra. It was shown previously that Gβ1

exhibits a single sharp peak in the amide proton of Phe 52 while MonB shows peak broadening and a set of three peaks for the same amide proton [19].

The differences in thermal stabilities of Ub-G, Ub-MonA and Ub-MonB are only mirrored minimally in the correspondent HSQC spectra. Consistently, the HSQC spectra of the non-fused proteins Gβ1, MonB and MonA are comparable in signal dispersion even though these proteins are different in regards to their thermal stability (Table 3.2) [19]. Therefore is not surprising that the differences in the thermal stabilities of the fusions are not reflected on HSQC spectra [19, 55]. A comparison of the HSQC spectra of the fusions with those of the free proteins suggests that the addition of the N-terminal ubiquitin does not adversely affect the folding of the C-terminal extensions. This is supported by the fact that several peaks in the free proteins are also found in the spectra of the ubiquitin fusions (Fig. 3.12).

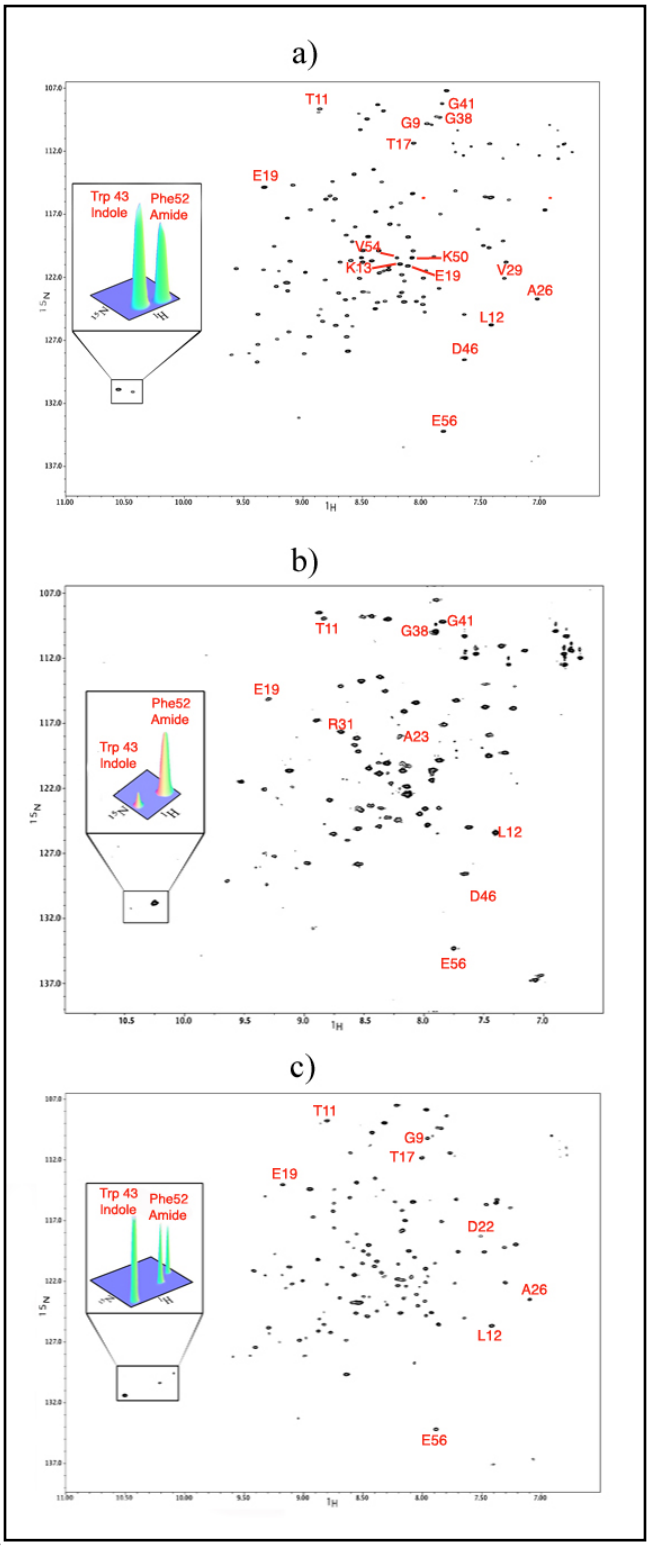


**Figure 3.12.** [$^{1}$H, $^{15}$N] HSQC spectra of ubiquitin fusions. a) Ub-G, b) Ub-MonA and c) Ub-MonB. The insets correspond to a 3D representation of W43 indole amide and F52 backbone amide. Amino acids identified in spectra of the correspondent non-fused proteins are indicated (see text for details) [ 18, 19, 56].

Tables 3.5, 3.6 and 3.7 contain the chemical shifts of peaks found in both the fused and the non-fused proteins. The positions of some amino acids in the spectra of Fig. 3.12 were determined by using the assignments on Gβ1, MonA and MonB previously published [18, 19, 56].

Complementing the data obtained from CD spectroscopy, the NMR experiments show that the small Gβ1 variants are only slightly influenced by attachment to ubiquitin, which is in agreement with several publications. Hagai et al., have demonstrated in *silico* that protein modification by a single ubiquitin molecule minimally affects the thermal stability of the modified protein [40]. The negative effect introduced by ubiquitin is only evident when proteins are modified by the addition of four ubiquitin moieties, suggesting that multiple ubiquitination may facilitate protein degradation at the 26S proteasome [40]. This hypothesis agrees with a report by Thrower et al. who established that a single ubiquitin is an inefficient degradation signal, although is still recognized by the proteasome with high affinity [57]. Thrower et al. determined that efficient proteasomal degradation of a target protein required a polyubiquitin chain of least four units linked to the same lysine residue [57]. Moreover, Freudenthal et al., found that ubiquitin had a narrow effect on the structure of an N-terminally mono-ubiquitinated protein. The structure of PCNA, a factor involved in DNA replication, displayed only minor structural differences in regards to the ubiquitinated form (*i.e.,* r.m.s. deviation of 0.6 Å over all the 254 Cα). The functional characterization of $^{Ubi}$PCNA established that this ubiquitinated protein self-assembled into a functional trimer capable of stimulating DNA polymerization [58].

**Table 3.5.** Chemical shift of peaks in the HSQC spectra of Ub-G also found in the HSQC spectra of Gβ1 [19]. The position of some residues has been determined using as reference the assignments on Gβ1 published elsewhere [56].

| Position | [$^{1}$H] Chemical Shift (ppm) | [$^{15}$N] Chemical Shift (ppm) |
|---|---|---|
| 1. Gly9 | 7.95 | 110 |
| 2. Thr11 | 8.9 | 108.5 |
| 3. Leu12 | 7.4 | 125.8 |
| 4. Lys13 | 8.2 | 120.8 |
| 5. Thr17 | 8.08 | 111.8 |
| 6. Glu19 | 8.18 | 121 |
| 7. Ala26 | 7.02 | 123.5 |
| 7. Val29 | 7.3 | 122 |
| 8. Gly38 | 7.88 | 109.2 |
| 9. Gly41 | 7.82 | 108 |
| 10. Trp 43 | 10.6 | 131 |
| 11. Asp46 | 7.65 | 128.5 |
| 12. Lys50 | 8.08 | 120.5 |
| 13. Phe52 | 10.4 | 131.2 |
| 14. Val54 | 8.2 | 120.5 |
| 15. Glu56 | 7.82 | 134.2 |
| 16. | 9.57 | 121.3 |
| 17. | 9.4 | 125 |
| 18. | 9.4 | 127.2 |
| 19. | 9.4 | 128.8 |
| 20. | 9.2 | 117.2 |
| 21. | 9.42 | 114.9 |
| 22. | 9.8 | 114.5 |
| 23. | 9.12 | 122.5 |
| 24. | 9.22 | 122.8 |
| 25. | 9.12 | 123 |
| 26. | 8.98 | 119.8 |
| 27. | 8.8 | 108.5 |
| 28. | 8.62 | 125 |
| 29. | 9.7 | 125.8 |
| 30. | 8.58 | 126.5 |
| 31. | 8.62 | 127 |
| 32. | 8.62 | 128 |
| 33. | 7.8 | 107.2 |
| 34. | 7.85 | 109 |
| 35. | 7.9 | 109.8 |
| 36. | 8.6 | 120.5 |
| 37. | 8.5 | 120.8 |
| 38. | 8.5 | 121 |

**Table 3.6.** Chemical shift of peaks in the HSQC spectra of Ub-MonA also found in the HSQC spectra of MonA [19]. The position of some residues has been determined using as guide the assignments on Gβ1 and MonA published elsewhere [56, 18].

| Position | [$^{1}$H] Chemical Shift (ppm) | [$^{15}$N] Chemical Shift (ppm) |
|---|---|---|
| 1. Thr11 | 8.8 | 108.9 |
| 2. Leu12 | 7.4 | 125.5 |
| 3. Glu19 | 9.3 | 115 |
| 4. Ala23 | 8.2 | 118 |
| 5. Arg31 | 8.6 | 117.5 |
| 6. Gly38 | 7.9 | 109.9 |
| 7. Gly41 | 7.8 | 110 |
| 8. Asp46 | 7.6 | 128.5 |
| 9. Trp43 | 10.4 | 131 |
| 10. Phe52 | 10.5 | 130.5 |
| 11. Glu56 | 7.75 | 134.5 |
| 12 | 10.1 | 129.5 |
| 13 | 9.4 | 128 |
| 14 | 9.25 | 125 |
| 15 | 9.05 | 122 |
| 16 | 9.0 | 121.5 |
| 17 | 9.45 | 121 |
| 18 | 8.8 | 120 |
| 19 | 9.2 | 114 |
| 20 | 8.95 | 126.5 |
| 21 | 8.85 | 125.5 |
| 22 | 8.8 | 126 |
| 23 | 8.77 | 108 |
| 24 | 8.75 | 126 |
| 25 | 8.6 | 129.9 |
| 26 | 8.6 | 127 |
| 27 | 7.95 | 124.9 |
| 28 | 7.85 | 124.5 |
| 29 | 7.85 | 110 |
| 30 | 7.8 | 125.2 |
| 31 | 7.4 | 116.25 |
| 32 | 7.35 | 116.2 |
| 33 | 7.3 | 123 |
| 34 | 7.2 | 119 |

**Table 3.7.** Chemical shift of peaks in the HSQC spectra of Ub-MonB also found in the HSQC of MonB [19]. The position of some residues has been determined using as guide the assignments on Gβ1 and MonB published elsewhere [56, 18].

| Position | [$^{1}$H] Chemical Shift (ppm) | [$^{15}$N] Chemical Shift (ppm) |
|---|---|---|
| 1. Gly9 | 7.98 | 110 |
| 2. Leu12 | 7.4 | 126 |
| 3. Thr11 | 8.8 | 108.5 |
| 4. Thr17 | 8 | 111.8 |
| 5. Glu19 | 9.15 | 114 |
| 6. Asp22 | 7.5 | 117.8 |
| 7. Ala26 | 7.1 | 123.5 |
| 8. Trp43 | 10.5 | 131.5 |
| 9. Phe52 | 10.2 | 130.2 |
| 10. Glu56 | 7.85 | 134 |
| 11. | 9.3 | 115 |
| 12. | 9.7 | 117.5 |
| 13. | 7.6 | 128.5 |
| 14. | 9.37 | 125 |
| 15. | 9.3 | 124 |
| 16. | 9.2 | 124 |
| 17. | 9.85 | 109 |
| 18. | 9.85 | 109 |
| 19. | 7.3 | 112.5 |
| 20. | 6.8 | 112.5 |

Acknowledgment:

This chapter, in part, is a reprint of the material as it appears in Navarro M., Carmody L., Romo O., and Love J. “Biochemical and biophysical effects of N-terminal monoubiquitination of small protein”. Manuscript in final stages of preparation.

## References

1. Hicke, L. (2001). Protein regulation by monoubiquitin. *Nat Rev Mol Cell Biol* **2**, 195-201.

2. Muyang Li, C. L. B., Foon Wu-Baer, Delin Chen, Richard Baer, Wei Gu. (2003). Mono- Versus Polyubiquitination: Differential Control of p53 Fate by Mdm2. *Science* **302**.

3. Boutet, S. C., Disatnik, M. H., Chan, L. S., Iori, K. & Rando, T. A. (2007). Regulation of Pax3 by proteasomal degradation of monoubiquitinated protein in skeletal muscle progenitors. *Cell* **130**, 349-62.

4. Torres, M. P., Lee, M. J., Ding, F., Purbeck, C., Kuhlman, B., Dokholyan, N. V. & Dohlman, H. G. (2009). G Protein Mono-ubiquitination by the Rsp5 Ubiquitin Ligase. *J Biol Chem* **284**, 8940-50.

5. Xu, G. & Jaffrey, S. R. (2011). The new landscape of protein ubiquitination. *Nat Biotechnol* **29**, 1098-100.

6. Ciechanover, A. & Ben-Saadon, R. (2004). N-terminal ubiquitination: more protein substrates join in. *Trends Cell Biol* **14**, 103-6.

7. Aviel, S., Winberg, G., Massucci, M. & Ciechanover, A. (2000). Degradation of the Epstein-Barr Virus Latent Membrane Protein 1 (LMP1) by the Ubiquitin-Proteasome Pathway. *J Biol Chem* **275**, 23491-23499.

8. Bloom, J., Amador, V., Bartolini, F., DeMartino, G. & Pagano, M. (2003). Proteasome-Mediated Degradation of p21 via N-Terminal Ubiquitinylation. *Cell* **115**, 71-87.

9. Reinstein, E., Scheffner, M., Oren, M., Ciechanover, A. & Schwartz, A. (2000). Degradation of the E7 human papillomavirus oncoprotein by the ubiquitin-proteasome system: targeting via ubiquitination of the N-terminal residue. *Oncogene* **19**, 5944-5950.

10. Jackson, S. E. (2006). Ubiquitin: a small protein folding paradigm. *Org Biomol Chem* **4**, 1845-53.

11. Falkenberg, C., Bjorck, L., Akerstrom, B. & Nilsson, S. (1987). Purification of streptococcal protein G expressed by Escherichia coli by high performance liquid affinity chromatography using immobilized immunoglobulin G and albumin. *Biomed Chromatogr* **2**, 221-5.

12. Byeon, I. J., Louis, J. M. & Gronenborn, A. M. (2003). A protein contortionist: core mutations of GB1 that induce dimerization and domain swapping. *J Mol Biol* **333**, 141-52.

13. Gallagher, T., Alexander, P., Bryan, P. & Gilliland, G. L. (1994). Two crystal structures of the B1 immunoglobulin-binding domain of streptococcal protein G and comparison with NMR. *Biochemistry* **33**, 4721-9.

14. Ramirez-Alvarado, M., Merkel, J. S. & Regan, L. (2000). A systematic exploration of the influence of the protein stability on amyloid fibril formation in vitro. *Proc Natl Acad Sci U S A* **97**, 8979-84.

15. Ramirez-Alvarado, M., Cocco, M. J. & Regan, L. (2003). Mutations in the B1 domain of protein G that delay the onset of amyloid fibril formation in vitro. *Protein Sci* **12**, 567-76.

16. Strop, P., Marinescu, A. M. & Mayo, S. L. (2000). Structure of a protein G helix variant suggests the importance of helix propensity and helix dipole interactions in protein design. *Protein Sci* **9**, 1391-4.

17. Malakauskas, S. M. & Mayo, S. L. (1998). Design, structure and stability of a hyperthermophilic protein variant. *Nat Struct Biol* **5**, 470-5.

18. Huang, P. S., Love, J. J. & Mayo, S. L. (2007). A de novo designed protein protein interface. *Protein Sci* **16**, 2770-4.

19. Barakat, N. H., Carmody, L. J. & Love, J. J. (2007). Exploiting elements of transcriptional machinery to enhance protein stability. *J Mol Biol* **366**, 103-16.

20. Barakat, N. H. & Love, J. J. (2010). Combined use of experimental and computational screens to characterize protein stability. *Protein Eng Des Sel* **23**, 799-807.

21. Ibarra-Molero, B., Loladze, V. V., Makhatadze, G. I. & Sanchez-Ruiz, J. M. (1999). Thermal versus guanidine-induced unfolding of ubiquitin. An analysis in terms of the contributions from charge-charge interactions to protein stability. *Biochemistry* **38**, 8138-49.

22. Loladze, V. V., Ibarra-Molero, B., Sanchez-Ruiz, J. M. & Makhatadze, G. I. (1999). Engineering a thermostable protein via optimization of charge-charge interactions on the protein surface. *Biochemistry* **38**, 16419-23.

23. Vijay-Kumar, S., Bugg, C. E. & Cook, W. J. (1987). Structure of ubiquitin refined at 1.8 A resolution. *J Mol Biol* **194**, 531-44.

24. Larsen, C. N., Krantz, B. A. & Wilkinson, K. D. (1998). Substrate specificity of deubiquitinating enzymes: ubiquitin C-terminal hydrolases. *Biochemistry* **37**, 3358-68.

25. Wintrode, P. L., Makhatadze, G. I. & Privalov, P. L. (1994). Thermodynamics of ubiquitin unfolding. *Proteins* **18**, 246-53.

26. Groenenborn, A. (1991). Similarity of Protein G and Ubiquitin. *Science* **254**, 581-582.

27. Ibarra-Molero, B., Makhatadze, G. I. & Sanchez-Ruiz, J. M. (1999). Cold denaturation of ubiquitin. *Biochim Biophys Acta* **1429**, 384-90.

28. Privalov, P. L. (1990). Cold denaturation of proteins. *Crit Rev Biochem Mol Biol* **25**, 281-305.

29. Davidovic, M., Mattea, C., Qvist, J. & Halle, B. (2009). Protein cold denaturation as seen from the solvent. *J Am Chem Soc* **131**, 1025-36.

30. Lopez, C. F., Darst, R. K. & Rossky, P. J. (2008). Mechanistic elements of protein cold denaturation. *J Phys Chem B* **112**, 5961-7.

31. Setsuie, R., Sakurai, M., Sakaguchi, Y. & Wada, K. (2009). Ubiquitin dimers control the hydrolase activity of UCH-L3. *Neurochem Int* **54**, 314-21.

32. Rahighi, S., Ikeda, F., Kawasaki, M., Akutsu, M., Suzuki, N., Kato, R., Kensche, T., Uejima, T., Bloor, S., Komander, D., Randow, F., Wakatsuki, S. & Dikic, I. (2009). Specific recognition of linear ubiquitin chains by NEMO is important for NF-kappaB activation. *Cell* **136**, 1098-109.

33. Olvera, J. & Wool, I. G. (1993). The carboxyl extension of a ubiquitin-like protein is rat ribosomal protein S30. *J Biol Chem* **268**, 17967-74.

34. Finley, D., Bartel, B. & Varshavsky, A. (1989). The tails of ubiquitin precursors are ribosomal proteins whose fusion to ubiquitin facilitates ribosome biogenesis. *Nature* **338**, 394-401.

35. Whitmore, L. & Wallace, B. A. (2008). Protein secondary structure analyses from circular dichroism spectroscopy: methods and reference databases. *Biopolymers* **89**, 392-400.

36. Rohaim, A., Kawasaki, M., Kato, R., Dikic, I. & Wakatsuki, S. (2012). Structure of a compact conformation of linear diubiquitin. *Acta Crystallogr D Biol Crystallogr* **68**, 102-8.

37. Patel, M. M., Sgourakis, N. G., Garcia, A. E. & Makhatadze, G. I. (2010). Experimental test of the thermodynamic model of protein cooperativity using temperature-induced unfolding of a Ubq-UIM fusion protein. *Biochemistry* **49**, 8455-67.

38. Alexander, P., Orban, J. & Bryan, P. (1992). Kinetic analysis of folding and unfolding the 56 amino acid IgG-binding domain of streptococcal protein G. *Biochemistry* **31**, 7243-8.

39. Predki, P. F., Agrawal, V., Brunger, A. T. & Regan, L. (1996). Amino-acid substitutions in a surface turn modulate protein stability. *Nat Struct Biol* **3**, 54-8.

40. Hagai, T. & Levy, Y. (2010). Ubiquitin not only serves as a tag but also assists degradation by inducing protein unfolding. *Proc Natl Acad Sci U S A* **107**, 2001-6.

41. Van Horn, W. D., Simorellis, A. K. & Flynn, P. F. (2005). Low-temperature studies of encapsulated proteins. *J Am Chem Soc* **127**, 13553-60.

42. Babu, C. R., Hilser, V. J. & Wand, A. J. (2004). Direct access to the cooperative substructure of proteins and the protein ensemble via cold denaturation. *Nat Struct Mol Biol* **11**, 352-7.

43. Kumar, S., Tsai, C. J. & Nussinov, R. (2000). Factors enhancing protein thermostability. *Protein Eng* **13**, 179-91.

44. Sinha, S. & Surolia, A. (2005). Oligomerization endows enormous stability to soybean agglutinin: a comparison of the stability of monomer and tetramer of soybean agglutinin. *Biophys J* **88**, 4243-51.

45. Tanaka, Y., Tsumoto, K., Yasutake, Y., Umetsu, M., Yao, M., Fukada, H., Tanaka, I. & Kumagai, I. (2004). How oligomerization contributes to the thermostability of an archaeon protein. Protein L-isoaspartyl-O-methyltransferase from Sulfolobus tokodaii. *J Biol Chem* **279**, 32957-67.

46. Komander, D., Reyes-Turcu, F., Licchesi, J. D., Odenwaelder, P., Wilkinson, K. D. & Barford, D. (2009). Molecular discrimination of structurally equivalent Lys 63-linked and linear polyubiquitin chains. *EMBO Rep* **10**, 466-73.

47. Freestone, P., Nystrom, T., Trinei, M. & Norris, V. (1997). The universal stress protein, UspA, of Escherichia coli is phosphorylated in response to stasis. *J Mol Biol* **274**, 318-24.

48. Polevoda, B. & Sherman, F. (2007). Methylation of proteins involved in translation. *Mol Microbiol* **65**, 590-606.

49. Sherlock, O., Dobrindt, U., Jensen, J. B., Munk Vejborg, R. & Klemm, P. (2006). Glycosylation of the self-recognizing Escherichia coli Ag43 autotransporter protein. *J Bacteriol* **188**, 1798-807.

50. Zhang, J., Sprung, R., Pei, J., Tan, X., Kim, S., Zhu, H., Liu, C. F., Grishin, N. V. & Zhao, Y. (2009). Lysine acetylation is a highly abundant and evolutionarily conserved modification in Escherichia coli. *Mol Cell Proteomics* **8**, 215-25.

51. Ecker, D. J., Butt, T. R., Marsh, J., Sternberg, E. J., Margolis, N., Monia, B. P., Jonnalagadda, S., Khan, M. I., Weber, P. L., Mueller, L. & et al. (1987). Gene synthesis, expression, structures, and functional activities of site-specific mutants of ubiquitin. *J Biol Chem* **262**, 14213-21.

52. Stulik, K., Pacakova, V. & Ticha, M. (2003). Some potentialities and drawbacks of contemporary size-exclusion chromatography. *J Biochem Biophys Methods* **56**, 1-13.

53. Komander, D. (2009). The emerging complexity of protein ubiquitination. *Biochem Soc Trans* **37**, 937-53.

54. Hirano, T., Serve, O., Yagi-Utsumi, M., Takemoto, E., Hiromoto, T., Satoh, T., Mizushima, T. & Kato, K. (2011). Conformational dynamics of wild-type Lys-48-linked diubiquitin in solution. *J Biol Chem* **286**, 37496-502.

55. Madl, T., Bermel, W. & Zangger, K. (2009). Use of relaxation enhancements in a paramagnetic environment for the structure determination of proteins using NMR spectroscopy. *Angew Chem Int Ed Engl* **48**, 8259-62.

56. Selenko, P., Serber, Z., Gadea, B., Ruderman, J. & Wagner, G. (2006). Quantitative NMR analysis of the protein G B1 domain in Xenopus laevis egg extracts and intact oocytes. Proc Natl Acad Sci U S A 103, 11904-9.

57. Thrower, J. S., Hoffman, L., Rechsteiner, M. & Pickart, C. M. (2000). Recognition of the polyubiquitin proteolytic signal. EMBO J 19, 94-102.

58. Freudenthal, B. D., Gakhar, L., Ramaswamy, S. & Washington, M. T. (2010). Structure of monoubiquitinated PCNA and implications for translesion synthesis and DNA polymerase exchange. Nat Struct Mol Biol 17, 479-84.

# CHAPTER IV
# Hydrolysis of N-Terminally Monoubiquitinated Proteins that Exhibit Different Thermal Stabilities using the Enzyme UCH-L3

## 4.1 Introduction

The human carboxy hydrolase–L3 (UCH-L3) enzyme is a cysteine hydrolase that removes several types of extensions covalently attached to the C-terminus of monoubiquitin *in vitro*. Some of these extensions include α-linked peptides, ε-linked peptides, amides and thioester-linked adducts [1]. Is been proposed that these activities may function *in vivo* to recycle ubiquitin or to release molecules inappropriately conjugated to it. Intriguingly in humans the physiological substrate of this enzyme still remains to be identified [2]. The biochemical characterization of UCH-L3 shows that this enzyme exhibits a preference for unfolded and small leaving groups as the activity towards larger ubiquitin conjugates of lysozyme and cytochrome C is low [3]. When the structure of UCH-L3 was solved Johnston *et al.* speculated that a 20 amino acid crossover loop formed by residues 146-167 acted as a filter to restrict the size of the ubiquitin extensions processed by this enzyme [1]. Recently, independent research from two groups provided convincing evidence to validate this long-standing speculation. In the work of one of these groups the length of the loop was extended by inserting three amino acids (Thr-Lys-Pro), thus conferring UCH-L3 with the capacity to accept and disassemble a larger diubiquitin substrate shown not to be cleaved by the wild type enzyme [4].

In chapter III we introduced a panel of designed proteins derived from Gβ1 that span a thermal stability range 38 °C to >100 °C. Upon the addition of a ubiquitin moiety at the N-terminus of the designed variants we observed that this modification did not affect the thermal stability of the designed proteins. Importantly, the thermal stability of the ubiquitin fusions resembles that of corresponding Gβ1 variant than that of ubiquitin (or for that matter the average of both proteins). In the present chapter we describe the semi-quantitative characterization of the hydrolytic properties of UCH-L3 in the context of the designed ubiquitin substrates characterized in chapter III. In doing so we look to explore the relevance of the thermal stability of proteins attached to the C-terminus of ubiquitin to their hydrolysis by UCH-L3.

## 4.2 Results and Discussion

### 4.2.1 Hydrolysis of Ubiquitin Fusions Assessed by Co-translational assays

To begin to explore the catalytic properties of UCH-L3 in the context of the designed substrates we performed co-translational assays in which the expression of both the enzyme and the substrates take place simultaneously inside of *E. coli*. In order to accomplish this we engineered a two plasmid system with compatible origins of replication in which the genes coding for the enzyme and the substrates are cloned. After co-transforming *E. coli* cells with both plasmids, protein production was induced upon the addition of IPTG and hydrolysis of the substrates is allowed to proceed *in vivo*. The results of this type of experiments was readily assessed using SDS-PAGE. Figure 3.1a-c shows that 30 minutes after induction increasing amounts of Ub-G, Ub-MonA and Ub-MonA(Y45A) accumulate, and at the same time no products of possible hydrolysis were

observed even after 180 minutes. In the case of Ub-MonB only limited amounts of this fusion are visible after 60 minutes after induction while extensive products of hydrolysis accumulate there after. On the other hand, a more stable chimeric substrate Ub-MonB(A45F), is only partially hydrolyzed and accumulates in a pattern similar to that of Ub-G, Ub-Mon A and Ub-Mon(Y45A).

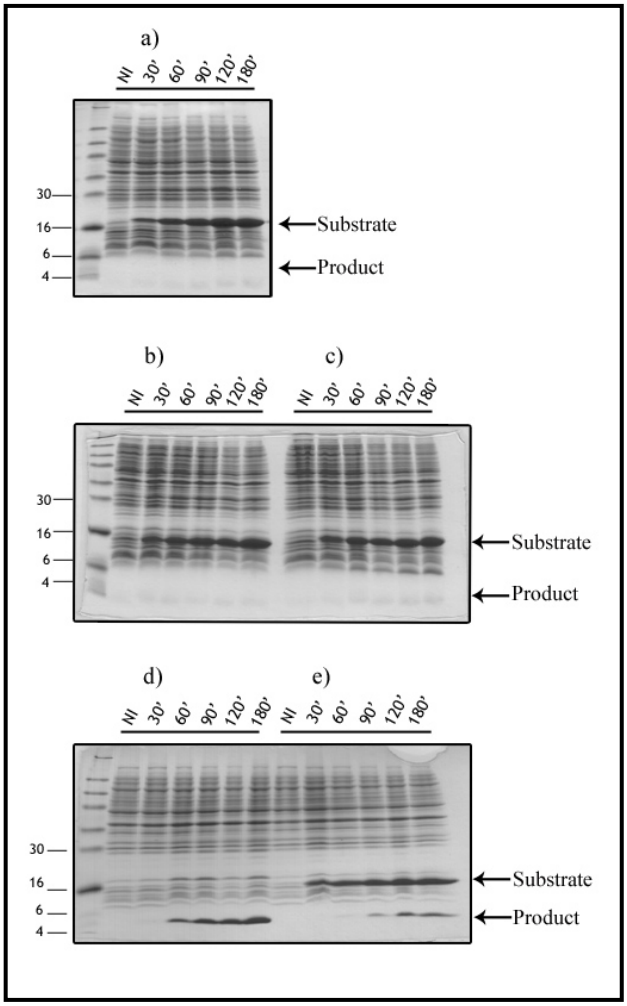


**Figure 4.1.** Co-translational expression and hydrolysis of ubiquitin fusions by UCH-L3. a) Ub-G, b) Ub-MonA, c) Ub-MonA(Y45A), d) Ub-MonB and e) Ub-MonB(Y45A). Post induction, aliquots of 500 μL of culture were taken at the time points indicated and cell pellets normalized by adding 40 μL of 2X loading dye per $OD_{600}$ of 1. The positions of the fusions are indicated on the top (~16 kDa) and the position of hydrolysis products are indicated on bottom (~9.7 kDa and ~6.3 kDa). NI, non-induced.

According to Larsen *et al.*, UCH enzymes hydrolyze peptides attached to the C-terminus of ubiquitin more efficiently if the enzyme is present during the synthesis of the substrate, before the C-terminal extension has a chance to fold into a stable domain [5]. This is a reasonable statement however we observe this to be the case only for Ub-MonB variant ($T_m$ = 36.2 °C) and to smaller extent for the Ub-MonB(A45F) variant ($T_m$ = 59.8 36.2 °C) since the other three fusions were not observed to be hydrolyzed.

Although the convenience of this format in analyzing hydrolysis is obvious, a major drawback is that expression levels for both the enzyme and substrates are unknown and cannot be precisely controlled. Therefore the data presented in figure 4.1 may be the result of unequal enzyme or substrate expression throughout the cultures. Since we desired to ascertain how the thermal stability of the ubiquitin substrates may be related to their hydrolysis rates, the unequal expression of enzyme and substrates is relevant. This is particularly true when the differences in thermal stabilities between protein substrates are small, as in the cases of Ub-MonA(Y45A) and Ub-MonB(A45F) that differ only by 3.2 °C (Table 3.2).

### 4.2.2 Hydrolysis of Ubiquitin Fusions Assessed by FRET

In an attempt to develop a technique that would enable the accurate measurement of various catalytic parameters of UCH-L3 we developed a method based on Fluorescence Resonance Energy Transfer (FRET). This method has been previously used to study enzyme catalysis, kinetics and protein folding [6, 7, 8]. A fundamental condition of a FRET experiment is the presence of a donor-acceptor pair and spectral overlap between the two. A donor-acceptor that is convenient when studying proteins is one in

which the amino acid tryptophan (Trp) acts as the donor and the molecule referred to as IAEDANS (a small thiol-reactive probe) acts as the acceptor [9]. We decided to use this pair by taking advantage of a naturally occurring Trp residue present at position 43 (Trp43) in all Gβ1 variants. However since cysteine is required for the conjugation of IAEDANS in one of the proteins (*i.e.,* ubiquitin), it was necessary to mutate a particular surface position of ubiquitin to cysteine. Searching for a surface residue in the structure of ubiquitin we found that a threonine at position 14 was a reasonable candidate and the mutation T14C was introduced in all five Gβ1 variants (Fig. 4.2).

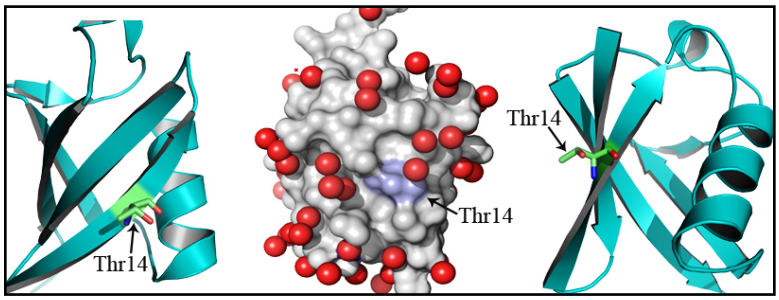


**Figure 4.2.** Threonine at position 14 (Thr14) in ubiquitin is located on the second β-sheet and is a solvent exposed residue. Thr14 was chosen to be mutated to cysteine, a residue necessary for the conjugation to the fluorescent probe IAEDANS. Different views are provided for comparison. The structure in the center shows a surface projection and the red spheres indicate solvent molecules.

As a proof of concept for our design we generated the mutant Ub(T14C)-MonB and successfully labeled it with IAEDANS. The fusion that contained the Mon-B variant was selected based on the fact that this fusion is readily hydrolyzed by UCH-L3 (Fig. 4.1). Experimentally, FRET would be induced by excitation of Trp43 in the labeled protein and signal detected by measuring the emission of radiation from IAEDANS (Fig 4.3). Theoretically, upon incubation of Ub(T14C)-MonB with UCH-L3, hydrolysis of the

fusion will release MonB away from ubiquitin, causing the signal emitted by IAEDANS to decrease as the FRET signal is dependent on the distance between the donor-acceptor pair. Figure 4.4a shows the fluorescence spectra from Ub-MonB in which the emission peak for Trp43 can be seen at ~353 nm. When that variant was labeled with IAEDANS [Ub(T14C)-MonB] and excited at 295 nm the emission peak for the IAEDANS moiety was observed at 473 nm which indicated that FRET was occurring (Fig 4.4b).

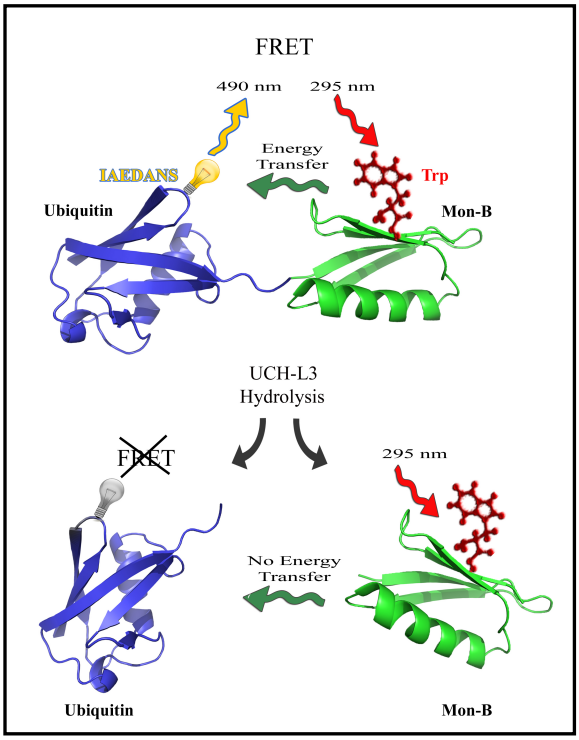


**Figure 4.3.** The engineered FRET system consists of a ubiquitin fusion in which position T14 in ubiquitin has been mutated to cysteine, producing Ub(T14C) variants necessary for conjugation to IAEDANS. Since the FRET signal depends on the distance between the donor-acceptor pair its intensity is expected to decay as the ubiquitin fusion is hydrolyzed by UCH-L3. Trp: $\lambda_{abs}$= 280-295 nm, $\lambda_{em}$= 330-340 nm; IAEDANS: $\lambda_{abs}$= 336 nm, $\lambda_{em}$= 490 nm.

These observations suggested that this technique could be useful to characterize the kinetic properties of UCH-L3, and we proceeded to react the labeled substrate with

the enzyme. The overlay of spectra collected at several time points during the reaction of UCH-L3 with Ub(TC)-MonB indicates that FRET signal between the sample with no enzyme and those incubated with enzyme decreased only very minimally (Fig 4.4c). Our previous con-translational analysis demonstrated that hydrolysis of Ub-MonB almost reaches completion after 60 minutes (Fig. 4.1). Therefore we expected a significant decrease in FRET signal after incubating labeled Ub(T14C)-MonB with UCH-L3 .

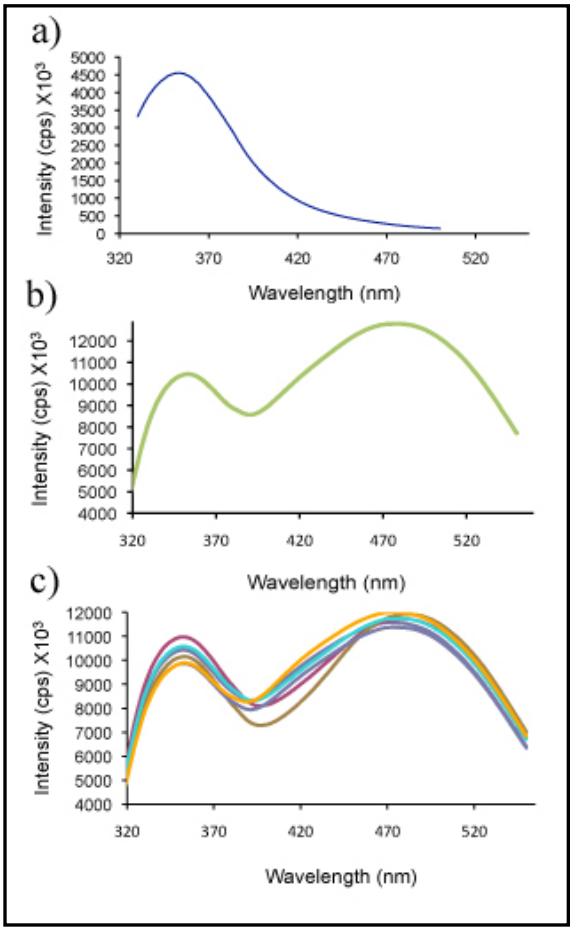


**Figure. 4.4.** Fluorescence emission spectra. a) Upon excitation at 295 nm, the emission peak for tryptophan in Ub-MonB is detected at 353 nm. b) Spectra for IAEDANS-labeled Ub(T14C)-MonB after excitation at 295 nm. The emission peak of IAEDANS at 473 nm indicates FRET. c) 50 µM of labeled Ub(T14C)-MonB was incubated with 1.5 µM UCH-L3 at 37 °C and spectra recorded at various times: (●) No enzyme, (●) 5 minutes, (●) 15 minutes, (●) 30 minutes, (●) 80 minutes and (●) 210 minutes.

These results indicated that the FRET assay, in the current implementation, provided a limited dynamic range of analysis, even for Ub-MonB, a substrate that normally undergoes extensive hydrolysis. To explain these findings we considered the possibility that two tryptophan residues in positions 6 and 29 of UCH-L3 could be acting as FRET donors for IAEDANS. The analysis of the crystal structure of UCH-L3 in complex with a ubiquitin substrate shows that Trp6 and Trp29 in UCH-L3 are only 38.5 Å and 36.5 Å away from Thr14 of ubiquitin, both of which are within the distance range known to be necessary for FRET (*i.e.,* 10-100 Å) [1, 10]. For this reason Trp6 and Trp29 were mutated to Val (a somewhat conservative mutation in respect to hydrophobicity) and the hydrolysis capacity of these mutants tested. Unfortunately although the single mutant UCH-L3(W6V) was active, the single mutant UCH-L3(W29V) and the double mutant UCH-L3(W6V/W29V) suffered considerable loss of activity and this avenue was no longer explored (data not shown).

Another possibility as to why the FRET signal did not diminish upon hydrolysis is that the Gβ1 variant, after cleavage, possibly forms a weak dimer with ubiquitin through extension β-sheets of both molecules. Since this scenario would result in the free Gβ1 variant remaining in close proximity to the IAEDANS moiety attached to ubiquitin, the FRET signal would presumably not diminish upon hydrolysis of the engineered substrate. This supposition is only speculative and thus would need to be verified experimentally. During the preparation of this thesis Ohayon *et al.* reported the successful design of a FRET system consisting of ubiquitin and a p53- derived pentapeptide [11]. In this system the fluorescence donor (Dpn) was attached in the pentapeptide and the quencher (MCA) was reacted with Asp54 of ubiquitin. By using this system Ohayon *et al.* isolated a novel

and potent inhibitor of UCH-L3 from a library of 1,000 compounds. Within the context of our research this system may be adapted and represents a viable alternative in which the acceptor we used, IAEDANS, could be incorporated in position 54 after generating the mutant of ubiquitin D54C.

### 4.2.3 Hydrolysis of Ubiquitin Fusions Assessed by SDS-PAGE

Given the limitations of our design using the FRET assay, we turned to a more fundamental form of analysis, SDS-PAGE. Previously, we used this technique to visualize the results of co-translation studies (described above, Fig. 4.1). Here we applied a similar approach and ran a time course assay in which purified enzyme and purified substrates were incubated for set time points, quenched at the end of the predetermined time, run on SDS-PAGE and analyzed afterwards by densitometry using ImageJ software [12].

The reaction of 10.0 pmole of UCH-L3 with 70.0 pmole of Ub-G and Ub-MonA, results in no hydrolysis even when the incubation periods were extended to 1,440 minutes (Fig. 4.5a and 4.5b). In contrast to this, hydrolysis of Ub-A(Y45A) and Ub-MonB(A45F) occurs within minutes and Ub-MonB is hydrolyzed within seconds. In addition to visual inspection of these gels we carried out a semi-quantitative comparison based on the densitometric analysis of unreacted substrates. From the data obtained we calculated the time that takes for UCH-L3 to hydrolyze 50% of the substrate ($H_{50\%}$). This analysis shows that the more stable hyperthermophile variants such as Ub-G and Ub-MonA require more than 1,440 minutes to reach $H_{50\%}$, whereas mesothermophile variants such as Ub-MonA(Y45A) and Ub-MonB(A45F) have $H_{50\%}$ of 22 minutes and 50 minutes, and

the variant of lowest thermal stability Ub-MonB is hydrolyzed quite quickly with a measured $H_{50\%}$ of 0.52 minutes (Table 4.1).

This data parallels the data obtained in the co-translational assay with the exception of the result obtained for Ub-A(Y45A). Co-expression of UCH-L3 and Ub-A(Y45A) resulted in no hydrolysis (Fig. 4.1c) but when both the enzyme and the substrate are purified and then assayed together hydrolysis is observed (Fig. 4.5c). To our surprise a similar discrepancy has been described previously. Larsen *et al.* report that purified UCH-L3 does not hydrolyze bacterial lysates from *E. coli* containing UbCEP52 (a 52 amino acid ribosomal protein fused to the C-terminus of ubiquitin) but if pure UCH-L3 is reacted with pure UbCEP52, this is efficiently hydrolyzed [5].

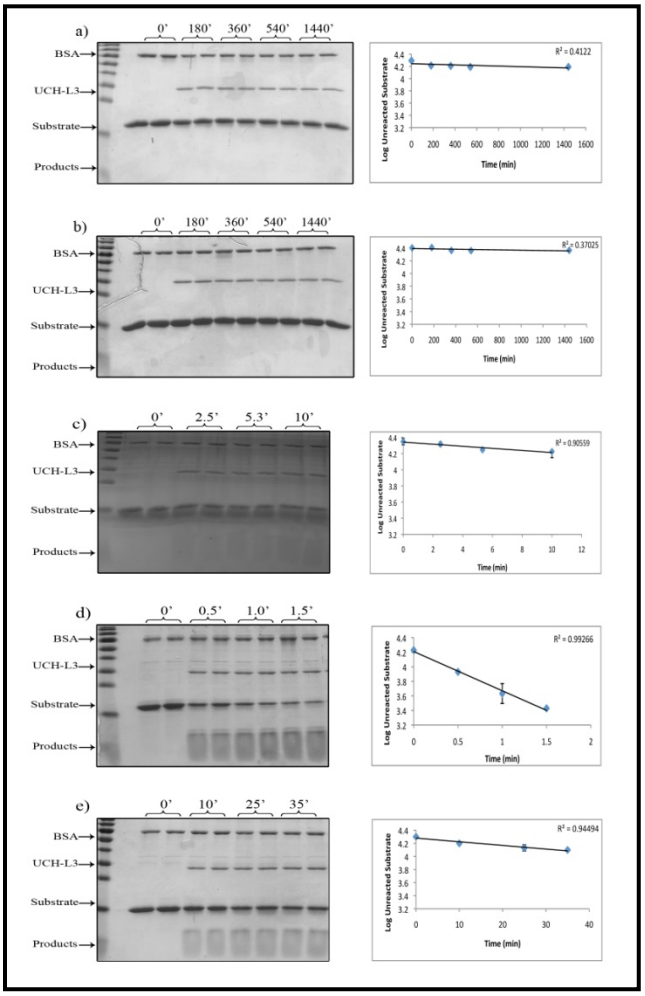


**Figure 4.5.** Time-dependent hydrolysis of a) Ub-G, b) Ub-MonA, c) Ub-MonA(Y45A), d) Ub-MonB and e) Ub-MonB(A45F) by UCH-L3. Time points were assayed in duplicates. The graphs in the right panel show the results of the densitometric analysis (see text). Line represents best fit. $R^2$ values are indicated on top right corner of each graph. BSA is included in the reaction mixture as an internal loading control. For time point at 0 minutes no enzyme was included to avoid possible hydrolysis during sample processing observed in fast-reacted substrates such as Ub-MonB.

The authors of this report suggests that bacterial lysates may contain a component that interferes with the cleavage of UbCEP52 and in the context of our work the same is possibly true for Ub-Mon(Y45A). Thus, although the data obtained in the co-translational assays are valuable we assign more validity to the experiments in which both purified enzyme and substrates were used.

**Table 4.1.** Quantification of hydrolysis of ubiquitin fusions. Respective $T_m$ values are included for direct comparison.

| Protein | $H_{50\%}$ (min) | $T_m$ (°C) |
|---|---|---|
| Ub-G | >1,440 | 82.7 |
| Ub-MonA | >1,440 | 90.7 |
| Ub-MonA(Y45A) | 22 | 56.6 |
| Ub-MonB | 0.52 | 36.2 |
| Ub-MonB(A45F) | 50 | 59.8 |

As seen in figure 4.5 substrates Ub-G and Ub-MonA are not hydrolyzed by UCH-L3 even when the incubation periods are extended to 1,440 minutes (24 hours). We wondered if these substrates could ultimately be hydrolyzed in the presence of greater enzyme concentrations. To test this hypothesis we devised another assay in which a fixed incubation time of 30 minutes was used and a constant amount of substrate (70.0 pmole) was incubated with increasing amounts of UCH-L3, from 3.5 pmole to 278.0 pmole. In this assay Ub-G and Ub-MonA are not hydrolyzed from 3.5 to 70.0 pmole and only begin to be cleaved with 140.0 pmole (Fig. 4.6). With 278.0 pmole of UCH-L3, Ub-G was cleaved to 33%, while Ub-MonA is hydrolyzed to 84%. On the contrary Ub-A(Y45A) is partially reacted with 7.0 pmole of UCH-L3 and using an enzyme concentration of 70.0 pmole only 15% of the substrate remains after 30 minutes. For Ub-MonB full hydrolysis is almost reached at 3.5 pmole of UCH-L3 while its derivative, Ub-MonB(A45F) is partially hydrolyzed by 10% and most of it is hydrolyzed at 140.0 pmole. This assay demonstrates that Ub-G and Ub-MonA are also substrates for UCH-L3 although to a lesser extent.

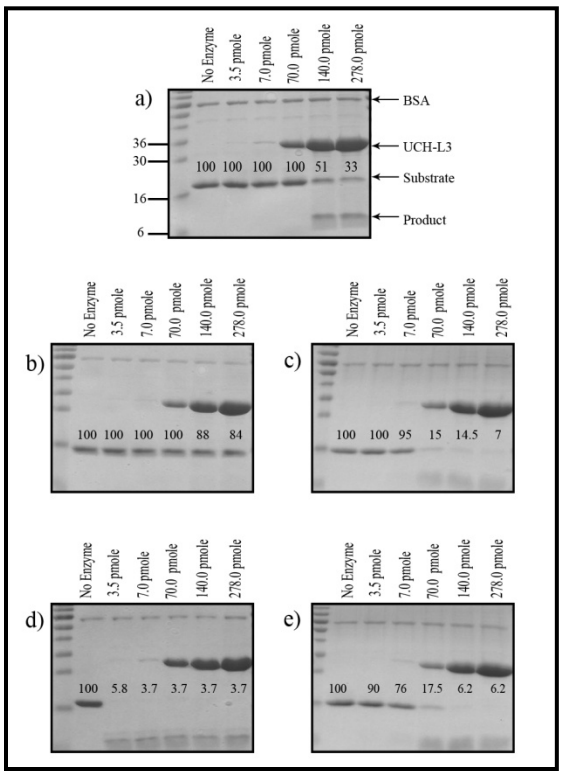


**Figure 4.6.** Concentration-dependent hydrolysis of a) Ub-G, b) Ub-MonA, c) Ub-MonA(Y45A), d) Ub-MonB and e) Ub-MonB(A45F) by UCH-L3. Fixed amounts of substrates were reacted with increasing amounts of UCH-L3 (indicated on top of every lane). Percent of unreacted substrate (in relationship to the lane in which no enzyme was added) is indicated on top of each band.

### 4.2.4 Hydrolysis of the Linear Ubiquitin Dimer by UCH-L3

Thus far we have demonstrated that the rate of hydrolysis of ubiquitin fusions by UCH-L3 is slow when the attached Gβ1 substrates are thermally stable. Considering this we theorized that the lack of hydrolysis for different ubiquitin dimers by UCH-L3 (reported elsewhere) could possibly be associated with the thermal stability of ubiquitin as well [13, 14]. Of special interest to us is the Ub-Ub linear dimer because this protein occurs naturally [14] and the two ubiquitin units are fused in the same format as all the other fusions studied thus far (N- to C-terminus). As described in chapter III Ub-Ub is a relatively stable protein ($T_m$ = 85 °C) and we were interested in determining if this

substrate could be hydrolyzed by UCH-L3 under the same experimental conditions used to characterize the other ubiquitin fusions. In the assay in which a fixed amount of enzyme and substrate were incubated for various time periods, Ub-Ub was not hydrolyzed into monomeric ubiquitin by UCH-L3, even after an incubation period of 1,440 minutes (Fig. 4.7a). Similarly in the enzyme-concentration dependent experiment, Ub-Ub is not reacted when incubated with up to 278.0 pmole of UCH-L3 (Fig. 4.7b). Under these conditions the two stable ubiquitin fusions derived from Gβ1, Ub-MonA and Ub-G were hydrolyzed to 33% and 84%, respectively (Fig. 4.6a and 4.6b), therefore Ub-Ub turns out to be the most hydrolytically stable substrate.

In addition to the ubiquitin dimer just described, another ubiquitin fusion was (inadvertently) created. This fusion resulted from an error during the design of the reverse oligonucleotide, OCN68 Ubi:Ubi Rev, used in the PCR reaction to amplify the ubiquitin gene (see chapter II). Cloning of this construct generated a read-through of the stop codon and continued into the vector multiple cloning site. The resulting protein consisted of a linear ubiquitin dimer with a scrambled 22-amino acid peptide fused to the C-terminus of the second C-terminal ubiquitin (UbUb-22). Considering that short extensions attached to the C-terminus of mono-ubiquitin are generally good leaving groups for UCH-L3 we looked to determine if this property remained when the leaving group was preceded by two ubiquitin moieties. Using the time-dependent assay and the concentration-dependent hydrolysis assay described above we found that unlike Ub-Ub, UbUb-22 is a good substrate for UCH-L3 and the 22-mer is rapidly removed from the distal ubiquitin with a $H_{50\%}$ of 1.3 minutes (Figs 4.7c and 4.7d). The $H_{50\%}$ of UbUb-22 is comparable to that of Ub-MonB (0.52 minutes), the least thermally stable construct.

Although we did not determine the thermal stability of UbUb-22 two possible arguments that may explain such similar $H_{50\%}$ values are its small size and its sequence. The random amino acid sequence of the 22-mer derives from the multiple cloning site of the vector used to clone Ub-Ub. Therefore we would not expect that the 22-mer would have secondary structure or to be folded. In conjunction the lack of folding and the small size of a leaving group are properties found in good substrates of UCH-L3 [5].

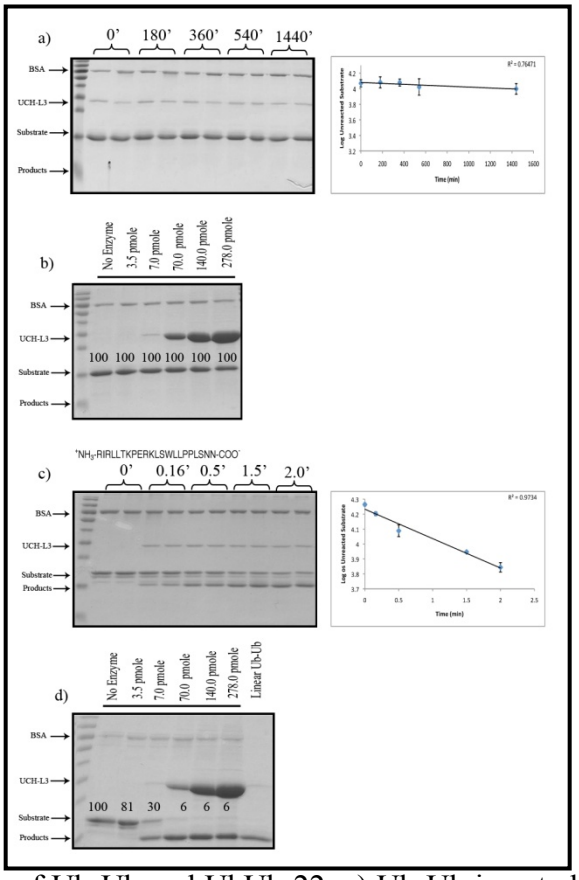


**Figure 4.7.** Hydrolysis of Ub-Ub and UbUb-22. a) Ub-Ub is not cleaved by UCH-L3. b) UCH-L3 is not capable of hydrolyzing Ub-Ub at the largest enzyme amount used to react all other substrates (278.0 pmole). c) UbUb-22 is a good substrate for UCH-L3 and the 22-mer is rapidly cleaved off the distal ubiquitin. d) UbUb-22 is nearly hydrolyzed completely when reacted with 70.0 pmole of enzyme. The last lane in d) was included as a reference for molecular weight. Sequence of the 22-mer is shown on top of c). Graphs to the right of a) and c) show the results of the densitometric analysis. Line represents best fit. $R^2$ values are indicated on top right corner of each graph.

An additional observation arising from the fast hydrolysis of UbUb-22 is that the human UCH-L3 can remove extensions attached to the C-terminus of ubiquitin dimers and not just from monoubiquitin as currently established in the literature. So far, the largest extension described to be cleaved from a ubiquitin dimer is 11 amino acids [4]. Our results with UbUb-22 support this published work and imply that UCH-L3 may be involved not only in the recycling or regeneration of mono-ubiquitin from small peptides or adducts (*i.e.*, amino acids, thiolesters or esters) [1, 15] but also in the recycling or regeneration of ubiquitin dimers and possibly other ubiquitin polymers. This may seem a trivial observation, however every reaction involving ubiquitin requires its C-terminal to be free in order to be polymerized into other ubiquitin molecules or into targeted substrates [16, 17, 18, 19]. Monoubiquitin or ubiquitin polymers with a C-terminus blocked by amino acids, peptides or any adduct may not be integrated into reaction cycles.

### 4.2.5 Hydrolysis of Ubiquitin Fusions by an Insertion Mutant of UCH-L3

The lack of activity of UCH-L3 towards linear, Lys48-linked and Lys63-linked ubiquitin dimers has been attributed to the presence of a 20 amino acid crossover loop positioned on top of the active site of the enzyme [5, 14]. This loop was theorized to confer UCH-L3 with specificity by restricting the size of the substrate cleaved by the enzyme, thus acting as a filter to prevent large and folded substrates from reaching the active site [4, 20]. Two groups independently proved this theory by engineering versions of UCH-L3 that disassembled Lys48 or Lys63 diubiquitin. Specifically the work of Zhou

*et al.* entailed the extension of the loop by inserting three consecutive amino acids (threonine, lysine and threonine) towards the C-terminus end of the loop. This modification enabled the engineered enzyme to accept and hydrolyze a Lys48 dimer that the wild type enzyme could not. We wondered if the engineered version of UCHL-3 described by Zhou *et al.* (UCHL3-TKT) could also process the linear ubiquitin dimer Ub-Ub and the thermally stable variants derived from Gβ1.

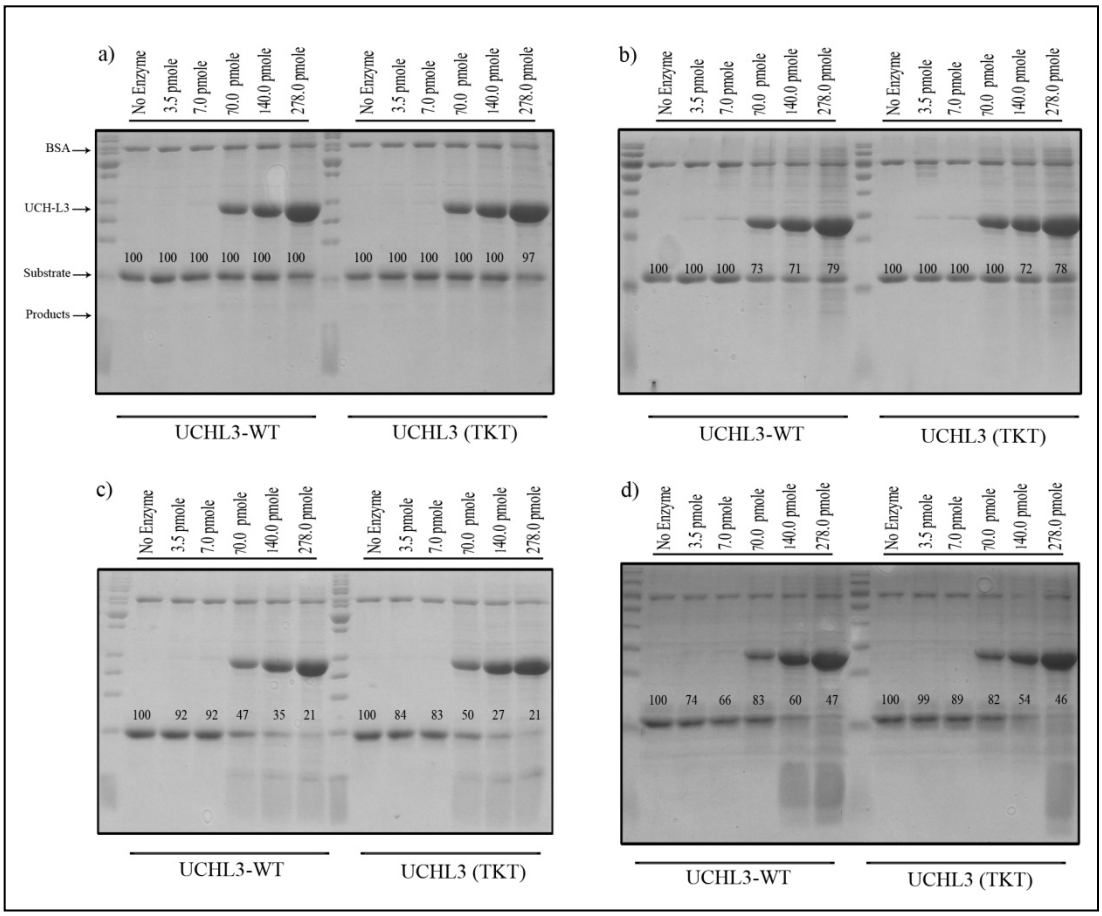


**Figure 4.8.** Concentration-dependent hydrolysis of a) Ub-Ub, b) Ub-G, c) Ub-MonA(Y45A) and d) Ub-MonB(A45F) by UCH-L3 and UCHL3-TKT. Each fusion was reacted in parallel with both forms of the enzyme and ran on the same gel. The percent of unreacted substrate is indicated on top of each band. Reactions were incubated for 30 minutes at 37 °C.

Hydrolysis of Ub-Ub, Ub-G, Ub-MonA(Y45A) and Ub-MonB(A45F) by wild-type UCH-L3 and the insertion mutant, UCHL3-TKT, resulted in a the nearly identical hydrolysis rates observed for the wild-type enzyme (Fig. 4.8). The extent of hydrolysis observed was mirrored for all substrates for all concentrations used for wild type UCH-L3 and the mutant UCHL3-TKT. Since Zhou *et al.* demonstrated that UCHL3-TKT partially hydrolyzed the Lys48-linked dimer of ubiquitin we expected similar results for the linearly fused ubiquitin dimer. This was not the case and hydrolysis of stable variants, including Ub-Ub was not improved by elongation of the cross over loop in UCHL3-TKT.

### 4.3.1 Thermal Stability vs. Hydrolytic Stability

Taken together, the results presented here suggest a general correlation between the hydrolysis of the ubiquitin substrates by UCH-L3 and their thermal stability. The ranking of ubiquitin fusions according to increasing order of thermal stability is as follows: Ub-MonA> Ub-G> Ub-MonB(Y45A)> Ub-MonA(A45F)> Ub-MonB. Likewise the ranking of the fusions in increasing order of hydrolytic stability is as follows: Ub-MonA> Ub-G> Ub-MonB(Y45A)> Ub-MonA(A45F)> Ub-MonB. From this comparison we observe that the thermal stability and the hydrolytic stability of the fusions parallel each other, a concept illustrated in figure 4.9.

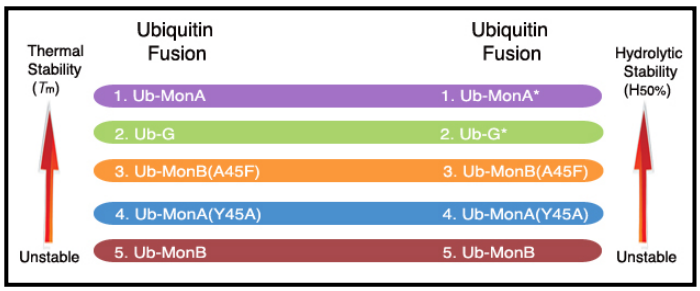


**Figure 4.9.** Ranking of thermal stability and hydrolytic stability of the ubiquitin fusions. The most thermally stable fusion is also the most hydrolytically stable. Likewise, the least thermally stable protein is also the least hydrolytically stable. *The ranking of hydrolytic stability is based on the values of $H_{50\%}$, except for Ub-G and Ub-MonA. These two fusions are ranked based on the hydrolytic stabilities seen in the concentration-dependent assay (Figs. 4.6a and 4.6b).

Complementing this work, Carmody L. developed comparable research in our laboratory by engineering proteins derived from the B domain of the Staphylococcal protein A and found a similar correlation [21]. The B domain from protein A is a small protein of 59 amino acids that forms a three-helix bundle. Integration of the results from Carmody and this thesis indicates an exponential relationship between the hydrolysis of ubiquitin fusions by UCH-L3 and their thermal stability (Fig. 4.10). Ubiquitin fusions with $T_m$'s <60 °C are hydrolyzed within 50 minutes or less while fusions with higher thermal stabilities require more than 180 minutes. In the opposite ends of this gradient of hydrolytic stabilities are Ub-MonA and Ub-MonB with a >2000-fold difference in the $H_{50\%}$ (*i.e.*, >1,440 minutes and 0.52 minutes).

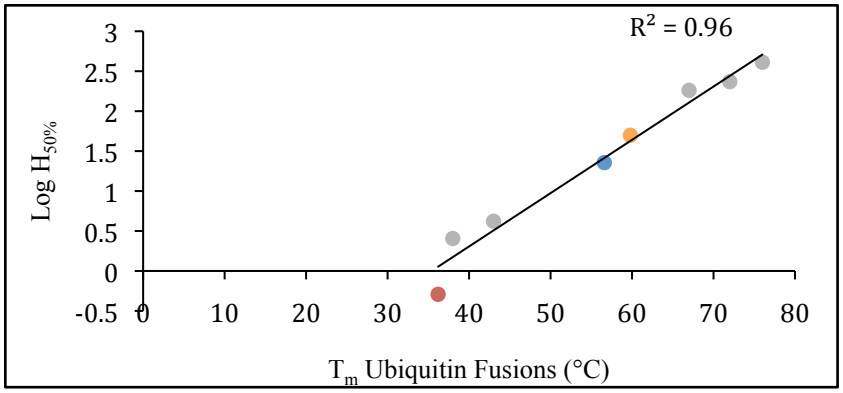


**Figure 4.10.** Relationship between thermal stability and the hydrolytic stability of ubiquitin fusions. ● Ub-MonB, ● Ub-MonA(Y45A) and ● Ub-Mon-B(A45F). In grey (●) are data points derived from ubiquitin fusions of Staphylococcal Protein A [21]. This graph only includes fusions for which $T_m$ and $H_{50\%}$ could be experimentally determined (Ub-G and Ub-Mon-A are excluded).

Next we consider a series of arguments that can be ruled out to explain the differences on hydrolysis seen in all fusions namely: primary structure and oligomerization of the substrate, size of the leaving group and finally the accessibility of the enzyme for the signal recognition and the scissile bond.

*Primary structure of the substrate*. The specificity of UCH-L3 for the P1' site (the position immediate to the scissile bond in relation to the C-terminus) has been previously studied at length [5, 22]. These studies showed no preference of UCH-L3 at this site or at the first ten amino acids in the leaving group regardless of the charge or size of the residue. The only exception occurred if proline was at the P1' site. When Pro was substituted at the P1' position UCH-L3 could not hydrolyze a short ubiquitin extension of just seven amino acids [5]. Within the framework of our research not only all five fusions contain the same amino acid at the P1' site, methionine, but also in all of these constructs the first 15 amino-terminal residues are the identical (Fig. 2.1). Therefore we exclude the possibility of inadvertently introducing sequences from the P1' to the P15' sites that may

be more preferentially hydrolyzed by UCH-L3. The low specificity of UCH-L3 for positions adjacent to the scissile bond represents a functional advantage since this confers on the enzyme the ability to process a larger variety of substrates, a scenario most likely found in the cellular environment. Following the analysis of the primary structure of the substrates Drag *et al.* defined the specificities of UCH-L3 at the P4-P1 sites (positions immediately N-terminal to the scissile bond). It was determined throughout the reported characterization that UCH-L3 exhibits a broad tolerance to different amino acids in position P2 and P4 but is highly selective for amino acids at the P3 and P1 positions. Nonetheless positions P1-P4, located in the C-terminus of ubiquitin, were not the subject of our engineering efforts and no influence on the hydrolytic properties of the enzyme should be expected [23].

*Oligomerization of the substrates*. A positive correlation has been found between the state of protein homo-oligomerization and thermal stability [24, 25, 26]. In the case of the soybean agglutinin the stability of the monomeric form is 9.8 kcal/mol and that of the tetramer is 50.2 kcal/mol. This five-fold difference illustrates the extensive contribution of intersubunit interaction to the stability of proteins [25]. In addition, substrate oligomerization may mask critical sites for the interaction of the enzyme with the substrate and inhibit their hydrolysis. Therefore we contemplated the possibility that if some fusions formed oligomers these could be structurally more stable and present increased resistance to hydrolysis. Data from size exclusion chromatography demonstrate that the fusions we engineered do not form oligomers (table 3.4). In consequence the differences in hydrolysis of the protein substrates obtained are not due to the presence of

oligomers that may increase their stability or mask amino acids necessary for the interaction with the enzyme.

*Size of the leaving group*. It has been demonstrated that UCH-L3 has a preference for small (~20 residues) and unfolded leaving groups, a property shared with the yeast homolog (YUH) and UCH-L1 [1]. The molecular mechanism for this selectivity is attributed to the crossover loop positioned on top of the active site that acts as a filter to restrict the size of the leaving group cleaved by the enzyme [20]. Therefore we could consider the size of the leaving group as a factor to explain the hydrolysis differential observed. Figure 2.1 illustrates that all the Gβ1 variants engineered have the same size, 56 amino acids (~6 kDa). This indicates that substrates such as Ub-MonB and Ub-MonA(Y45A) are not hydrolyzed more extensively because of their differences in their size. A secondary consideration is that the N-terminal Histag included to aid protein purification may interfere with the enzyme. Earlier studies have found that this short stretch of amino acids has a marginal role on the cleaving rates of UCH-L3 [27, 28]. This seems to be the case because the structure of the enzyme in complex with Ub-VME (a suicide substrate) reveals that the N-terminus of the ubiquitin moiety lies away from the active site of the enzyme and does not interact with it at all (Fig. 1.6). Still, since the His tag is present in all of substrates the effect, if any, would be the same for all fusions.

*Accessibility of the recognition signal and the scissile bond.* A basic principle in the processing of peptides by hydrolases is the accessibility of the recognition signal and the scissile bond located in the substrate. UCH-L3 recognizes the sequence $Arg^{72}$-$Leu^{73}$-$Arg^{74}$-$Gly^{75}$-$Gly^{76}$~P1', located at the C-terminus of ubiquitin (where P1' is the first amino acid in the leaving group and ~ represents the scissile bond) [29]. The packing of

the leaving group against ubiquitin may block both the recognition signal and the scissile bond, slowing or preventing its cleavage by UCH-L3. This structural arrangement is found in dimers and tetramers of ubiquitin linked through Lys48. These polymers adopt a closed conformation with a tight compact structure sustained by multiple intermolecular hydrogen bonds [13, 19, 30]. In contrast to this the structure of two linear fusions, Ub-Ub and Ub-UIM (Ubiquitin Interacting Motif) illustrates that the region that connects the individual domains (which contains the motif recognized by UCH-L3 and the scissile bond) is solvent-accessible and exists in a fairly open conformation and does not contain any element of secondary structure (Fig. 4.11) [13, 31, 32]. Thus we consider that for our substrates the sequence motif recognized by UCH-L3 and the scissile bond should be accessible for catalysis to proceed (Fig 4.11). In addition the unstructured character of the region connecting ubiquitin to other domains is extensively recognized as the preferred structural element where protease cleavage occurs [33, 34].

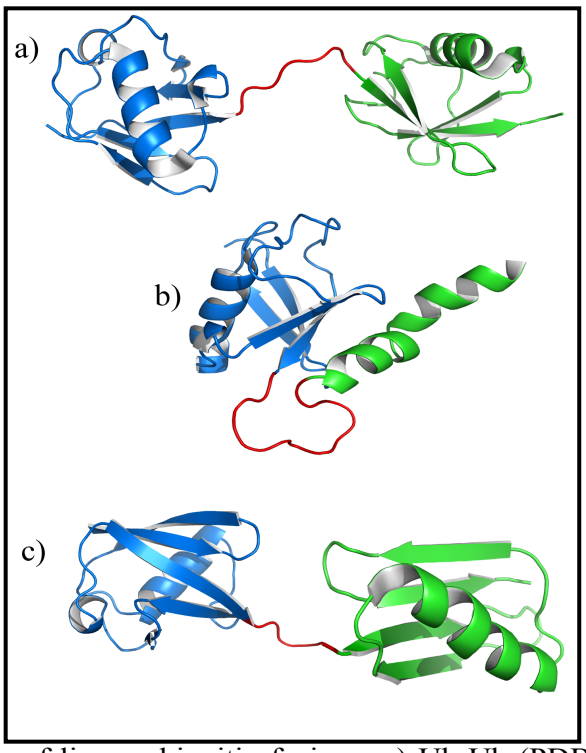


**Figure 4.11.** Structure of linear ubiquitin fusions: a) Ub-Ub (PDB: 2W9n), b) Ub-UIM (PDB: UIM1) and c) Ub-G. In all structures ubiquitin is shown in blue and the corresponding C-terminal domain is shown in green. As seen in the actual structures of Ub-Ub and Ub-UIM the region connecting ubiquitin to the C-terminal domain (red) extends from 7 to 11 amino acids, is solvent-accessible and disordered. Structure in c) was generated for purposes of illustration using the actual PDB files of ubiquitin (1UBQ) and Gβ1 (2GB1).

The substrates studied here share a number of biophysical and biochemical properties: these occur in monomeric state, the leaving groups have the same N-terminal sequence, the amino acid length is the same, the overall fold is maintained and the accessibility to the recognition signal and the scissile bond by the enzyme are likely highly similar. Still, we observe that thermally stable substrates such as Ub-G and Ub-MonA are minimally hydrolyzed, intermediately stable substrates, Ub-MonA(Y45A) and Ub-MonB(A45F) are hydrolyzed more efficiently and the most unstable fusion, Ub-MonB is an excellent substrate for UCH-L3. Hence a valid question is what is the basis

for the relationship between the thermal and hydrolytic stability of the ubiquitin fusions? A potential answer can be formulated by considering the folding and dynamic properties of the substrates and the enzyme. First, the structure of the complex UCH-L3/Ub-VME shows that the unfolded C-terminus of ubiquitin contacts several residues in UCH-L3. The most prominent example of this is Arg74 that forms and extensive network of hydrogen bonds and electrostatic interactions with 11 residues in UCH-L3 [23, 28]. These contacts allow the alignment and positioning of the ubiquitin extensions in proximity to the catalytic site prior to catalysis (Fig. 1.6). In addition, several studies have shown that hyperthermophiles tend to be less flexible than their mesophilic homologs suggesting an inverse relationship between stability and flexibility [35, 36]. Therefore it is possible to assume that more thermally stable and more slowly hydrolyzed substrates may not be malleable enough to be accommodated in the active site of UCH-L3 and subsequently be hydrolyzed. In support of this hypothesis, HSQC experiments of [1H15N] single-labeled samples show that the least thermally stable protein, Mon-B and the more extensively hydrolyzed fusion, Ub-MonB, display increased backbone dynamics (Fig 3.11) when compared to Gβ1 or MonA [37, 38]. Also, proteins exist in a dynamic equilibrium between a folded and an unfolded state. Possibly, in some substrates the unfolded state of the leaving groups is favored and this condition confers the enzyme with the capacity to hydrolyze these fusions more rapidly. The structure of the substrate-bound enzyme shows that some ligand-induced changes in the structure of UCH-L3 are required to render its active site accessible to the C-terminus of ubiquitin. The most prominent structural change in the enzyme is the stabilization of the 20 amino acids-crossover loop into an α-helix followed by and S shaped-loop [28]. Perhaps a major

structural rearrangement in UCH-L3 as the one just described is not possible or is limited when hydrolyzing more rigid substrates, compromising the catalytic efficiency of the enzyme. The validation of the three arguments just presented is beyond the scope of this thesis but we can propose that experiments previously performed to study the dynamics and folding of ubiquitin and Gβ1 can be applied to study the fusion in the free form and also in complex with the enzyme. Some of these experiments include $^{15}N$ and $^{13}C$ relaxation of backbone amide nitrogens and methyl carbon centers to probe internal dynamics [39, 40]. Another approach entails the study of chemical denaturation in methanol or urea, analyzed by 1D 1H NMR and CD, to determine the thermodynamics of unfolding [41]. Finally accelerated molecular dynamic simulations in combination with experimental NMR measurements (*i.e.*, residual dipolar couplings) might be useful to assess dynamic events at certain timescales (*i.e.,* μs to ms) that are significant for biochemically relevant processes such as enzymatic catalysis and protein-protein interactions [42, 43].

Acknowledgment:

This chapter, in part, is a reprint of the material as it appears in Navarro M., Carmody L., Romo O., and Love J. "Biochemical and biophysical effects of N-terminal monoubiquitination of small protein". Manuscript in final stages of preparation.

**References**

1. Johnston, S. C., Larsen, C. N., Cook, W. J., Wilkinson, K. D. & Hill, C. P. (1997). Crystal structure of a deubiquitinating enzyme (human UCH-L3) at 1.8 A resolution. *EMBO J* **16**, 3787-96.

2. Nijman, S. M., Luna-Vargas, M. P., Velds, A., Brummelkamp, T. R., Dirac, A. M., Sixma, T. K. & Bernards, R. (2005). A genomic and functional inventory of deubiquitinating enzymes. *Cell* **123**, 773-86.

3. Wilkinson, K. D., Cox, M. J., Mayer, A. N. & Frey, T. (1986). Synthesis and characterization of ubiquitin ethyl ester, a new substrate for ubiquitin carboxyl-terminal hydrolase. *Biochemistry* **25**, 6644-9.

4. Zhou, Z. R., Zhang, Y. H., Liu, S., Song, A. X. & Hu, H. Y. (2012). Length of the active-site crossover loop defines the substrate specificity of ubiquitin C-terminal hydrolases for ubiquitin chains. *Biochem J* **441**, 143-9.

5. Larsen, C. N., Krantz, B. A. & Wilkinson, K. D. (1998). Substrate specificity of deubiquitinating enzymes: ubiquitin C-terminal hydrolases. *Biochemistry* **37**, 3358-68.

6. Franke, A. E., Danley, D. E., Kaczmarek, F. S., Hawrylik, S. J., Gerard, R. D., Lee, S. E. & Geoghegan, K. F. (1990). Expression of human plasminogen activator inhibitor type-1 (PAI-1) in Escherichia coli as a soluble protein comprised of active and latent forms. Isolation and crystallization of latent PAI-1. *Biochim Biophys Acta* **1037**, 16-23.

7. Teilum, K., Maki, K., Kragelund, B. B., Poulsen, F. M. & Roder, H. (2002). Early kinetic intermediate in the folding of acyl-CoA binding protein detected by fluorescence labeling and ultrarapid mixing. *Proc Natl Acad Sci U S A* **99**, 9807-12.

8. Jeganathan, S., von Bergen, M., Brutlach, H., Steinhoff, H. J. & Mandelkow, E. (2006). Global hairpin folding of tau in solution. *Biochemistry* **45**, 2283-93.

9. Liang, J. J. & Liu, B. F. (2006). Fluorescence resonance energy transfer study of subunit exchange in human lens crystallins and congenital cataract crystallin mutants. *Protein Sci* **15**, 1619-27.

10. Szollosi, J., Damjanovich, S., Nagy, P., Vereb, G. & Matyus, L. (2006). Principles of resonance energy transfer. *Curr Protoc Cytom* **Chapter 1**, Unit1 12.

11. Ohayon, S., Spasser, L., Aharoni, A. & Brik, A. (2012). Targeting deubiquitinases enabled by chemical synthesis of proteins. *J Am Chem Soc* **134**, 3281-9.

12. Abramoff, M. D., Magalhaes, P. J. & Ram, S. J. (2004). Image Processing with ImageJ. *Biophotonics International* **11**, 36-42.

13. Komander, D., Reyes-Turcu, F., Licchesi, J. D., Odenwaelder, P., Wilkinson, K. D. & Barford, D. (2009). Molecular discrimination of structurally equivalent Lys 63-linked and linear polyubiquitin chains. *EMBO Rep* **10**, 466-73.
14. Setsuie, R., Sakurai, M., Sakaguchi, Y. & Wada, K. (2009). Ubiquitin dimers control the hydrolase activity of UCH-L3. *Neurochem Int* **54**, 314-21.

15. Pickart, C. M. & Rose, I. A. (1985). Functional heterogeneity of ubiquitin carrier proteins. *J Biol Chem* **260**, 1573-81.

16. Kensche, T., Tokunaga, F., Ikeda, F., Goto, E., Iwai, K. & Dikic, I. (2012). Analysis of nuclear factor-kappaB (NF-kappaB) essential modulator (NEMO) binding to linear and lysine-linked ubiquitin chains and its role in the activation of NF-kappaB. *J Biol Chem* **287**, 23626-34.

17. Zeng, W., Sun, L., Jiang, X., Chen, X., Hou, F., Adhikari, A., Xu, M. & Chen, Z. J. (2010). Reconstitution of the RIG-I pathway reveals a signaling role of unanchored polyubiquitin chains in innate immunity. *Cell* **141**, 315-30.

18. Komander, D. & Rape, M. (2012). The ubiquitin code. *Annu Rev Biochem* **81**, 203-29.

19. Kulathu, Y. & Komander, D. (2012). Atypical ubiquitylation - the unexplored world of polyubiquitin beyond Lys48 and Lys63 linkages. *Nat Rev Mol Cell Biol* **13**, 508-23.

20. Popp, M. W., Artavanis-Tsakonas, K. & Ploegh, H. L. (2009). Substrate filtering by the active site crossover loop in UCHL3 revealed by sortagging and gain-of-function mutations. *J Biol Chem* **284**, 3593-602.

21. Carmody, L. (2011). Contrasting the Biophysical Properties of Two Small Protein Domains that are Similar in Size Yet Differ in Secondary Structure *Master in Science Thesis. San Diego State University*, 1-148.

22. Schechter, I. & Berger, A. (1967). On the size of the active site in proteases. I. Papain. *Biochem Biophys Res Commun* **27**, 157-62.

23. Drag, M., Mikolajczyk, J., Bekes, M., Reyes-Turcu, F. E., Ellman, J. A., Wilkinson, K. D. & Salvesen, G. S. (2008). Positional-scanning fluorigenic substrate libraries reveal unexpected specificity determinants of DUBs (deubiquitinating enzymes). *Biochemical Journal* **415**, 367-375.

24. Kumar, S., Tsai, C. J. & Nussinov, R. (2000). Factors enhancing protein thermostability. *Protein Eng* **13**, 179-91.

25. Sinha, S. & Surolia, A. (2005). Oligomerization endows enormous stability to soybean agglutinin: a comparison of the stability of monomer and tetramer of soybean agglutinin. *Biophys J* **88**, 4243-51.

26. Tanaka, Y., Tsumoto, K., Yasutake, Y., Umetsu, M., Yao, M., Fukada, H., Tanaka, I. & Kumagai, I. (2004). How oligomerization contributes to the thermostability of an archaeon protein. Protein L-isoaspartyl-O-methyltransferase from Sulfolobus tokodaii. *J Biol Chem* **279**, 32957-67.

27. Beers, E. P. & Callis, J. (1993). Utility of polyhistidine-tagged ubiquitin in the purification of ubiquitin-protein conjugates and as an affinity ligand for the purification of ubiquitin-specific hydrolases. *J Biol Chem* **268**, 21645-9.

28. Misaghi, S., Galardy, P. J., Meester, W. J., Ovaa, H., Ploegh, H. L. & Gaudet, R. (2005). Structure of the ubiquitin hydrolase UCH-L3 complexed with a suicide substrate. *J Biol Chem* **280**, 1512-20.

29. Wilkinson, K. D., Laleli-Sahin, E., Urbauer, J., Larsen, C. N., Shih, G. H., Haas, A. L., Walsh, S. T. & Wand, A. J. (1999). The binding site for UCH-L3 on ubiquitin: mutagenesis and NMR studies on the complex between ubiquitin and UCH-L3. *J Mol Biol* **291**, 1067-77.

30. Eddins, M. J., Varadan, R., Fushman, D., Pickart, C. M. & Wolberger, C. (2007). Crystal structure and solution NMR studies of Lys48-linked tetraubiquitin at neutral pH. *J Mol Biol* **367**, 204-11.

31. Rohaim, A., Kawasaki, M., Kato, R., Dikic, I. & Wakatsuki, S. (2012). Structure of a compact conformation of linear diubiquitin. *Acta Crystallogr D Biol Crystallogr* **68**, 102-8.

32. Patel, M. M., Sgourakis, N. G., Garcia, A. E. & Makhatadze, G. I. (2010). Experimental test of the thermodynamic model of protein cooperativity using temperature-induced unfolding of a Ubq-UIM fusion protein. *Biochemistry* **49**, 8455-67.

33. Timmer, J. C., Zhu, W., Pop, C., Regan, T., Snipas, S. J., Eroshkin, A. M., Riedl, S. J. & Salvesen, G. S. (2009). Structural and kinetic determinants of protease substrates. *Nat Struct Mol Biol* **16**, 1101-8.

34. Kazanov, M. D., Igarashi, Y., Eroshkin, A. M., Cieplak, P., Ratnikov, B., Zhang, Y., Li, Z., Godzik, A., Osterman, A. L. & Smith, J. W. (2011). Structural determinants of limited proteolysis. *J Proteome Res* **10**, 3642-51.

35. Pechkova, E., Sivozhelezov, V. & Nicolini, C. (2007). Protein thermal stability: the role of protein structure and aqueous environment. *Arch Biochem Biophys* **466**, 40-8.

36. Tsai, A. M., Udovic, T. J. & Neumann, D. A. (2001). The inverse relationship between protein dynamics and thermal stability. *Biophys J* **81**, 2339-43.

37. Barakat, N. H., Carmody, L. J. & Love, J. J. (2007). Exploiting elements of transcriptional machinery to enhance protein stability. *J Mol Biol* **366**, 103-16.

38. Huang, P. S., Love, J. J. & Mayo, S. L. (2007). A de novo designed protein protein interface. *Protein Sci* **16**, 2770-4.

39. Schneider, D. M., Dellwo, M. J. & Wand, A. J. (1992). Fast internal main-chain dynamics of human ubiquitin. *Biochemistry* **31**, 3645-52.

40. Wand, A. J., Urbauer, J. L., McEvoy, R. P. & Bieber, R. J. (1996). Internal dynamics of human ubiquitin revealed by 13C-relaxation studies of randomly fractionally labeled protein. *Biochemistry* **35**, 6116-25.

41. Jourdan, M. & Searle, M. S. (2001). Insights into the stability of native and partially folded states of ubiquitin: effects of cosolvents and denaturants on the thermodynamics of protein folding. *Biochemistry* **40**, 10317-25.

42. Markwick, P. R., Bouvignies, G. & Blackledge, M. (2007). Exploring multiple timescale motions in protein GB3 using accelerated molecular dynamics and NMR spectroscopy. *J Am Chem Soc* **129**, 4724-30.

43. Henzler-Wildman, K. & Kern, D. (2007). Dynamic personalities of proteins. *Nature* **450**, 964-72.

**Appendix I.**
DNA Oligonucleotide sequences. Sequences are listed in 5'-3' direction. All oligonucleotides were purchased from Integrated DNA technologies (IDT).

---

**Oligonucleotides to generate monomer B(A45F)**

| | |
|---|---|
| OCN58 monB (A45F) For | gggtgaatggacattcgacgaagcgaccaag |
| OCN59 monB (A45F) Rev | cttggtcgcttcgtcgaatgtccattcaccc |

**Oligonucleotides to amplify Protein G, monomer A, monomer B to generate in frame fusions with ubiquitin**

| | |
|---|---|
| OCN25 Ubi:ProG For | ctccgtctccgcggtggtatgactacttacaaa |
| OCN26 Ubi:ProG Rev | atctaggatccgttattcagtaactgtaaa |
| OCN27 Ubi:MonAB For | ctccgtctccgcggtggtatgacctataagctg |
| OCN28 Ubi:MonAB Rev | atctaggatccgttattcggtcacggtgaa |

**Oligonucleotides to amplify ubiquitin to generate a di-ubiquitin fusion**

| | |
|---|---|
| OCN67 Ubi:Ubi For | ctccgtctccgcggtggtatgcagatcttcgtaaag |
| OCN68 Ubi:Ubi Rev | atctaggatccgaccaccgcggagacg |
| OCN69 Ubi:Ubi Rev | atctaggatccgttaaccaccgcggagacg |

**Oligonucleotides to amplify ubiquitin to generate a UbUb-22 fusion**

| | |
|---|---|
| OCN67 Ubi:Ubi For | ctccgtctccgcggtggtatgcagatcttcgtaaag |
| OCN68 Ubi:Ubi Rev | atctaggatccgaccaccgcggagacg |

**Oligonucleotides to modify pBT**

| | |
|---|---|
| OCN4 pBT --LcI –For | gatggcgcggccgcatcgaattcccgg |
| OCN5 pBT--LcI-Rev | ccactgccgcatatgcatacgctgtttcctgtgtga |

**Oligonucleotides to sequence genes in pBT inserted outside of the multiple cloning site**

| | |
|---|---|
| OCN18 Seq pBT LcI-For | ggcaccccaggctttacactt |
| PC19 seq pBT LcI-Rev | gataactttccccacaacgga |

**Oligonucleotides to amplify UCH-L3 for its cloning in pBT**

| | |
|---|---|
| OCN6 UCH-Nde I-For | ccactgccgcatatgggccatcatcatcatcat |
| OCN7 UCH-EcoR I-Rev | cgctagcatgaattctgctgcagaaagagcaatcgc |

**Oligonucleotides to generate ubiquitin (T14C) in fusions**

| | |
|---|---|
| OCN39 Ubi:GABTto CFor | accggaaagaccatctgtcttgaagttgagccctcc |
| OCN40 Ubi:GABTto CRev | ggagggctcaacttcaagacagatggtctttccggt |

**Oligonucleotides to insert amino acid sequence Thr, Lys, Thr (TKT) in UCH-L3 by Site-Directed Mutagenesis**

| | |
|---|---|
| OCN71 UCHL3TKT(SDM)-For | ggtcagactgaggcaacgaagactccaagtatagatgag |
| OCN72 UCHL3TKT(SDM)-Rev | ctcatctatacttggagtcttcgttgcctcagtctgacc |